Redox-dependent differentiation and dedifferentiation

Inaugural-Dissertation

zur Erlangung des Doktorgrades
der Mathematisch-Naturwissenschaftlichen Fakultät
der Heinrich-Heine-Universität Düsseldorf

vorgelegt von

Christina Wilms
aus Mönchengladbach

Düsseldorf, Mai 2021

Aus der Klinik für Neurologie
der Heinrich-Heine-Universität Düsseldorf

Gedruckt mit der Genehmigung der
Mathematisch-Naturwissenschaftlichen Fakultät der
Heinrich-Heine-Universität Düsseldorf

Berichterstatter:

1. **Priv.-Doz. Dr. Carsten Berndt**
Klinik für Neurologie, Heinrich-Heine-Universität Düsseldorf

2. **Univ.-Prof. Dr. Charlotte von Gall**
Institut für Anatomie, Heinrich-Heine-Universität Düsseldorf

Tag der mündlichen Prüfung: 23.08.2021

Manuscripts related to this thesis:

Wilms C, Lepka L, Häberlein F, Edwardson S, Felsberg J, Pudelko L, Lindenberg T, Poschmann G, Qin N, Volbracht K, Meuth S, Kahlert U, Remke M, Aktas O, Reifenberger G, Bräutigam L, Odermatt B, Berndt C, Glutaredoxin 2 promotes Sp1-dependent NG2/CSPG4 transcription and increases migration of wound healing NG2-glia cells and invasion of glioblastoma cells: enzymatic Taoism (2021), manuscript in preparation

Further manuscripts not related to this thesis:

Hanschmann EM, **Wilms C**, Falk L, Holubiec MI, Mennel S, Lillig CH, Godoy JR, Glutaredoxin 1 is a novel regulator of retinal pigment epithelial cell proliferation, submitted to Antioxidants

Invited bookchapter:

Berndt C, **Wilms C**, Thauvin M, Vriz S, Redox-regulated brain development in: "Oxidative Stress", Sies, H., Ed., Elsevier (2019)

Berndt C, **Wilms C**, Gellert M, Lillig CH, Functional plasticity in the glutaredoxin protein family in Redox Chemistry and Biology of Thiols, Elsevier, in preparation

As oral presentation (selected from abstract):

Wilms C, Lepka K, Häberlein F, Engelke A, Ingold I, Conrad M, Odermatt B, Aktas O, Berndt C, Differentiation of oligodendrocytes is redox regulated. (Symposium of the SPP1710 & GBM, 2018, Berlin –Germany)

Wilms C, Lepka K, Häberlein F, Engelke A, Ingold I, Conrad M, Odermatt B, Aktas O, Berndt C, Glutaredoxin 2 affects differentiation of neural progenitor cells. (Symposium of the SPP1710 (2019, Rauischholzhausen Castle - Germany)

As poster contribution:

Wilms C, Lepka K, Aktas O, Berndt C, Glutaredoxin differentiation of oligodendrocytes. Symposium of the SPP1710 (2018, Rauischholzhausen Castle - Germany)

Wilms C, Lepka K, Odermatt B, Aktas O, Bogeski I, Berndt C, Glutaredoxin 2c, probably the most abundant protein in Speedy Gonzales, speeds up cell migration. Mechanisms and Organizing Principles in Redox Signaling - Implications for Age-Related Disease (Gordon Research Conference 2018, Barcelona - Spain)

Wilms C, Lepka K, Lindenberg T, Häberlein F, Odermatt B, Aktas O, Berndt C, Glutaredoxin 2 affects cellular processes of oligodendrocytes. Current Topics in Myelin Research (2019, Kassel - Germany)

Wilms C, Lepka K, Lindenberg T, Häberlein F, Odermatt B, Aktas O, Berndt C, Glutaredoxin 2 affects cellular processes of oligodendrocytes. Symposium of the SPP1710 (2019, Rauischholzhausen Castle - Germany)

Wilms C, Lepka K, Pudelko L, Lindenberg T, Häberlein F, Odermatt B, Aktas O, Bräutigam L, Berndt C, Redox regulated migration of glia cells. (2019, XIV European Meeting on Glial Cells in Health and Disease, Porto - Portugal)

Wilms C, Lepka K, Poschmann G, Aktas O, Reifenberger G, Bräutigam L, Berndt C, Glutaredoxin 2-regulated redox state of the transcription factor Sp1 affects migration of oligodendrocytes and tumor cell invasion. Symposium of the SPP1710 (2021, online meeting)

„Nothing in life is to be feared,
it is only to be understood.
Now is the time to understand more,
so that we may fear less."

Marie Curie

Table of Contents

1 Abstract

Differentiation and dedifferentiation of cells share many processes like proliferation, survival, cell fate decision, migration, cytoskeletal reorganization and angiogenesis. Over the last decades redox regulation has emerged as one of the central mechanisms in cellular signaling and it has been shown, that under physiological as well as under pathological conditions cells need a delicate redox balance. Many essential cellular functions like proliferation, differentiation and apoptosis are regulated by reversible redox events. Oxidoreductases, like Glutaredoxins (Grxs), control various important signaling pathways via regulation of the protein thiol redox state. Dysregulation of redox signaling is correlated with numerous pathologies, including cancer, (neuro-) inflammation and degenerative disorders. It seems that expression of neuron-glial antigen 2 (NG2) plays a crucial role in most of these diseases, contributing to the maintenance and differentiation of progenitor cell populations as well as proliferation and migration. The aims of this study are, to investigate the effect of Grx2c on migration and differentiation of oligodendrocytes as well as proliferation and migration of cells in diseases like glioblastoma, melanoma and endometriosis and further to examine the molecular mechanism of NG2 regulation via Grx2.

Our findings demonstrate that Grx2c is upregulated during early differentiation of oligodendrocyte precursor cells (OPCs) and down regulated in later stages of differentiation. Treatment with recombinant Grx2c protein blocked differentiation of $NG2^+$-cells, resulting in an increased amount of $NG2^+$-cells, while the amount of more mature cells was decreased. The opposite effect was shown after Grx2 knock-down by siRNA and even more pronounced in OPCs generated from Grx2 knock-out mice. Further, these Grx2 knock-out mice showed a loss of visual function. In addition, our results demonstrated that increased levels of Grx2c promote migration of OPCs. The opposite effect was shown after Grx2 knock-down by siRNA. We were also able to show these effects in the zebrafish model, where decreased Grx2 amount also led to a decreased amount of migrated oligodendrocytes, while Grx2 overexpressing zebrafish displayed an increased number of migrated OPCs. Also in cancer cells, namely glioblastoma cells, we found that overexpression of Grx2 led to an increased amount of NG2, while Grx2 knock-down decreased NG2 expression. In this study we were able to show that Grx2c also promotes migration, invasion and metastasis of glioblastoma and melanoma cells. Also *in vivo* Grx2 knock-down decreased number and lengths of human glioblastoma tumor protrusions in zebrafish. In patient samples Grx2c expression correlated with NG2 expression. Our results further demonstrate that Sp1 is an interaction partner of Grx2. Via electrophoretic mobility shift assay (EMSA) we were able to demonstrate that Grx2 knock-down decreased Sp1 binding to

the NG2 promoter/enhancer in HeLa and glioblastoma cells. In addition, the Sp1 inhibitor Mithramycin A, abolished the Grx2c effect on migration.

In conclusion, we were able to show that Grx2c plays an essential role concerning differentiation of oligodendrocytes as well as dedifferentiation of cancer cells. In both cases Grx2 enhances binding of Sp1 to the NG2 promoter, acting as an activator of gene expression leading to an increase of NG2 protein level, which blocks differentiation and promotes migration as well as invasion of cells. We hypothesize Grx2c to be a helpful tool as a diagnostic marker as well as a promising therapeutic target in the future.

2   Zusammenfassung

Die Differenzierung und Dedifferenzierung von Zellen teilen viele gemeinsame Prozesse wie Proliferation, Migration, Reorganisation des Cytoskeletts sowie Angiogenese. In den letzten Jahrzehnten hat sich Redox-Regulation als ein zentraler Mechanismus verschiedener Zellsignalwege herausgestellt und es hat sich gezeigt, dass Zellen sowohl unter physiologischen als auch pathologischen Bedingungen eine empfindliche Redox-Balance benötigen. Viele essentielle zelluläre Funktionen wie Proliferation, Differenzierung und Apoptose werden durch reversible Redox-Ereignisse reguliert. Zum Beispiel kontrollieren Oxidoreduktasen, wie Glutaredoxine (Grxs), verschiedene wichtige Signalwege über die Regulation des Protein-Thiol-Redoxstatus. Auf der anderen Seite ist eine Disregulation von Redox-Signaling mit einer Vielzahl von Krankheiten wie Krebs, (Neuro-)Inflammation und degenerativen Erkrankungen assoziiert. Es scheint so, als würde auch das neuronale-gliale Antigen 2 (NG2) in den meisten dieser Erkrankungen eine zentrale Rolle spielen, da es zur Erhaltung und Differenzierung von Vorläuferzell-Populationen sowie zur Proliferation und Migration von Zellen beiträgt. Die Ziele dieser Arbeit sind es, den Effekt von Grx2c auf die Migration und Differenzierung von Oligodendrozyten sowie die Proliferation und Migration von Zellen in verschiedenen Krankheiten wie Glioblastoma, Melanoma und Endometriose zu untersuchen, sowie den molekularen Mechanismus der NG2-Regulation durch Grx2 zu erforschen.

Unsere Ergebnisse demonstrieren, dass Grx2c während der frühen Differenzierung von Oligodendrozyten-Vorläuferzellen (OPCs) hochreguliert und in späteren Stadien der Differenzierung runterreguliert ist. Eine Behandlung mit rekombinantem Grx2c-Protein blockierte die Differenzierung von NG2$^+$-Zellen, was zu einer erhöhten Anzahl an NG2$^+$-Zellen führte, während die Anzahl an differenzierten Zellen abnahm. Den gegenteiligen Effekt zeigte ein Grx2 „knockdown" mittels siRNA, welcher noch ausgeprägter in OPCs war, welche aus Grx2 „knockout" Mäusen generiert wurden. Zusätzlich zeigten die Grx2 „knock-out" Mäuse einen Verlust ihrer visuellen

Funktion. Unsere Ergebnisse zeigen außerdem, dass ein erhöhtes Grx2c-Level die Migration von OPCs fördert. Den gegenteiligen Effekt zeigte ein Grx2 „knockdown" mittels siRNA. Des Weiteren konnten wir diesen Effekt in einem Zebrafisch-Modell zeigen, wo ein Grx2 „knockdown" ebenfalls zu einer reduzierten Anzahl an migrierenden Oligodendrozyten führte, während Grx2 überexprimierende Fische eine erhöhte Anzahl an migrierenden OPCs aufwiesen. Auch in Krebszellen, genauer Glioblastomazellen, führte eine Überexpression an Grx2 zu einem Anstieg an NG2, während ein Grx2 „knockdown" die NG2-Expression verringerte. Zudem zeigt diese Studie, dass Grx2c auch die Migration, Invasion und Metastasierung von Glioblastoma- und Melanomazellen fördert. Auch *in vivo* reduzierte ein Grx2 „knockdown" die Anzahl und Länge von humanen Glioblastoma-Tumor-Auswüchsen im Zebrafisch. Ferner korrelierte die Grx2c-Expression mit der NG2-Expression in Patientenproben. Unsere Ergebnisse zeigen überdies, dass Sp1 ein Interaktionspartner von Grx2 ist. Durch Electrophoretic Mobility Shift Assays (EMSA) waren wir in der Lage zu zeigen, dass ein Grx2 „knockdown" in HeLa- und Glioblastomazellen die Bindung von Sp1 an den NG2-Promoter/Enhancer verringert. Zusätzlich verhinderte der Sp1-Inhibitor Mithramycin A den Effekt von Grx2 auf die Migration.

Zusammenfassend konnten wir in dieser Studie zeigen, dass Grx2c sowohl eine essentielle Rolle in Bezug auf die Differenzierung von Oligodendrozyten als auch die Dedifferenzierung von Krebszellen spielt. In beiden Fällen fördert Grx2 als Aktivator der Genexpression die Bindung von Sp1 an den NG2-Promoter, was zu einem Anstieg an NG2-Protein führt, welches wiederum die Differenzierung, Migration sowie Invasion von Zellen fördert. Wir nehmen an, dass Grx2c in der Zukunft sowohl ein hilfreicher diagnostischer Marker als auch ein vielversprechendes therapeutisches Target sein wird.

3 Introduction

3.1 Redox regulation and Glutaredoxin 2 (Grx2)

Reactive oxygen species (ROS) and reactive nitrogen species (RNS), like superoxide ($O_2 \cdot -$), hydroxyl- and nitric oxide-radicals (OH·; NO·) as well as hydrogen peroxide (H_2O_2) and peroxynitrite ($ONOO^-$) are generated throughout our whole lives (Hybertson et al., 2011). The pathological production of ROS and RNS causing damage is known as oxidative stress. Describing the imbalance between cellular pro- and antioxidant systems the term "oxidative stress" was introduced in 1985 by Sies and Cadenas (Sies and Cadenas, 1985). Due to the caused oxidative damage to proteins, lipids and DNA, accumulation of ROS and RNS can be harmful (Hybertson et al., 2011). However, during the last decade the importance of reactive species has shifted from an entirely disadvantageous view towards the function of ROS and RNS as signaling molecules under physiological conditions, where they act as specific second messengers (Jones and Sies, 2015). Therefore redox regulation has emerged as one of the central mechanisms in cellular signaling (Hanschmann et al., 2013a). Lipids, nucleic acids and proteins can be redox modified (Brigelius-Flohé and Flohé, 2011; Schafer and Buettner, 2001). It has been demonstrated that local changes in the redox state at certain time points lead to specific reversible oxidative modifications of key proteins (Hanschmann et al., 2013a). Proteins are very sensitive to oxidative modifications due to their thiol groups (-SH), the functional group of the amino acid cysteine. These oxidative modifications can regulate protein activity, structure, subcellular distribution and interactions with substrates and thereby affect a protein's functions (Berndt et al., 2014; Lillig and Berndt, 2013). The reactive thiol group can be reversibly or irreversibly posttranslational modified by the formation of disulfide bridges, glutathionylation, nitrosylation, formation of sulfenic acid and latter sulfinic and sulfonic acid and the coordination of metal clusters (Fig. 1) (Hanschmann et al., 2013a). It has been shown, that essential cellular functions like proliferation (Zhang et al., 2008), differentiation (Gellert et al., 2013) and apoptosis (Enoksson et al., 2005) are regulated by reversible redox events. Furthermore, dysregulation of redox signaling and an increased formation of ROS and RNS are correlated with numerous pathologies, including cancer, (neuro-)inflammation, cardiovascular- and degenerative disorders (Hanschmann et al., 2013a).
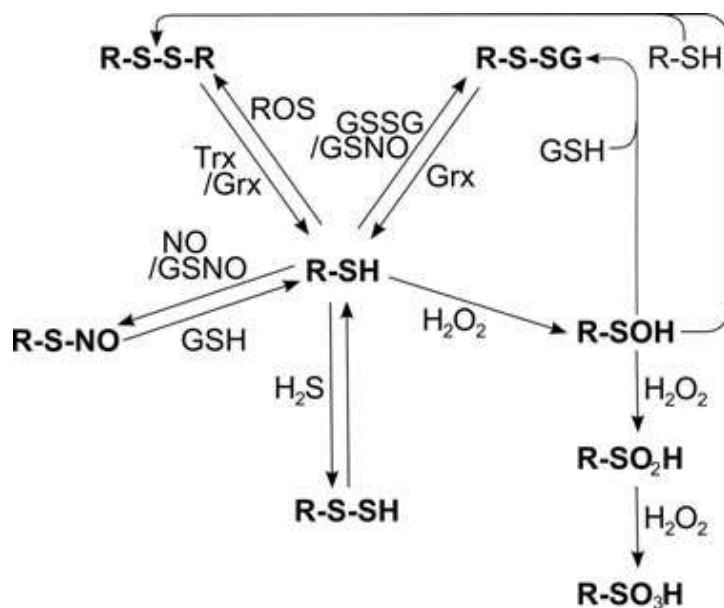
Figure 1: Redox modifications at cysteinyl residues. Free thiol groups (R-SH) can be reversibly modified by ROS, leading to the formation of protein disulfides (R-S-S-R), which can be reduced by the Trx and Grx systems. Thiols can also be glutathionylated (R-S-SG) by oxidized glutathione (GSSG) or S-nitroso glutathione (GSNO). The de-glutathionylation is exclusively catalyzed by Grxs. Furthermore, GSNO can lead to the nitrosylation of cysteinyl residues, which can be reversed by GSH or transferred to other thiols. Another modification, induced by peroxides, is the formation of sulfenic acid (R-SOH). In the presence of another free thiol, it can be modified to a protein disulfide. However, in the presence of excessive peroxides, it can be irreversibly over-oxidized to sulfinic (R-SO2H) and sulfonic acid (R-SO3H). (Hanschmann et al., 2013a)

Those oxidative modifications can be reversed by proteins of the thioredoxin (Trx) family. The Trx family proteins constitute key players in maintaining cellular redox homeostasis and redox signaling (Lillig et al., 2008). Apart from the name giving Trxs the family of proteins includes glutathione peroxidases (GPxs), glutaredoxins (Grxs), protein disulfide isomerases (PDIs) and Peroxiredoxins (Prxs), sharing the Trx fold as well as the oxidoreductase activity (Hanschmann et al., 2013a). The Trx fold consist of a central core of four- to five-stranded β-sheets surrounded by three to four α-helices, and the conserved active site motif Cys-X-X-Cys, which is crucial for the transfer of electrons (Hanschmann et al., 2013a). GPxs and Prxs as peroxidases are known to catalyze the reduction of H_2O_2 to water and oxygen. Mammalian cells contain six Prx isoforms that are located in different cellular compartments (Hanschmann et al., 2013b). The GPx family of proteins is the largest group in vertebrates containing selenoproteins. Five out of the eight members in human incorporate the 21st amino acid selenocysteine (Sec) instead of the functional analog cysteine (Cys) in their catalytic site (Buday and Conrad, 2021).

Grxs are small, glutathione (GSH)-dependent oxidoreductases and part of the Trx-family of proteins (Lillig and Berndt, 2013). First discovered as electron donor for ribonucleotide reductase, Grxs are ubiquitously expressed in all organisms (Lönn et al., 2008). Depending on the number of active site cysteine residues, Grxs are divided into dithiol (Cys-X-X-Cys) and monothiol (Cys-X-X-Ser) Grxs. The latter group is further subdivided into single and multi-domain monothiol Grxs (Hanschmann et al., 2013a). So far, four Grxs have been discovered in mammals: the dithiol Grxs 1 and 2 and the monothiol Grxs 3 and 5 (Lillig and Berndt, 2013). While dithiol Grxs take part in reduction of

disulfides and glutathionylated thiols, monothiol Grxs play a role in iron homeostasis and biosynthesis of iron sulfur (FeS) clusters (Lillig and Berndt, 2013).

Grx2 has a molecular mass of 14 kDa and is characterized as vertebrate specific oxidoreductase by two conserved additional cysteine residues forming an intramolecular disulfide (Hanschmann et al., 2013a). Its active site motif (Cys-Ser-Tyr-Cys) enables Grx2 to fulfill dithiol reaction mechanisms, to be reduced by GSH (Fig. 2) and also by thioredoxin reductase (TrxR) and to coordinate an FeS cluster (Berndt and Lillig, 2017; Lillig et al., 2005).
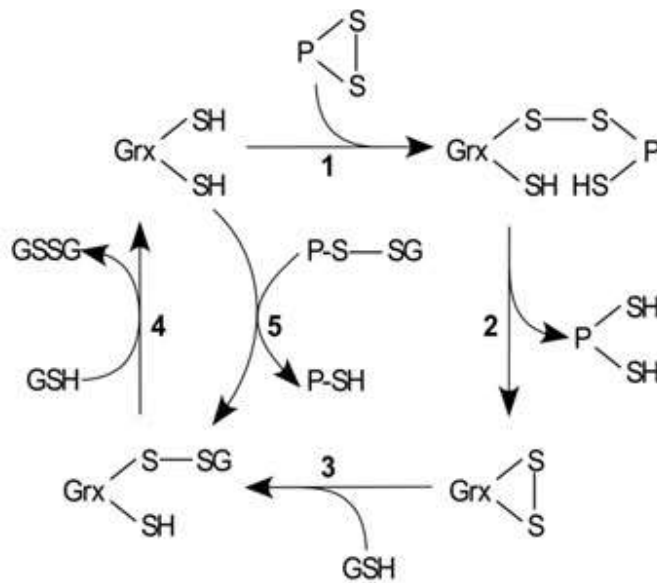
Figure 2: Reaction mechanisms of Grxs. Grxs reduce protein disulfides via the dithiol mechanism and are reduced by two GSH molecules (1–4). In addition, they reduce glutathionylated proteins via the monothiol mechanism (5–4), only depending on the N-terminal active site Cys that attacks the GSH moiety and forms a GSH-mixed disulfide intermediate (5), which is reduced by another GSH molecule (4). (Hanschmann et al., 2013a)

In humans the gene for glutaredoxin 2 (GLRX2) gives rise to different isoforms through alternative splicing: the mitochondrial variant Grx2a, which is also present in mice, and the cytosolic/nuclear isoforms Grx2b and Grx2c in humans and Grx2c and Grx2d in mice (Hudemann et al., 2009; Lönn et al., 2008). Until now the specific function of Grx2d has not been investigated. Grx2a and Grx2c differ only in their localization. Cleavage of the mitochondrial translocation motif of Grx2a results in an identical protein constitution of Grx2a and Grx2c (Lundberg et al., 2004). In adult humans Grx2a is ubiquitously expressed in all tissues, while Grx2b and Grx2c expression is limited to spermatogenic and cancer cells (Lönn et al., 2008). In mice Grx2a and Grx2c are conserved and expressed ubiquitously. Even other vertebrate species, like zebrafish, contain genes that encode homologues to cytosolic Grx2c (Bräutigam et al., 2011). Different studies indicate a participation of Grx2 in different processes. For example the susceptibility to apoptosis by preventing cytochrome c release (Enoksson et al., 2005), a regulatory function in vascular and brain development (Bräutigam et al., 2013, 2011) as well as participation in axon formation by regulation of the thiol redox state of the collapsing response mediator protein 2 (CRMP2) (Bräutigam et al., 2011).

3.2 Redox regulation in differentiation

3.2.1 Oligodendrocytes

Oligodendrocytes are one type of glial cells of the CNS, forming the structures of myelin for rapid saltatory conduction (Mirsky and Jessen, 1996). Oligodendrocyte precursor cells (OPCs) represent a major proliferative population in the adult CNS of mammals and approximately 5–8 % of the cells in the brain are OPCs (Lopez Juarez et al., 2016). Since their first identification in the early 80s (Raff et al., 1983), OPCs have been always described as an abundant glial population widely distributed in the mammalian CNS throughout the cerebellar white matter, granular and molecular layers at postnatal and adult ages (Buffo and Rossi, 2013; Viganò and Dimou, 2016).

During embryonic development, oligodendrocytes arise from neuroectodermal stem cells that also generate neurons and astrocytes (Bradl and Lassmann, 2010). OPCs arise in three different populations, which are functionally redundant to guarantee a normal complement of oligodendrocytes and myelin production. The first wave of OPCs originates in the medial ganglionic eminence and anterior entopeduncular area of the ventral forebrain, populating the entire embryonic telencephalon including the cerebral cortex. The second wave of OPCs derives from the lateral and caudal ganglionic eminences, while the finally third wave of OPCs arises within the postnatal cortex (Bradl and Lassmann, 2010). To produce the insulating sheath of axons they have to undergo a complex and precisely timed program of proliferation, migration, differentiation and myelination (Bradl and Lassmann, 2010). From their site of origin oligodendrocytes have to migrate to their final site of function before acquiring their myelinating phenotype during terminal differentiation (Bradl and Lassmann, 2010). These processes require coordinated changes in gene expression that are induced by defined stimuli from the environment. These stimuli include paracrine and juxtacrine signaling molecules like platelet-derived growth factor (PDGF), fibroblast growth factor (FGF), bone-morphogenetic proteins, Wnt molecules, neuregulins, notch ligands, hormones and neurotransmitters. One important source of these signaling molecules are axons, which additionally influence myelination process by their adhesive properties and electrical activity (Sock and Wegner, 2019). Migration of OPCs is tightly controlled by secreted growth factors (PDGF, FGF, hepatocyte growth factor), chemotropic molecules (netrins, semaphorins) and chemokines (CXCL1). The exact mode of action of these factors is still a matter of controversy. OPC migration is regulated by contact-mediated mechanisms involving different extracellular matrix proteins, cell surface molecules and N-cadherins (Bradl and Lassmann, 2010). Once migrated to their final destination, some OPCs persist into adulthood, but the majority differentiates into myelin-producing oligodendrocytes (Bradl and Lassmann, 2010). Differentiation of oligodendrocytes from their progenitors follows a stepwise

morphological transformation from bipolar progenitors to immature pro-oligodendrocytes, mature oligodendrocytes and myelinating oligodendrocytes. This morphological change goes along with the sequential expression of molecular markers characteristic for the differentiation state. A2B5 antigen, platelet-derived growth factor receptor-α (PDGFRα) and chondroitin sulphate proteoglycan NG2 in progenitors, 2',3'-cyclic nucleotide 3'-phosphodiesterase (CNPase) in mature oligodendrocytes as well as myelin basic protein (MBP) and proteolipid protein (PLP) in further developed oligodendrocytes (Fig. 3) (Zhang, 2001).
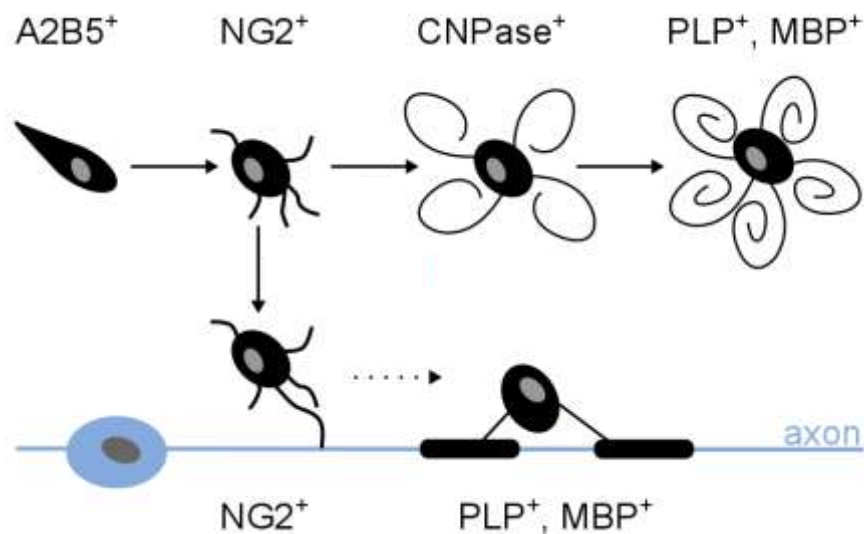
Figure 3: Morphological and antigenic markers for oligodendroglia during development. The differentiation of oligodendrocytes from their progenitors follows a stepwise morphological transformation from bipolar progenitors to immature pro-oligodendrocytes, mature oligodendrocytes and myelinating oligodendrocytes. This morphological change goes along with the sequential expression of molecular markers characteristic for the differentiation state. A2B5 antigen, platelet-derived growth factor receptor- (PDGFRα) and chondroitin sulphate proteoglycan NG2 in progenitors, 2',3'-cyclic nucleotide 3'-phosphodiesterase (CNPase) in mature oligodendrocytes and myelin basic protein (MBP) and proteolipid protein (PLP) in further developed oligodendrocytes. NG2 expressing progenitors are the migrating cells in this stepwise transformation, which are capable to get in contact with axons and start myelination.

Due to their unique metabolism and the very complex processes of differentiation, myelination and maintenance of myelin sheaths oligodendrocytes count among the most vulnerable cells of the CNS. Further disturbance of these processes is associated with major diseases of the CNS (Bradl and Lassmann, 2010). Oligodendrocytes are particularly vulnerable to oxidative damage, which is a common contributor to myelin damage in diseases like multiple sclerosis (MS) and ischemia (Bradl and Lassmann, 2010). This is due to the high metabolic rate of oligodendrocytes with toxic byproducts like hydrogen peroxide, the high intracellular iron concentration, which can evoke free radical formation and lipid peroxidation as well as the low concentrations of the antioxidative glutathione (Juurlink, 1997; Thorburne and Juurlink, 1996). Moreover, the intracellular redox state in oligodendrocytes regulates the balance between progenitor cell division and differentiation. It

seems, that cells that are slightly more reduced showed increased proliferation, while cells that are slightly more oxidized show a greater response to inducers of differentiation (Noble et al., 2005). Furthermore, it was shown, that myelin gene expression of mature oligodendrocytes is redox-sensitive (Jana and Pahan, 2005). ROS and RNS also contribute to adult neural cell fate decision and neural stem cell maintenance. In a concentration-dependent manner reactive species either maintain neural stem cell population or induce differentiation (Yuan et al., 2015). Moreover, exposure to NO shifts the cell fate of neural progenitors from neurogenesis to astrogliosis (Covacu et al., 2006). The essential signaling molecule H_2O_2 mediates self-renewal and therefore maintains neural stem population in the brain (Dickinson et al., 2011; Le Belle et al., 2011). Here, H_2O_2-dependent up-regulation of the deacetylase Sirt2 increased neural progenitor proliferation and generation of both neurons and oligodendrocytes (Pérez Estrada et al., 2014). Taken together these findings highlight the importance of redox regulation in cell fate decision.

3.3   Oligodendrocyte damage

3.3.1 Neuroinflammation and Multiple sclerosis

Neuroinflammation in the CNS is characterized by increased production of chemokines and cytokines, influx of leukocytes, activation of microglia and astroglia and an altered integrity of the blood-brain-barrier (Lepka et al., 2016). Diseases that result in demyelination in the CNS are major causes of neurological mortality and are among the most disabling and cost-intensive neurological disorders (Lopez Juarez et al., 2016). Multiple sclerosis (MS) is the prototype for an autoimmune inflammatory and degenerative disorder of the CNS. It is characterized by infiltration of immune cells, as well as myelin and axonal damage, resulting in impaired axonal conduction and neurological dysfunctions (Dimou and Gallo, 2015; Lopez Juarez et al., 2016; Trapp and Nave, 2008). Majority of patients show disease onset between 20 and 40. Symptoms are diverse but the most frequent ones are visual disturbances, paresthesias, ataxia and muscle weakness (Ellwardt and Zipp, 2014). Until now, MS is not curable and therapeutic approaches aim at the suppression of immune attacks, but fail to address repair of damaged brain and spinal cord areas. (Lepka et al., 2016). The etiology of MS is not known to this date but there are hypotheses addressing both environmental and genetic factors (Trapp and Nave, 2008). These suggested MS-specific genes and risk genes, like *HLA-DRB1,* code for cytokine pathways, signaling molecules of immunological relevance and environmental MS risk factors like vitamin D dependent metabolism (Sawcer et al., 2011). However, the molecular mechanisms concerning the specific immune reactivity towards myelin and oligodendrocytes are still unclear (Hohlfeld et al., 2016).

Myelin damage is characteristic for MS. In chronic MS, demyelination and disturbed remyelination lead to lesion areas and subsequently to neuronal cell loss responsible for neurological dysfunctions (Franklin and Blakemore, 1997; Lopez Juarez et al., 2016). Regeneration after damage or CNS demyelination is accomplished by OPCs proliferation, migration and differentiation (Adams et al., 1989). Although neural stem cells are able to produce oligodendrocytes in the adult brain, their capacity to replenish oligodendrocytes and thus the capacity for remyelination is limited (Chari, 2007; Franklin and Ffrench-Constant, 2008; Lopez Juarez et al., 2016). While in early stages of MS remyelination may occur, regeneration is severely compromised with progression of the disease (Kremer et al., 2016). However, remyelination is never complete and the newly formed myelin is thinner, less compacted and with shorter internodes (Dimou and Gallo, 2015). However, in the peripheral nervous system (PNS) remyelination is a quick and efficient process. After demyelination of the PNS Schwann cells, the myelinating cells of the PNS, proliferate, migrate and contribute to regeneration (Arthur-Farraj et al., 2012). In the CNS altered migration capacities of OPCs into demyelinated lesion areas are the major cause for disturbed myelin regeneration (Franklin and Blakemore, 1997). OPC proliferation, migration and differentiation in lesion areas are crucial steps for functional remyelination and repair of destroyed myelin by treating demyelinating diseases in the CNS by enhancing the production of oligodendrocytes and their precursors has become an area of major interest in MS research (Kocsis and Waxman, 2007; Lopez Juarez et al., 2016). One reason for failed CNS remyelination could be the accumulation of factors like chemokines, cytokines, growth factors, reactive species and semaphorins, that are characteristic for MS lesions and reduce regeneration (Costa et al., 2015; Kremer et al., 2016; Robinson and Miller, 1999). Also the inhibition of OPC recruitment and extensive OPCs cell death are discussed as possible reasons, as well as a possible misregulation in the process of differentiation (Rudick et al., 2008). Moreover, neuroinflammation has been linked to other neurodegenerative disorders like Alzheimer's and Parkinson's disease concerning the mechanisms of disease as well as clinical outcomes (Amor et al., 2010).

Over the last two decades ROS and RNS have attracted increasing interest and oxidative stress is considered as a major contributor to neuroinflammatory diseases including MS (Aktas et al., 2007; Greco et al., 1999; Koch et al., 2006; van Horssen et al., 2011). It has been shown, that nitrotyrosine (Pacher et al., 2007) as well as iron accumulations in lesion areas promote oxidative damage of proteins, lipids and nucleotides (Hametner et al., 2013). So far, there is not much known about the role of oxidoreductases or other antioxidant enzymes during MS (Lepka et al., 2016). It has been shown, that oxidoreductases are important during inflammatory processes like activation of

macrophages (Salzano et al., 2014). Furthermore, it has been investigated, that activity of GPx is decreased in cerebrospinal fluid and in serum of MS patients (Calabrese et al., 1994; Socha et al., 2014). In contrast Prx5, Trx2 and Prx3 are upregulated in MS lesions (Holley et al., 2007; Nijland et al., 2014). Furthermore, it was shown that in active lesion areas of human MS brain tissue Grx2, Grx3 and Grx5 were enriched (Lepka, 2017). In line, brain lesions in the cerebellum of mice suffering from experimental autoimmune encephalomyelitis (EAE), an animal model of multiple sclerosis, showed increased expression of Grx2 in the disease peak, but downregulated expression in chronic disease phase (Lepka, 2017). Moreover, spinal cord of EAE mice displayed increased Prx6 levels. The identification of oxidants and antioxidants involved in disease processes also brought up the idea of treatment with antioxidants, but the majority of clinical studies failed. This failure might be due to negation of the role of specific ROS as important second messengers in cellular signaling (Lepka et al., 2016). Therefore, instead of unspecific application of ROS scavengers, therapies aiming at specific enzyme-based thiol redox modulations might be more promising. For example Collapsin response mediator protein 2 (CRMP2), which is redox regulated was proposed as a potential novel drug target for axonal regeneration after neuroinflammation (Bräutigam et al., 2011; Petratos et al., 2010).

3.4 Redox regulation in dedifferentiation

3.4.1 Cancer

The World Health Organization defines cancer as "a large group of diseases that can start in almost any organ or tissue of the body when abnormal cells grow uncontrollably, go beyond their usual boundaries to invade adjoining parts of the body and/or spread to other organs". With 9.8 million deaths, or one in sixth deaths, in 2018 cancer is the second leading cause of death globally and the cancer rates are increasing. In men the most common types of cancer are lung, prostate, colorectal, stomach and liver cancer. In women breast, colorectal, lung, cervical and thyroid cancer are most frequent (https://www.who.int/health-topics/cancer#tab=tab_1).

In this study we will focus on glioblastoma and melanoma. Glioblastoma (GBM) is the most common and malignant brain tumor in adults (Svendsen et al., 2011). These tumors are characterized by high intra- and intertumor heterogeneity, diffuse brain infiltration, necrosis and high rate of cell proliferation (Salazar-Ramiro et al., 2016). Glioblastoma multiforme has two origins: 90–95% of all GBMs are tumors arising *de novo*, called primary GBM. Usually they are diagnosed between the sixth and seventh decade of life. 5-10% are secondary GBMs, arising from lower grade tumors through several genetic mutations. Usually they are diagnosed around the fourth decade of life

(Salazar-Ramiro et al., 2016). Prognosis for GBM is poor and never considered curable. The survival for untreated tumors is about 5 months and even the best current available therapy, including surgery, chemotherapy and radiotherapy, can expand survival only to 14 months, due to the tumor's intrinsic resistance to radio- and chemotherapy (Salazar-Ramiro et al., 2016; Svendsen et al., 2011). Even after treatment with the most widely used chemotherapeutic agent temozolomide (TMZ) approximately 90% of the patients suffered from disease recurrence within two years of treatment (Chang et al., 2017). Also malignant melanoma is one of the most aggressive cancers, which also shows a high frequency of metastases (Obrador et al., 2019). Cutaneous melanoma arises from epidermal melanocytes and is therefore predominantly a disease of the skin but it may also occur on mucous membranes and the eyes (Obrador et al., 2019). In contrast to many other tumor types showing a decreasing incidence in the 21st century, melanoma incidence continues to increase. Nowadays the average lifetime risk for melanoma has reached 1 in 50 in many Western populations (Rastrelli et al., 2014). Melanoma mostly affects young and middle-aged people. The median age at the time of diagnosis is 57 years (Rastrelli et al., 2014). Early detection of malignant melanoma is essential for lowering mortality, because prognosis in melanoma is directly proportionate to the depth of the neoplasm, which increases over time (Rastrelli et al., 2014). Melanoma is considered as a multi-factorial disease arising from genetic susceptibility and environmental exposure, especially the exposure to genotoxic UV rays (Rastrelli et al., 2014).

It is also well known that UV radiation causes oxidative stress and there is strong evidence that melanoma cells display increased ROS levels (Obrador et al., 2019). Also in GBM a cellular redox imbalance has been found, showing high basal levels of ROS (Salazar-Ramiro et al., 2016). Recent studies showed that this is due to an increased basal metabolic activity, mitochondrial dysfunction, hypoxia or mitophagy, peroxisomal activity, uncontrolled growth factors of cytokine signaling, oncogene activity, as well as enhanced activity of known ROS sources like NADPH oxidase, cyclooxygenases or lipoxygenases (Salazar-Ramiro et al., 2016). Redox systems play important roles in the control of growth, apoptosis, angiogenesis and drug resistance of cancer cells (Mollbrink et al., 2014). Deactivation of tumor suppressor genes, oncogene expression and mutations in mitochondrial DNA are ROS-regulated mechanisms, which can again regulate tumorigenic ROS production (Idelchik et al., 2017). Higher ROS levels can induce apoptosis or necroptosis in cancer cells, showing that cancer cells need a delicate redox balance in terms of cellular growth and proliferation such as healthy cells (Idelchik et al., 2017). Several studies displayed an increased expression of Trx1, Trx2, Grx2, Grx3 and Grx5 in various cancer types correlating with a worse prognosis for patients (Fernandes et al., 2009; Mollbrink et al., 2014). It is not known which event is the first trigger for

gliomagenesis, whether if it's a DNA alteration as result of an imbalance of redox homeostasis or if the imbalance in the redox state involves alterations in key genes. However, also chronic inflammation is critical for tumor development in various tissues and it is postulated, that some tumors may arise from chronic inflammation. In melanoma tumor tissues oxidative stress and inflammation markers are frequently much higher than in the surrounding control tissue or even non-melanoma skin cancer and high nitrotyrosine levels are associated with poor survival of melanoma patients (Obrador et al., 2019). Furthermore, inflammation is also linked to redox modulation (Salazar-Ramiro et al., 2016). For example monocyte infiltrations into GBM result in a proinflammatory microenvironment leading to alterations in redox homeostasis (Feng et al., 2015). During the inflammatory process TNF-α, a cytokine, is released leading to activation of pro- and anti-apoptotic pathways. In GBM TNF-α increases ROS production and activates the PI3K/Akt pathway, which is involved in regulation of cell growth and apoptosis resistance. Akt plays a role in cytoskeletal reorganization promoting invasion and migration of GBM cells. Phosphorylation of Akt is redox state-dependent (Radeff-Huang et al., 2007; Salazar-Ramiro et al., 2016). The redox balance in the tumor environment is also affected by other alterations. Primary GBMs show amplification in epidermal growth factor receptor (EGFR), PTEN mutation and loss of chromosome 10 (Reardon et al., 2015). In cancer cell lines ligation of EGFR by EGF induces endogenous production of ROS. This leads to further activation of several intracellular signal pathways, such as phosphatidylinositol 3′ kinase (PI3K)/Akt and Ras/mitogen-activated protein kinase (MAPK), leading to increased DNA synthesis (Bae et al., 1997). Besides, the chronic amounts of H_2O_2 are high enough to induce DNA damage. Acting as a second messenger inducing several pathways H_2O_2 increases the expression of antioxidant enzymes protecting malignant cells from apoptosis induction (Salazar-Ramiro et al., 2016). Also in melanocytes the generation of melanin leads to the generation of H_2O_2 and the consumption of reduced glutathione (GSH) (Obrador et al., 2019). Secondary GBMs often display mutations in tumor protein p53 (Reardon et al., 2015). P53 is a protein involved in regulation of energetic metabolism and expression of genes that are involved in redox regulation, for example mitochondrial superoxide dismutase 2 (SOD2) (Hussain et al., 2004) or glutathione peroxidase 1 (GPX1) (Salazar-Ramiro et al., 2016; Tan et al., 1999). Patients with Germline mutations in *TP53* display more damages upon oxidative stress (Macedo et al., 2012). Inactivation of p53 enables tumor cells to escape apoptosis inhibiting the therapeutic effects of radio- and chemotherapy. Due to the important role of the redox environment in initiation, progression and regression of tumor cells new redox therapies have been investigated over the last years. Until now redox therapies failed to cure glioblastoma. However, most of these therapies give insights about the involved mechanism and therefore enables the discovery of new cancer-specific therapies (Salazar-Ramiro et al., 2016).

3.4.2 Endometriosis

Endometriosis is a chronic, estrogen-dependent gynaecological disease, characterized by the implantation and growth of endometrial tissue (glands and stroma) outside of the uterine cavity (Attar and Bulun, 2006; Choi et al., 2015). This tissue can be subdivided into ovarian endometriomas, small peritoneal lesions or deep infiltrating lesions, which are often rectovaginal or gut lesions. In some cases endometriosis was also found in the lung, lymph nodes or pancreas (Zeitvogel et al., 2001). Endometriosis is often associated with pelvic pain and infertility as well as dyspareunia and dysmenorrhea (Attar and Bulun, 2006; Bruner-Tran et al., 2018). Affecting 10-15% of women of reproductive age it is a common disorder (Scutiero et al., 2017).

Although the etiology is still unclear there are three main theories for the establishment of endometriosis: retrograde menstruation, coelomic metaplasia and induction theory (Scutiero et al., 2017). Origin of endometric lesions also depends on the type of tissue that is affected, but the most accepted theory at the moment is, that viable endometrial cells are transported to the peritoneal cavity by retrograde menstruation. Here these cells adhere to the peritoneal wall, proliferate and form lesions (Zeitvogel et al., 2001). However, since retrograde menstruation is a common process among women in reproductive age, but only 10-15% of women develop endometriosis, other mechanisms seems to be involved. The induction theory, meaning the peritoneal activation of embryonic cell rests, could explain the unusual and rare occurrence of endometriosis in men and children (Bruner-Tran et al., 2018). Recently, ectopic endometrial tissue has been described in human fetuses. It was suggested that it developed as a consequence of ectopic localization of primitive endometrial tissue during organogenesis (Bruner-Tran et al., 2018). In addition, genetics and epigenetics as well as immune dysregulation and environmental toxicant exposure seem to affect an individual's risk for developing endometriosis (Bruner-Tran et al., 2018; Scutiero et al., 2017).

Recent studies have put attention on the role of oxidative stress in the initiation and progression of endometriosis, causing a general inflammatory response in the peritoneal cavity (Chen et al., 2019; Scutiero et al., 2017). In patients with endometriosis, markers of oxidative stress are significantly increased in peritoneal fluid, follicular fluid and peripheral circulating blood (Chen et al., 2019; Lambrinoudaki et al., 2009). Here, oxidative stress positively correlates with the proliferation and migration of endometrial cells in the peritoneal cavity, promoting endometriosis and infertility (Chen et al., 2019; Scutiero et al., 2017). Although endometriosis is considered as a benign disorder it shares some features with cancer, like invasion, proliferation and migration (Chen et al., 2019). In endometriotic and in tumor cells, the increased production of ROS is associated with an increase in

the proliferation rate (Scutiero et al., 2017). Furthermore, endometriosis is associated with inflammatory changes in the intrafollicular microenvironment. Here, levels of inflammatory cytokines, such as interleukin 6, IL1b and TNFα are increased in the follicular fluid of patients with endometriosis. These pro-inflammatory cytokines increase the levels of ROS inducing oxidative modifications of cellular macromolecules (Choi et al., 2015). In infertile patients with endometriosis additionally changes in the thiol–redox system were found (Choi et al., 2015). Here, GSH levels were significantly reduced, while TBP2 levels were increased compared to women without endometriosis (Choi et al., 2015). TBP2 was found as an interaction partner for Trx. It binds to the active site of Trx, inhibiting its disulfide reductase activity and therefore works as an endogenous Trx inhibitor (Hanschmann et al., 2013a).

Until now treatment options for women with endometriosis remain limited and involve a combination of hormonal manipulation and surgery to remove endometrial tissue. Surgical treatment alone is frequently non-curative due to the high risk of recurrence, but hormonal therapy for endometriosis shows many side effects. Therefore, current endometriosis research focuses on the identification of better diagnostic and treatment strategies (Bruner-Tran et al., 2018).

3.5 Neuron-glia protein 2 (NG2) in differentiation and dedifferentiation

Neuron-glial antigen 2 (NG2) in mouse and rat or chondroitin sulphate proteoglycan 4 (CSPG4) in human belong to the protein family of chondroitin sulphate proteoglycans (Schiffer et al., 2018). NG2 and CSPG4 are highly conserved through phylogenetic evolution (Price et al., 2011). Homologues in rat and mouse share 90% amino acid identity with each other and over 80% with the human sequence (Schiffer et al., 2018). The NG2/CSPG4 proteoglycan is encoded by the *NG2/CSPG4* gene and display some structural features that make it unique in the proteoglycan family (Schiffer et al., 2018). NG2 is a cell surface type I transmembrane protein, which consists of a core protein and a 450 kDa proteoglycan (Ampofo et al., 2017; Price et al., 2011; Schiffer et al., 2018). The NG2 core protein consists of three main structural domains: a large extracellular domain with 2.225 amino acids (290 kDa), which can be released into the extracellular matrix, a 25-amino acid transmembrane region (12 kDa), and a short cytoplasmic tail of 76 amino acids (8.5 kDa) (Price et al., 2011; Schiffer et al., 2018). The full-length NG2 protein is sequentially cleaved into the mentioned domains by the α-secretase ADAM10 and the γ-secretase complex. The proteolytic cleavage is enhanced in several types of injuries, like spinal cord injuries, multiple sclerosis and tumors and the three domains are associated with different functions (Schiffer et al., 2018). The extracellular domain, still partially unknown, acts in regulation of neuronal networks with neuromodulatory properties or in endothelial

cell and pericyte function for example (Ampofo et al., 2017; Schiffer et al., 2018). The intracellular domain acts as an acceptor site for the extracellular signal-regulated kinases (ERK) 1/2 and protein kinase C-alpha (PKC-α). Both are involved in the regulation of proliferation, migration, invasion, cytoskeletal reorganization, survival, angiogenesis, chemoresistance and modulation of the neuronal network (Ampofo et al., 2017; Schiffer et al., 2018).

NG2/CSPG4 is highly expressed in more than ten different tissues or organs, like brain, gastrointestinal tract and endocrine organs and more than 50 cell types, including chondroblasts, osteoblasts, keratinocytes, smooth muscle cells and macrophages. However, the correlation between transcript and protein levels is poor in most of them and its expression seems to be limited to precursor or progenitor cells of epithelial and mesenchymal origin (Schiffer et al., 2018). Taken together it seems, that NG2 plays an important role in the maintenance and differentiation of progenitor cell populations in the development and homeostasis of various tissues (Price et al., 2011). Interestingly, embryonic deletion of this gene in mice is not lethal (Price et al., 2011).

In developing and adult CNS NG2 occurs as a marker of oligodendrocyte precursor cells together with PDGFRα (Schiffer et al., 2018). NG2 cells expressing PDGFRα make up 5% of the cells in mature brain and are regarded as a novel "fifth neural cell type" after neurons, oligodendrocytes, astrocytes and microglia. Known as oligodendrocyte precursor cells (OPCs) or NG2-glia, the majority of them are located in the white matter of the cerebral cortex. NG2-glia are cells with high proliferative capacity being able to differentiate into mature, myelinating oligodendrocytes (Schiffer et al., 2018). Maturation of NG2-glia is characterized by a down regulation of NG2 as well as PDGFRα (Schiffer et al., 2018). Further NG2-glia can also produce astrocytes, remain as NG2-glia or generate neurons *in vivo* (Schiffer et al., 2018; Trotter et al., 2010). NG2 contributes to many processes and functions via its heterogenic expression level. Mice lacking NG2 display defective vasculature. Furthermore, its expression in OPCs indicates a role for NG2 in tissue development and stem cell niche maintenance (Price et al., 2011; Schiffer et al., 2018). Moreover, NG2 induces cell proliferation and migration (Schiffer et al., 2018). In general, NG2-glia react to many types of injury or pathological conditions by changes in cell morphology, proliferation rate and scar formation with a strong potential to repopulate areas of lesion (Dimou and Gallo, 2015; Schiffer et al., 2018). After acute experimental demyelination, local NG2 cells quickly proliferate and generate myelinating oligodendrocytes (Nishiyama et al., 2016). NG2 cells also generate myelinating oligodendrocytes in the inflammatory model of demyelination, experimental autoimmune encephalomyelitis, by becoming hypertrophic and undergoing rapid proliferation, differentiation into myelinating oligodendrocytes and partially remyelinate naked axons (Dimou and Gallo, 2015; Nishiyama et al.,

2016). Furthermore, remyelination in the adult brain requires migration of OPC in a precise direction to lesions. Binamé et al. showed that NG2 regulates the polarity of OPC via activation of RhoA, enhancing directional migration (Binamé et al., 2013).

But NG2/CSPG4 is not only expressed in benign tissue. CSPG4 was originally identified as a highly immunogenic tumor antigen on the surface of melanoma cells (Price et al., 2011). It is associated with melanoma tumor formation and poor prognosis for patients (Price et al., 2011). Its expression correlates with malignancy also in other tumor types, like oligodendrocytomas, astrocytomas, gliomas, triple-negative breast carcinomas and squamous cell carcinoma (Ampofo et al., 2017; Price et al., 2011; Schiffer et al., 2018). NG2 is expressed on the surface of tumor cells (Schiffer et al., 2018) and promotes tumor growth and angiogenesis in animal models (Svendsen et al., 2011). Svendsen et al. further demonstrated that increased expression of NG2 in tumor cells and vasculature in GBM biopsies was associated with shorter patient survival. This correlation was independent of age and clinical treatment (Svendsen et al., 2011). Although NG2 is not an oncogene per se, its expression activates multiple signaling pathways associated with the progression of several tumor types and oncogenic transformation. Pathways driving tumorigenesis that are affected by NG2 include cytoskeletal reorganization, survival (PI3K, AKT and NFκB) causing multi-drug chemoresistance, migration, adhesion (FAK and integrin function) and growth/motility (RTK, and ERK 1,2) (Price et al., 2011; Svendsen et al., 2011).

Although NG2 is frequently used as a marker for certain cell types little is known about the molecular mechanisms regulating its expression (Ampofo et al., 2017). What is known is that NG2 expression is influenced by inflammation and hypoxia and that it is intracellularly regulated by methyltransferases, miRNAs and transcription factors, like C/EBP, p300, CBP and Sp1 (Ampofo et al., 2017). Sp1 seems to play a crucial role in the regulation of NG2 gene expression. Sellers et al. showed, that transfection of COS cells with luciferase reporter gene constructs containing the NG2 promoter without TATA-box and Sp1 binding sites, results in increased cellular luciferase activity (Sellers et al., 2009). In contrast Bin et al. found that transcription of NG2 is down regulated in keratinocytes after Sp1 silencing (Bin et al., 2011). It seems, that Sp1 can either act as a transcriptional activator or repressor of NG2 and that this function depends on its additional post-transcriptional modifications (Ampofo et al., 2017).

3.6 Aims of the study

NG2/CSPG4 plays an important role in the maintenance and differentiation of progenitor cells, as well as proliferation and migration. Also redox regulation is connected to essential cellular functions like proliferation and differentiation. Previous studies of our group indicated an effect of Grx2 on NG2 expression in oligodendrocytes (Lepka, 2017; Wilms, 2017). Therefore this study aims at investigating the effect of NG2/CSPG4 and redox regulation on differentiation and dedifferentiation. Differentiation is important for rapid signal conduction and therefore proper brain functions. Dedifferentiation plays an important role in many diseases, like cancer. It is known that cells need a delicate redox balance under physiological as well as under pathological conditions. Until now the impact of redox regulation concerning NG2/CSPG4 regulation in terms of differentiation and dedifferentiation is not known. This study aims at:

I.   Investigating the effect of Grx2 on migration and differentiation of oligodendrocytes *in vitro* and *in vivo* under physiological conditions

II. Examining the effect of Grx2 on pathological migration of cells in dedifferentiating diseases such as cancer *in vitro* and *in vivo* also in terms of NG2/CSPG4 expression

III. Studying the molecular mechanism of NG2/CSPG4 regulation via Grx2
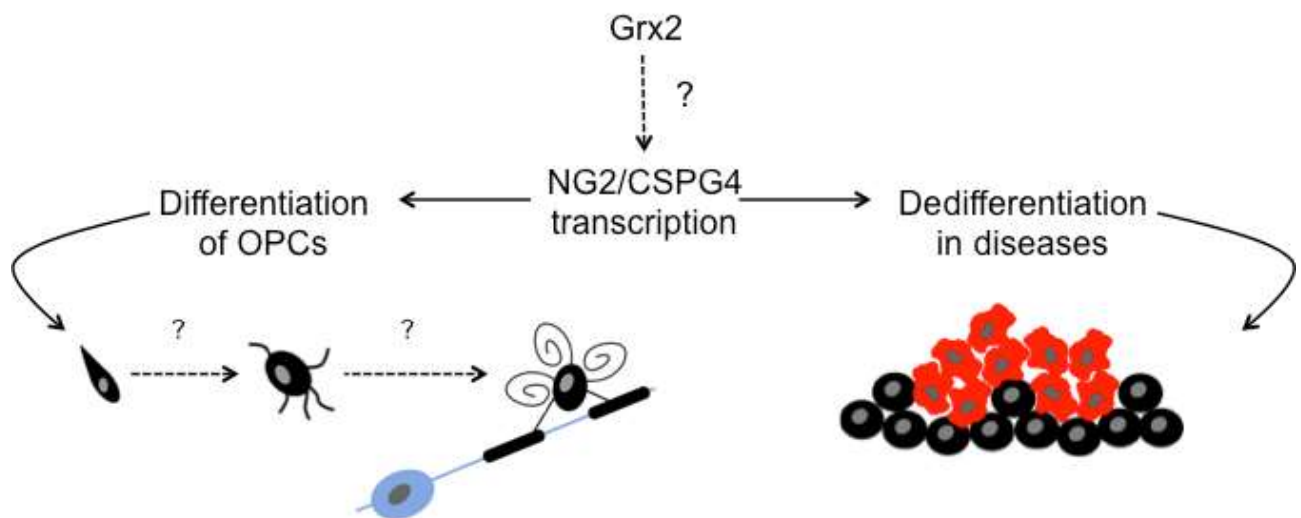
Figure 4: Graphical abstract. This study aims at investigating the impact of redox regulation via Grx2 concerning NG2/CSPG4 regulation in terms of differentiation of OPCs and dedifferentiation in diseases.

4 Material and Methods

4.1 Material

4.1.1 Chemicals

Table 1: List of chemicals and supplements

Chemical	Supplier
10x RT buffer	Applied Biosystems, USA
10x RT random primers	Applied Biosystems, USA
2 % Nitrocellulose membrane	Bio-Rad, USA
4 % Roti-Histofix	Carl Roth, Germany
4x SDS Loading Buffer	Life Technologies, USA
6-8 kD Spectra/Por Dialysis membrane	Spectrumlabs.com
Accutase	Life Technologies, USA
Acidic acid (100%)	Merck, Germany
Agar Noble	Sigma-Aldrich, USA
Ampicillin	Sigma-Aldrich, USA
Anti-A2B5 MicroBeads	Miltenyi Biotec, Germany
Anti-NG2 MicroBeads	Miltenyi Biotec, Germany
Antisense oligonucleotide Morpholinos	Gene Tools, USA
B-27 supplement 50x with vitamin A	Invitrogen, Germany
B-27 supplement 50x without vitamin A	Invitrogen, Germany
BC Assay Protein Quantification Kit	Interchim, France
Bovine Serum Albumin (BSA)	Carl Roth, Germany
Bromodeoxyuridin (BrdU)	Sigma-Aldrich, USA
Calcium chloride	Sigma-Aldrich, USA
CellTiter-Blue reagent	Promeg, USA
Chloramphenicol	Sigma-Aldrich, USA
Chloroform	Merck, Germany
Collagen I, bovine	Life Technologies, USA
cOmplete Tablets	Roche, CHE
Coomassie brilliant blue R-250	Sigma-Aldrich, USA
D-glucose	Sigma-Aldrich, USA
Digitonin	Sigma-Aldrich, USA

Disodium hydrogen phosphate	Sigma-Aldrich, USA
Distilled H2O DNase/RNase free	Invitrogen, Germany
DL-Dithiothreitol (DTT)	Sigma-Aldrich, USA
DMEM/F-12	Life Technologies, USA
DMSO	Honeywell International, USA
DNAse I	Sigma-Aldrich, USA
dNTP Mix (100 mM)	Applied Biosystems, USA
DpnI	New England BioLabs GmbH, Germany
Dulbecco`s Modified Eagles Medium (DMEM)	Life Technologies, USA
Dulbecco´s Phosphate Buffered Saline (PBS)	Life Technologies, USA
Duplex DNA probes	Metabion, Germany
EDTA	Invitrogen, USA
EGTA	Invitrogen, USA
Ethanol 96 %	VWR International, USA
Fetal Calf Serum (FCS)	Life Technologies, USA
Gelatine solution 0.1% in PBS	PAN Biotech GmbH, Germany
Geneticin™ Selective Antibiotic (G418 Sulfate)	Thermo Scientific, USA
GlutaMax	Life Technologies, USA
Glycine	GE Healthcare, UK
Hank´s Balanced Salt Solution (HBSS)	Life Technologies, USA
HEPES (4-(2-hydroxyethyl)-1-piperazineethanesulfonic acid)	Life Technologies, USA
HIS trap columns	GE health care, USA
Hoechst 33258	Sigma-Aldrich, USA
Hydrochloric acid (32%)	Merck, Germany
Imidazole	AppliChem, Germany
ImmoMount	Thermo Scientific, USA
IPTG (β-D-1-thiogalactopyranoside)	Sigma-Aldrich, USA
Isoflurane	Piramal, UK
Isopropanol	Merck, Germany
KOD Hot Start Mastermix	Millipore, USA
L15 Leibovitz-Medium	Biochrom, UK
LB Agar (Lennox L Agar)	Invitrogen, USA
LB Broth Base (Lennox L Broth Base)	Invitrogen, USA
L-Glutamine	Sigma-Aldrich, USA

L-Glutathione (GSH)	Sigma-Aldrich, USA
Lipofectamine™ 2000 Transfection Reagent	Thermo Scientific, USA
Low melt agarose	Sigma-Aldrich, USA
L-Thyroxine (T4)	Sigma-Aldrich, USA
Lysozym	Sigma-Aldrich, USA
Magnesium chloride	Sigma-Aldrich, USA
MCDB 153-Basalmedium	Biochrom, UK
Minimum Essential Media (MEM)	Life Technologies, USA
Minimum Essential Medium – Eagle with Earle's BSS	Lonza, Switzerland
Mini-PROTEAN TGX precast Gels (any KD)	Bio-Rad, USA
Mithramycin A	Cayman Chemical Company, USA
MS222	Sigma-Aldrich, USA
MultiScribe Reverse Transcriptase	Applied Biosystems, USA
NEBuffer	New England BioLabs GmbH, Germany
N-Ethylmaleimide (NEM)	Sigma-Aldrich, USA
Neural Tissue Dissociation Kit	Miltenyi Biotec, Germany
Normal Goat Serum (NGS)	Life Technologies, USA
NP-40	Sigma-Aldrich, USA
Nuclease-Free water	Ambion, Germany
NuPAGE LDS sample buffer (4x)	Life Technologies, USA
Penicillin/Streptomycin	Life Technologies, USA
PhosSTOP	Roche, CHE
Poly-L-Lysin	Sigma-Aldrich, USA
Polyvinylpyrrolidone (PVP)	Sigma-Aldrich, USA
Potassium chloride	Sigma-Aldrich, USA
*Power*SYBR Green PCR Master Mix	Applied Biosystems, USA
Protein Marker V	PeqLab Biotechnology, Germany
PTU	Sigma-Aldrich, USA
PureYield Plasmid Miniprep System	Promega, USA
Random hexamers (primers)	Life Technologies, USA
Recomb. mouse epidermal growth factor (EGF)	ImmunoTools, Germany
Recomb. mouse fibroblast growth factor-basic (FGF)	ImmunoTools, Germany
Recomb. mouse platelet-derived growth factor (PDGF)	ImmunoTools, Germany
Reverse Transcriptase	Life Technologies, USA

RIPA buffer	Sigma-Aldrich, USA
RNAse inhibitor	Life Technologies, USA
Sodium bicarbonate	Lonza, CHE
Sodium chloride	Sigma-Aldrich, USA
Sodium phosphate	Sigma-Aldrich, USA
Sodium tetraborate	Sigma-Aldrich, USA
Sucrose	Carl Roth, Germany
TaqMan Gene Expression Master Mix	Applied Biosystems, USA
ThinCert cell culture Inserts (8 μm)	Greiner Bio-One, Austria
Total RNA, human	Takara, Japan
Trichloroacetic acid (TCA)	Sigma-Aldrich, USA
Triiodo-L-Thyronine (T3)	Sigma-Aldrich, USA
Tris	Carl Roth, Germany
Tris/Glycin Running Buffer (10x)	Bio-Rad, USA
Tris-HCl	Carl Roth, Germany
Triton-X-100	Merck, Germany
Trizol Reagent	Life Technologies, USA
Trypsin (10x)	Life Technologies, USA
Tween-20	Sigma-Aldrich, USA
Urea	Sigma-Aldrich, USA

4.1.2 Laboratory equipment

Table 2: List of used laboratory equipment

Instrument	Supplier
7500 Fast Real-Time PCR Systems	Applied Biosystems, USA
BioPhotometer	Eppendorf, Germany
BioRad TL10 Automatic Cell counter	Bio-Rad Laboratories, USA
BTX Gemini Electroporation System	Thermo Scientific, USA
BX51 fluorescent microscope	Olympus, Japan
Centrifuge 5417R	Eppendorf, Germany
Centrifuge Minispin	Eppendorf, Germany
Centrifuge Rotanta 460 R	Hettich, Germany
CPS-100	Shimadzu, Germany

F-view CCD camera	Olympus, Japan
His GraviTrap	GE Healthcare Life Science, US
Intas GDS UV-Systeme	Intas, Germany
IX81 microscope	Olympus, Japan
Leica CM 1900 UV Cryostat	Leica, Germany
Leica S6 E Stereomicroscope	Leica Microsystems, Germany
Lightsheet Z.1	Zeiss, Germany
Microplate Reader	Tecan Group Ltd., Switzerland
Mini Protean tetra system	BioRad Laboratories, USA
Multiskan FC	Thermofisher, USA
Nanodrop 2000 Spectrophotometer	Thermo Scientific, USA
Odyssey Infrared Imaging System	LI-Cor, USA
OptoMotry HD	CerebralMechanics, Canada
Pipettes	Eppendorf, Germany
Sonoplus	Bandelin, Germany
Spectralis Plus Mulitcolor	Heidelberg Engineering, Germany
Sterile Incubator	Thermo Scientific, USA
TCS SP8 Confocal Microscope	Leica, Germany
Thermocycler T Gradient	Biometra, Germany
Trans-Blot Turbo transfer system	Bio-Rad Laboratories, USA
TriM Scope II - 2-Photon Microscope	LaVision BioTec GmbH, Germany
UV-1800	Shimadzu, Germany
Vortex Genie 2	Scientific industries, USA

4.1.3 Antibodies

Table 3: List of primary antibodies

Antibody (species)	Western Blot	Histology	Company
Anti-Actin (mouse)	1:5000	-	Abcam, UK
Anti-BrdU (mouse)	-	1:500	Sigma-Aldrich, USA
Anti-Grx2 (rabbit)	1:1000	1:500	Abcam, UK
Anti-Histone H3 (rabbit)	1:1000	1:1000	Abcam, UK
Anti-NG2 (rabbit)	-	1:500	Millipore, USA
Anti-Sp1 (mouse)	1:500	1:500	Santa Cruz Biotech., USA
Anti-α-Tubulin (rat)	1:5000	-	Acris Antibodies, USA

Secondary antibodies used for Western blot were IRDyes from LI-COR, USA, diluted 1:15000. Secondary antibodies for ICC were Cyanine Dye conjugates from Millipore, USA, diluted 1:500.

4.1.4 Primer- and siRNA sequences

Table 4: List of primer sequences for quantitative RT-PCR analysis

Gene	Primer sequences (5' -> 3')
mCNPase	Fw: 5'-TGC-TGC-ACT-GT-ACA-ACC-AAA-TTC-3'
	Rw: 5'-GAG-AGC-AGA-GAT-GGA-CAG-TTT-GAA-3'
mGAPDH	Fw: 5'-CTC-AAC-TAC-ATG-GTC-TAC-ATG-TTC-CA-3'
	Rw: 5'-CCA-TTC-TCG-GCC-TTC-ACT-AT-3'
mGrx2c	Fw: 5'-CGG-GGA-CCT-TTG-GCT-ATGTC-3'
	Rw: 5'-ATT-GTT-TCT-TGG-ATC-TGG-TTC-ACA-3'
mMBP	Fw: 5-'CAC-AGA-GAC-ACG-GGC-ATC-CT-3'
	Rw: 5'-TCT-GCT-TTA-GCC-AGG-GTA-CCT-T-3'
mNG2	Fw: 5'-CCC-CCC-CAT-ACC-CAT-GTC-3'
	Rw: 5'-CGA-TCG-GAA-ATA-ACC-TGA-AGC-T-3'
hGrx2c	Fw: 5'-CGA-GAT-AAG-CAA-GCA-AGA-TGG-AGA-GCA-3'
	Rw: 5'-GCC-TAT-GAG-TGT-CAG-TTG-CAC-C-3'
hGAPDH	Fw: 5'-GGA-TTT-GGT-CGT-ATT-GGG-3'
	Rw: 5'-GGA-AGA-TGG-TGA-TGG-GAT-T-3'
hNG2	Fw: 5'-CAC-GGC-TCT-AGC-CGA-CAT-AG-3'
	Rw: 5'-CCC-AGC-CCT-CTA-CGA-CAG-T-3'

Table 5: List of siRNA sequences

Gene	Sequences (5' -> 3') or Cat #	Company
mControl	D-001910-01-50	Dharmacon, USA
mGrx2	A-050282-13-0050	Dharmacon, USA
hControl	5'-CAU-UCA-CUC-AGG-UCA-G-3'	Eurogentec, Belgium
	5'-CUG-AUG-ACC-UGA-GUG-AAU-G-3'	
hGrx2	5'-GGU-GCA-ACU-GAC-ACU-CAU-A-3'	Eurogentec, Belgium
	5'- UAU-GAG-UGU-CAG-UUG-CAC-C-3'	

24

4.1.5 Software

Table 6: Software used for data analysis and presentation

Software	Company
Adobe Acrobat Reader 11.0	Adobe System Inc, USA
Adobe Photoshop CS4	Adobe System Inc, USA
GraphPad Prism 5	GraphPad Software, USA
Image J	Rasband, USA
Magellan Data Analysis Software	Tecan Group Ltd., Switzerland
Odyssey Imaging System Software	LI-Cor, USA
Office Professional Plus 2010	Microsoft Corporation, USA
Zotero	Corporation for Digital Scholarship

4.1.6 Plasmids

pet15b (Novagen): The pet15b vector was used for recombinant protein expression. It carries a T7 promoter, a His Tag sequence and an ampicillin resistance.

4.1.7 Bacteria

For expression of recombinant proteins the *E. coli* strain BL21(DE3)pRIL (hasdS gal (λIts857 ind 1 Sam7 nin5 lac UV5-T7 gene 1) from Stratagene (chloramphenicol resistance) was used.

For expression of recombinant proteins *E.coli* DH5α cells were generated as described in *4.2.27*.

4.1.8 Ethical approvals

All animal experiments were conducted according to the guidelines and protocols approved by the local animal welfare committee "Landesamt für Natur, Umwelt und Verbraucherschutz Nordrhein-Westfalen" (LANUV) under the protocol number O74/08.

4.1.9 Statistical analysis

Graphs and statistical analyses were performed using GraphPad Prism 5 (GraphPad Software). All graphs show bars or dot plots with mean value and standard error of the mean (SEM). Statistical significance was determined using the two-tailed student's t-test with the following p values:
ns: $p > 0.05$; *: $p < 0.05$; **: $p < 0.01$; ***: $p < 0.001$.

4.2 Methods

4.2.1 Cell culture

Cell culture work was performed using a sterile bench. Cultivation occurred in a sterile incubator at 37°C and a humidified atmosphere containing 5% CO_2. Medium was exchanged every 2-3 days and confluent cell cultures were passaged.

Primary cells:

A2B5⁺- and NG2⁺- cells were isolated using the Neural Tissue Dissociation Kit (Miltenyi Biotec, Germany) according to manufacturer´s instructions. Afterwards they were sorted by Magnetic associated cell sorting (MACS) using Anti-A2B5 MicroBeads (Miltenyi Biotec, Germany) or Anti-AN2 MicroBeads (Miltenyi Biotec, Germany) according to manufacturer´s instructions.

A2B5 and NG2 positive cells were cultivated either in proliferation (DMEM/F-12 medium with 1% HEPES, 1 % GlutaMax, 1 % Pen/Strep, B27- 1:50, FGF 1:1000, PDGFα 1:1000) or differentiation medium (DMEM/F-12 medium with 1% HEPES, 1 % GlutaMax, 1 % Pen/Strep, B27+ 1:50, T3 1:100, T4 1:100) using dishes or glasses coated with 0.1 mg/ml poly(L)-lysin. For splitting, cells were detached by incubation with accutase for 2-3 min and collected by washing with PBS. After centrifugation for 10 min at 300 g, the pellet was resuspended in medium and cells were counted and plated for further experiments.

Grx2 knockdown in primary cells was performed using membrane consistently Dharmacon siRNA resuspension. Therefore 1 µM control or Grx2 siRNA were added to the cells. The procedure was repeated after 72 h. 24 h later cells could be used for further experiments.

Cell lines:

HeLa-cells (endothelial cells, derived from a cervical carcinoma) and **HeLaGrx2c cells** (Grx2c overexpressing HeLa cells) were maintained in DMEM medium with 1 g/L D-glucose, 10 % FCS and 1 % Pen/Strep. Cells of both cell lines were passaged when confluent. For splitting, cells were detached by incubation with trypsin for 5 min and reaction was stopped using medium. After centrifugation for 5 min at 1,000 rpm, the pellet was resuspended in medium and cells were counted and plated for further experiments.

GBM18- and **U343-MGA-cells** (human glioblastoma cells) were maintained in Minimum Essential Medium (MEM) with 10 % FCS and 1 % Pen/Strep. Cells of both cell lines were passaged when confluent. For splitting, cells were detached by incubation with accutase for 5 min and reaction was

stopped using medium. After centrifugation for 10 min at 500 rpm, the pellet was resuspended in medium and cells were counted and plated for further experiments.

GBM1-cells (human glioblastoma stem cells) were maintained in DMEM/F-12 medium with 2 % B27 supplement with Vitamin A, 0.1 % EGF, 0.1% FGF, 0.1 % Heparin and 1 % Pen/Strep. For splitting, cells were collected and centrifuged for 5 min at 500 rpm, the pellet was resuspended in medium and cells were counted and plated for further experiments.

Skmel2-, **1205-LU-** and **WM3734-cells** (human melanoma cells) were maintained in TU-Medium (80 % MCDB 153-Basalmedium, 20 % L15 Leibovitz-Medium) with 2 % FCS, 1 % Pen/Strep, 1 mM $CaCl_2$ and 2 mM L-Glutamin. Cells of all three cell lines were passaged when confluent. For splitting, cells were detached by incubation with accutase for 5 min and reaction was stopped using medium. After centrifugation for 10 min at 500 rpm, the pellet was resuspended in medium and cells were counted and plated for further experiments.

Z12-cells (endometrial cells) were maintained in DMEM medium with 4.5 g/L D-glucose, 10 % FCS and 1 % Pen/Strep. Cells were passaged when confluent. For splitting, cells were detached by incubation with accutase for 5 min and reaction was stopped using medium. After centrifugation for 5 min at 1,000 rpm, the pellet was resuspended in medium and cells were counted and plated for further experiments.

4.2.2 Chemical transfection

To knockdown Grx2 expression in GBM18- and U343-MAG-cells cells were chemically transfected with siRNA. Therefore 15 µg siRNA (control and Grx2) were mixed with 1875 µl MEM medium and 37.5 µl Lipofectamine 2000 reagent were mixed with 1875 µl MEM medium. Both mixtures were incubated for 5 min at RT, before siRNA mixture was carefully added to the Lipofectamine mixture. After incubation for 20 min at RT the mixture was added to the cells. After 72 h the whole procedure was repeated and cells were harvested the next day and plated for further experiments.

4.2.3 Electroporation

HeLa cells were electroporated with Grx2 siRNA to knock-down Grx2 levels. Therefore $3,5x10^6$ cells were resuspended in 550 µl electroporation buffer (21 mM HEPES, 137 mM NaCl, 5 mM KCl, 0.7 mM Na_2HPO_4, 6 mM D-glucose, pH 7.15), mixed with 15 µg control or Grx2 siRNA and transferred

into a electroporation cuvette. HeLa cells were transfected with 250 V, 1500 µF and 500 Ω. 500 µl FCS were added and cells were transferred to a T175 flask with 1:5 old to fresh medium. The whole procedure was repeated after 72 h, after additionally 24 h cells were harvested and used for further experiments.

4.2.4 Immunocytochemistry

Cells were grown in petri dishes on poly(L)-lysin (PLL) coated glasses, washed with PBS and fixed for 15 min, shaking at RT by using 4 % Roti-Histofix (Carl Roth, Germany). After two washing steps with washing solution (PBS, 0.1 % Triton-X) cells were permeabilizied and blocked for 2 h in blocking buffer (PBS, 0.1 % Triton-X 100, 5 % NGS) to avoid unspecific binding. Primary antibodies were added in 1:1 blocking buffer:PBS and cells were incubated at 4°C overnight. After washing three times with PBS containing 1 % Triton-X 100, secondary antibodies (Cyanine Dyes) diluted in 1:1 blocking buffer:PBS were added for 1 h at RT. Then a staining with Hoechst diluted 1:500 for 10 min was performed. Glasses were washed 3x with PBS for 10 min and attached to object slides with ImmuMount (Thermo Fisher, USA). Object slides were dried overnight in the dark and pictures were taken using BX51 fluorescent microscope (Olympus, Japan) and F-view CCD camera (Olympus, Japan).

4.2.5 CellTiter-Blue® cell viability assay

To define a non-lethal Mithramycin A (MitA) concentration for transwell-migration assay a CellTiter-Blue® cell viability assay was performed. Therefore 10,000 GBM18-cells per well were seeded in 96 well-plates. After 24 h cells were treated with DMSO (control), 5 nM, 10 nM, 25 nM, 50 nM, 100 nM or 200 nM MitA. After 48 h medium with 20 % CellTiter-Blue reagent (Promega) was supplemented to the cells. After additional 1.5 h, absorption at 562 nm and at 612 nm (reference wavelength) was measured using the TECAN microplate reader and survival rates were calculated in comparison to untreated controls.

4.2.6 Transwell-migration assay

In order to analyze the influence of Grx2c on migration ability of A2B5[+]-, NG2^{+}-, GBM1-, GBM18- and U343-MGA-cells a quantitative cell invasion assay using ThinCert™ cell culture inserts with 8 µm pores was performed. The migration chamber consists of an upper and lower compartment with a porous PET membrane in-between. Cells may actively migrate from the upper to the lower compartment.

Glasses for microscopy were coated over night with PLL (A2B5$^+$-, NG2$^+$-, GBM18-, U343-MGA cells) or with gelatin (GBM1-cells). 50,000 cells were treated with or without 2 µM Grx2c. After 24 h (A2B5$^+$-, NG2$^+$-cells) or 48 h (GBM1-, GBM18- and U343-MGA-cells) inserts were removed and the cells were incubated for another 24 h to attach to the bottom of the wells before they were fixated with 4 % PFA for 15 min. Fixation was followed by staining with Hoechst diluted 1:500 for 10 min and by three washing steps with PBS for 10 min. Finally plates were removed from wells and mounted to an objective slide with a drop of ImmuMount. For analysis 5 randomly selected pictures per plate were made with the fluorescence microscope at 10x magnification and migrated cells were counted.

4.2.7 3D spheroid assay

To investigate the influence of Grx2 expression on 3D migration of cells a 3D spheroid assay with GBM18-, U343-MGA- and Z12-cells was performed. To generate spheroids each well of a 96 well plate was coated with 50 µl 1.5 % agar noble solution. After the agar cooled down to RT, 5,000 cells in 50 µl MEM medium were seeded per well. Spheroids were harvested after 48 h.

For the collagen mix 420 µl 10x EMEM, 38 µl L-glutamine (200 nM), 462 µl FCS, 78 µl NaHCO$_3$ (7.5 %) and 3.5 ml collagen (2 mg/ml in PBS) were prepared. NaHCO$_3$ was added until the color of the mixture appeared orange. 300 µl of the collagen mixture was added to each well of a 24 well plate, before the plate was incubated at 37°C for 30 min. Fresh collagen mix was prepared and spheroids were harvested with a 1000 µl pipette into a falcon. After the spheroids settled to the bottom the liquid was removed and spheroids were resuspended in 300 µl collagen mix and added on top of the first, solid collagen layer. After 30 min at 37°C 500 µl MEM medium was added on top. Pictures of the spheroids at bright field microscope at 4x magnification were taken after 24 h, 48 h and 72 h.

4.2.8 BrdU assay

BrdU, an analogon of thymidine, is incorporated during DNA replication. Therefore, proliferating cells can be visualized by anti-BrdU antibodies. 30,000 GBM18 and U343-MGA cells were seeded per well and incubated overnight. Each well contained glass plates for microscopy, which have been coated with PLL before. Cells were kept untreated as control or treated with 2 µM for 24 h. The next day 10 µM BrdU were applied for 2 h at 37°C. After three washing steps with PBS cells were fixated with 4 % PFA for 15 min. Afterwards the cells were exposed to 2 M HCl for 30 min at 37°C in order to denature DNA and to allow access of the antibodies against BrdU. One washing step with saturated tetraborate solution normalized pH levels and was followed by two washing steps with PBS containing 1 % Triton-X 100. Subsequently unspecific binding sites were blocked using blocking

buffer (5 % normal goat serum (NGS), 0.2 % Triton-X 100 in PBS) for 1 h. Before incubation with the primary mouse anti-BrdU antibodies and rabbit anti-H4 antibodies cells were washed three times with PBS. Anti-H4 antibodies were used for nuclear staining, since Hoechst needs double stranded DNA to intercalate. Antibodies were diluted in 1:1 blocking buffer and PBS and incubation occurred at 4°C overnight. Washing three times with PBS removed the surplus amount of antibodies. Secondary antibodies, also diluted in 1:1 blocking buffer and PBS, were applied and incubated for one hour at RT. After removing the secondary antibodies and washing three times for 10 min with PBS, the plates were removed from wells and mounted to an objective slide using ImmuMount. For analysis the number of BrdU positive cells was divided by the overall cell number indicated by H4 staining to determine the percentage of proliferating cells.

4.2.9 Acidic Wash

To remove recombinant proteins from the cell surface an acidic wash was performed before Western blot or immunocytochemistry (ICC) analyses. For acidic wash the medium was aspirated and cells were washed twice with PBS. Afterwards the cells were washed for 30 sec with acidic-wash buffer (200 mM glycine, 150 mM NaCl; cooled down to 4°C, before adjusting the pH to 3). After aspiration of the acidic-wash buffer cells were neutralized by adding cell culture medium. These steps were performed two times before harvesting or fixing the cells.

4.2.10 Generation of Grx2 overexpressing U343-MGA-cells

To generate Grx2 overexpressing U343-MGA-cells the cells were transfected with a pExpress Grx2 plasmid as described in *4.2.2*. Afterwards 700 µg/ml Neomycin/G418 was added to the medium for two weeks.

4.2.11 Optical Coherence Tomography (OCT) and Optomotor Response (OMR)

Optical Coherence Tomography (OCT) and Optomotor Response (OMR) as visual system readouts were kindly performed by Christina Hecker from the working group of Prof. Dr. Philipp Albrecht, Neurology, Düsselorf as described elsewhere (Dietrich et al., 2019).

4.2.12 Zebrafish housing and maintenance

Zebrafish experiments were conducted in cooperation with Prof. Dr. Odermatt (Institute of Anatomy, University of Bonn, Germany) and Dr. Bräutigam (Karolinska Institutet, Solna, Sweden). Adult

zebrafish were maintained at 28°C with a light/dark cycle of 14/10 h under actual husbandry license (§ 11). Embryos ≤5 days post fertilization (dpf) were kept at 28°C in an incubator in 0.3× Danieau's buffer (1× Danieau's buffer: 58 mM NaCl, 0.7 mM KCl, 0.4 mM $MgSO_4$, 0.6 mM Ca[NO_3]2, 5 mM HEPES, pH 7.2). Until 24 h post fertilization (hpf), 0.3× Danieau's buffer was supplemented with 0.00001% methylene blue solution. From 24 hpf, when used for imaging, 0.3× Danieau's buffer was supplemented with 0.003% phenylthiourea (PTU) to prevent pigmentation. All experiments were done according to institutional and national law, following ARRIVE guidelines.

Wildtype line and the following transgenic fishlines were used in this study:

/Tg(olig2:GFP) // (Shin et al., 2003)/

/Tg(mbp:EGFP) // (Almeida et al., 2011)/

/Tg(claudinK:EGFP) // (Münzel et al., 2012)/

/fli1a:EGFP // (Lawson and Weinstein, 2002)

A Grx2 overexpressing zebrafish strain (Tg(ßact:Grx2)) was provided by Dr. Bräutigam, Karolinska Institute, Solna, Sweden. For generation zebrafish Grx2 was amplified from whole embryo RNA. Primers were flanked from attB1 and attB2 sites for gateway cloning (forward: GGGG ACA AGT TTG TAC AAA AAA GCA GGC TTC ATGGGGAACTTCTCGTC; reverse: GGG GAC CAC TTT GTA CAA GAA AGC TGG GTC TCACTGATGAGGCTGATTTTG). PCR product was cloned into pDONR 221 vector and further cloned via the gateway/Tol2 system. The vector backbone express GFP under a heart-specific promotor for screening. Afterwards the construct (ßactin promotor – zfGrx2 – pA) was injected into zebrafish eggs together with tol2 transposase. Zebrafish were raised and outcrossed to AB zebrafish strain.

4.2.13 Morpholino injection into zebrafish

Grx2 expression in zebrafish was downregulated by injection of antisense oligonucleotide Morpholinos (MOs) from Genetools. Therefore control (5' CCTCTTACCTCAGTTACAATTTATA 3') and Grx2 (5′GTTGAAGATACTAGGAAAGCAAACG 3′) morpholino (stock concentration 3 mM) were diluted 1:40 in injectionbuffer. A volume of 1.5 nl was injected with a glass micropipette into Olig2-, ClaudinK- and MBP-GFP zebrafish at 1-2 cell stage. Water was changed to PTU the next and after 3 days (Olig2, ClaudinK) or 4 days (MBP), fish were sorted and prepared for 2-Photon microscopy. Therefore 5 fish were placed into the lid of a petridish, access water was removed, before 5 µl MS222 and 195 µl low melt agarose were added. Zebrafish were adjusted for microscopy and picture were taken at the 2-Photon microscope. For analysis dorsally migrating cells were counted.

4.2.14 Transplantation of glioblastoma cultures into zebrafish

Glioblastoma cultures were maintained as described in *4.2.1* and transferred to complete neural stem cell medium (Neurobasal medium/DMEM/F12 mixture containing B27 and N2 supplements as well as 10 ng/ml bFGF and 20 ng/ml EFG) 5 days before transplantation. Cells were washed with PBS, harvested, passed over a 20 μM nylon mesh and resuspended in medium containing 2 % polyvinylpyrrolidone (PVP) to avoid clogging of the micro-injection capillary. Directly before injection cells were centrifuged for 10 min at 500 g and the medium was almost entirely removed. The cell suspension was loaded in nonfilament microcapillaries and approximately 100 tumor cells were injected into blastula-stage zebrafish embryos, which have been immobilized in an agarose mold. After injection embryos were screened for successful transplantation, transferred into a 10 cm dish and incubated at 33°C for 24 h. 24 hpf embryos were mounted in a glass capillary containing 1 % low melt agarose and were extruded into an imaging chamber containing E3 medium supplemented with MS222. Time-lapse images were acquired on a Zeiss Lightsheet Z.1 using a 10x detection objective and 10x illumination objectives. Samples were illuminated from one or both directions and Z-stacks were acquired every 15 min using a 1x optical zoom, 6.4 μm light-sheet thickness and 1.8 μm Z-interval. Max intensity projections were generated and sample drift was corrected for using a rigid body transformation in the StackReg plugin of ImageJ. For analysis number of protrusions was counted and length of protrusions was measured.

4.2.15 Transplantation of melanoma cells into zebrafish

Skmel2 melanoma cells were maintained as described in 4.2.1 and were treated 24 h and 2h before transplantation with 2 μM Grx2c or were kept untreated as control. Cells were washed with PBS, harvested, passed over a 20 μM nylon mesh and resuspended in medium containing 2 % polyvinylpyrrolidone (PVP) to avoid clogging of the micro-injection capillary. Directly before injection cells were centrifuged for 10 min at 500 g and the medium was almost entirely removed. The cell suspension was loaded in nonfilament microcapillaries and approximately 100 tumor cells were injected into yolk sac of fli1a:EGFP zebrafish 48 hpf which have been immobilized in an agarose mold. After injection embryos were screened for successful transplantation, transferred into a 10 cm dish and incubated at 33°C for 48 h. Afterwards embryos were mounted in a glass capillary containing 1 % low melt agarose and were extruded into an imaging chamber containing E3 medium supplemented with MS222. Images were acquired on a Zeiss Lightsheet Z.1 using a 10x detection objective and 10x illumination objectives. Samples were illuminated from one or both directions and Z-stacks were acquired every 15 min using a 1x optical zoom, 6.4 μm light-sheet thickness and 1.8 μm Z-interval. Max intensity projections were generated and sample drift was corrected for using a

rigid body transformation in the StackReg plugin of ImageJ. For analysis zebrafish with and without metastasis were determined.

4.2.16 Generation of Grx2 knock-out mice

The *Glrx2-lacZ* mouse strain was established together with Dr. Marcus Conrad (Helmholz Zentrum München, Munich, Germany). Briefly in this mouse strain the *Glrx2* gene was replaced by *lacZ* gene, meaning that homozygous mice miss the *Glrx2* gene leading to a Grx2 knock-out.

4.2.17 Cell lysis and protein isolation

Cells were harvested, washed with PBS and centrifuged for 5 min at 300 g. The pellet was resuspended in 30-100 µl lysis buffer (RIPA or NP40) and incubated at RT for 10 min, before freezing in liquid nitrogen. Samples were stored at -80°C. Samples were thawn and centrifuged at 4°C for 20 min at 18000 g. Supernatants were transferred into new tubes and used for further analysis.

4.2.18 Crude cell fractionation (lysate, cytosol, organelles)

To analyze specific cellular compartments to investigate DNA-protein binding crude cell fractionation was performed to separate the cytosol from the organelles. Therefore cells were harvested as described before and cell pellets were resuspended in 120 µl digibuffer (0.01% digitonin in mitobuffer (5 mM Tris-HCl (pH 7.4), 250 mM sucrose, 1 mM EDTA, 1 mM EGTA, 1.5 mM MgCl$_2$) plus phosphatase and protease inhibitor). Samples were incubated on ice for 10 min before 20 µl were transferred as full lysate to a new tube and were shock frozen in liquid nitrogen. The rest of the sample was centrifuged at 13.000 rpm for 10 min at 4°C. Afterwards the supernatant was transferred as cytosolic fraction and was shock frozen in liquid nitrogen. The cell pellet was resuspended in 500 µl ice cold mitobuffer and centrifuged for 10 min at 13,000 rpm at 4°C. Afterwards the supernatant was discarded and the pellet was washed two additionally times before it was resuspended in 100 µl NP40 and incubated for 15 min at room temperature. The lysate was sonificated twice for 20 sec with 60% input before it was shock frozen in liquid nitrogen and stored as organelle fraction.

4.2.19 Bicinchoninic acid assay (BCA assay)

Bicinchoninic acid assay (BCA assay) was performed using BC Assay Protein Quantification Kit (Interchim, France) according to manufacturer´s instructions.

4.2.20 SDS polyacrylamide gel electrophoresis

To separate proteins by size SDS polyacrylamid gel electrophoresis (SDS-PAGE) was performed. 20-30 µg of total protein were diluted and combined with loading-buffer. Proteins were separated for approximately 30 min at 150 V using any KD Bio-RAD mini-PROTEAN TGX Gels (Bio-Rad, USA) in mini-PROTEAN Tetran System (Bio-Rad, USA) in Tris/Glycin running buffer (Bio-Rad, USA; 25mM Tris, 192mM Glycine, 0.1% (w/v) SDS, pH 8.3). Gels were washed with aqua dest, incubated for 1 h with coomassie-blue solution (0.1 % Coomassie brilliant blue R-250, 40 % ethanol, 10 % acidic acid in distilled water) to dye proteins. After incubation the gel was washed with coomassie-blue decoloration-solution (20 % ethanol, 10 % acidic acid in distilled water) and incubated for 30 min or overnight. The gel was washed again with aqua dest and imaged afterwards using Odyssey Infrared Imaging System (LI-COR Bioscience, USA).

4.2.21 Western blot

Cells were lysed as described in *4.2.8* on ice in RIPA buffer supplemented with a protease and phosphatase inhibitor cocktail (Roche, Germany). Protein concentrations in the supernatant were determined in triplicates with the BC Assay Protein Quantification Kit (Interchim, France) according to manufacturer´s instructions. Equal protein amounts (30 µg) were prepared with 4x SDS loading buffer. The samples were loaded on any KD Bio-RAD mini-PROTEAN TGX Gels (Bio-Rad, USA) and ran for 30 min at 150 V in mini-PROTEAN Tetran System (Bio-Rad, USA) in Tris/Glycin running buffer (Bio-Rad, USA). Proteins were electrophoretically transferred from SDS-Gel on 0.2 µm Nitrocellulose membrane (Bio-Rad Trans- Blot Turbo Transfer Pack mini format) using TransBlot Turbo Transfer System (Bio-Rad, USA) at 25 V, 2.5 A for 7 min. To prevent unspecific antibody bindings the membrane was blocked with blocking buffer (PBS, 0.05 % Tween 20, 5 % Bovine Serum Albumin) for 1 h at RT on shaker. Primary antibodies were diluted to the appropriate concentration in blocking buffer and applied to the membrane overnight at 4°C on shaker. After removal of primary antibodies the membrane was washed 3x with PBS-T (PBS, 0.05 % Tween 20) for 10 min and the secondary antibodies, diluted in blocking buffer, were applied for 1 h at RT on shaker. After removal of the secondary antibodies the membrane was washed 3x with PBS-T and the infrared signal was detected using Odyssey Infrared Imaging System (LI-COR Bioscience, USA).

4.2.22 EMSA (Electrophoretic mobility shift assay)

To shed light on protein-DNA interaction an Electrophoretic Mobility Shift Assay (EMSA) was conducted. Therefore duplex DNA with a IRD700 (NG2 promoter: ggctgggacagttcatgcctcctccctgagggggtctcc; ccgaccctgtcaagtacggaggagggactcccccagagg; NG2 enhancer: tgctgaaccagctgggccgccccccgcgcagatggtctgca; acgacttggtcgacccggcggggggcgcgtctaccagacgt; Metabion, Germany) was diluted in annealing buffer (60 mM KCl, 6 mM HEPES, 0.2 mM $MgCl_2$) to 0.1 µM. DNA was reannealed for 1 min at 95°C, then cooled down for more than 30 min to RT. 1 µl DNA and 20 µg cell lysate were incubated for 15 min at RT in the dark. SDS page was run as a native gel (Native PAGE buffer: 25 mM Tris, 192 mM Glycine, pH 8.3) for 45 min at 120 V. Afterwards the gel was detected at 700 nm using Odyssey Infrared Imaging System (LI-COR Bioscience, USA)

4.2.23 Intermediate trapping

To identify dithiol:disulfide substrates for specific Cys-X-X-Cys oxidoreductases intermediate trapping was used. By mutating the C-terminal Cys to a Ser, the substrates are trapped in the intermediate state. Grx2c wt and Grx2c C37S were expressed and purified as described in *4.2.31* and cell lysates were prepared as described in *4.2.17*. The protein concentration is determined by BCA assay as described in *4.2.19*. Columns were prepared with 10 ml PBS, followed with 10 ml PBS containing 20 mM Imidazol. Afterwards 1-2 mg Grx2c C37S or Grx2c wt as (as control) were diluted in 5 ml PBS and applied to the column. Flow-through was applied a second time to the column to guarantee efficient binding. The column was washed with 10 ml PBS containing 20 mM Imidazol, followed by 10 ml PBS with 10 mM DTT to reduce the protein and afterwards one washing step with 5 ml PBS was conducted. Afterwards the column was loaded with 10-20 mg lysate diluted in 5 ml PBS and flow-through was applied a second time before the column was washed with 10 ml PBS containing 20 mM Imidazol. Reductase-substrate complex was eluated using 3 ml PBS containing 20 mM GSH. Samples were precipitated with 20% TCA overnight at 4°C and centrifuged afterwards at 13,000 rpm for 15 min at 4°C. Pellet was washed with ice-cold aceton and centrifuged again before the pellet was dried at RT for a few minutes. Afterwards the pellet was resuspended in 50 µl urea buffer and 4x SDS loading buffer. Samples were analyzed by western blot as described in *4.2.21* or were send for mass spectrometry to Dr. Gereon Poschmann (Institute for Molecular Medicine I, Heinrich-Heine-University, Dusseldorf, Germany).

4.2.24 RNA isolation

RNA isolation of cells was performed using Trizol. Therefore, the cell pellet was resuspended in 500 µl Trizol. Afterwards 200 µl chloroform was added, the samples were vortexed and centrifuged for 15 min at 12,000 g and 4°C. The upper aqueous phase was transferred to a fresh RNAse-free tube and 500 µl isopropanol were added. The samples were mixed by inverting the tube and incubated for 10 min at RT. After another centrifugation step for 10 min at 12,000 g at 4°C the supernatant was removed and the pellet was washed with 1 ml 75% ethanol. The samples were vortexed again and centrifuged at 7,500 g for 5 min at 4°C. After another washing step the pellet was dried at 55-60°C. Isolated RNA was solved in 20 µl RNAse-free water and quantity of RNA was determined with Nanodrop 2000 (Thermo Scientific, USA). RNA was stored at -80°C or directly used for cDNA-synthesis.

4.2.25 cDNA synthesis

1-2 µg of total RNA were utilized for complementary DNA (cDNA) synthesis with 2 µl 10x buffer, 0.8 µl dNTP (100 mM), 2 µl random hexamer primer, 1 µl RNAse inhibitor (20 U/µl), 1 µl reverse transcriptase (50 U/µl) and RNAse-free water up to 20 µl. The samples were vortexed and centrifuged briefly. The reaction takes place in a T Gradient Thermocycler (Biometra, Germany). The cDNA synthesis reaction was incubated for 10 min at 25°C, before incubation for 2 h at 37°C. Afterwards reverse transcriptase was inactivated at 85°C for 5 min. The synthesized cDNA was diluted with RNAse-free water 1:3 and stored at -20°C.

4.2.26 Quantitative real time PCR (qRT-PCR)

5 µl of diluted cDNA were applied to 15 µl of the adequate master mix. Genes of interest were analyzed in duplicates with AB 7500 Real-Time PCR System (Life Technologies, USA) using the following reaction program: 15 min at 95°C, 45 cycles at 94°C for 15 sec, 20 sec at 60°C, 35 sec at 72°C. After the reaction cycles, a dissociation step was performed by heating the samples to 95°C for 15 sec, 1 min at 60°C and 15 sec at 95°C to identify possible primer dimers. Comparative threshold cycle method served as basis for relative gene expression quantification with GAPDH expression level as internal control.

4.2.27 Generation of calcium competent E.coli DH5α cells

For generation of competent cells a preculture was prepared. Therefore, a single colony or 5-10 µl of competent cells were inoculated overnight at 37°C in 10 ml LB medium. The next day 6 ml of the overnight culture were inoculated with 300 ml LB medium and cells were grown until they had

reached an OD 600 of 0.2. Cells were incubated on ice for 30 min and were centrifuged at 1,000 g for 10 min. The pellet was resuspended in 100 ml of ice cold 0.1 M sterile filtered $CaCl_2$ and was incubated on ice for 15 min. The bacteria were centrifuged at 1,000 g for another 10 min. Afterwards the pellet was resuspended in 12.5 ml of ice cold 0.1 M sterile filtered $CaCl_2$ containing 15 % glycerol. After another incubation on ice for 15 min, the cells were aliquoted, frozen in liquid nitrogen and stored at -80°C.

4.2.28 Chemical Transformation

For chemical transformation DH5α- (for mini plasmid DNA preparation) or BL21-cells (for protein expression) were used. 25 ng Plasmid-DNA was added to a chilled Eppendorf tube with an aliquot (200 µl) of the appropriate *E.coli* strain and were incubated on ice for 20 min.

A heat shock was performed at 42°C for 90 seconds in a heating block. After incubation on ice for 5 min, the sample was incubated with 800 µl LB medium at 37°C for 45 min. Afterwards the cells were centrifuged for 5 min at 5,000 rpm, the supernatant was decanted and the pellet was resuspended in the remaining fluid. The suspension was spread on preheated LB-Agar plates containing the appropriate antibiotic. The plates were incubated overnight at 37°C.

The next day single colonies were picked and preculture was prepared. Therefore, 5 ml LB-Medium for mini plasmid DNA preparation or 10 ml for protein expression were incubated overnight at 37°C in the shaking incubator.

4.2.29 Mini Plasmid DNA Preparation

Mini plasmid DNA preparation was performed using PureYield Plasmid Miniprep System (Promega, USA) according to manufacturer´s instructions.

4.2.30 Expression of recombinant proteins

400 ml of LB medium, supplemented with ampicillin and chloramphenicol (final concentration: 100 µg/ml) were inoculated at 37°C with 10 ml of an overnight culture of *E.coli* BL21, transformed with the pet15b plasmid. Cells were grown at 37°C and optical density at 600 nm was measured until it reached 0.7. 1 ml of culture was taken as control for the protein expression. The expression of the protein of interest was induced by adding β-D-1-thiogalactopyranoside (IPTG) (final concentration 1 mM). The culture was incubated shaking at RT overnight. Cells were harvested the next day. Therefore, the culture was put on ice, a sample for the control of the protein expression was taken and the culture was centrifuged for 10 min at 4°C with 5,000 rpm. The pellet was washed in 20 ml

cold PBS, centrifuged another time for 10 min at 4°C with 5,000 rpm and stored for protein purification at -20°C. To control the success of the protein expression a SDS-PAGE and Coomassie-staining were performed.

4.2.31 Purification of recombinant proteins

The bacteria pellets were thawn and resuspended in 20 ml sodium phosphate buffer (20 mM sodium phosphate, 0.5 M NaCl, pH 7.4) containing 20 mM imidazole. 20 mg lysozyme and a spatula top DNAseI were added to the suspension, mixed and incubated for 30 min at room temperature. Following the enzymatic lysis, a mechanical lysis was performed. Therefore, the bacteria were sonicated 3 times with an intensity of 85 % for 2 min 30 sec. After sonification the cell suspension was centrifuged at 4°C and 10,000 rpm for 30 min. The supernatant was transferred into a new tube and the pellet was discarded. Proteins cloned as His-tagged fusion proteins were purified according to the IMAC (immobilized metal affinity chromatography) technique using columns (GE Healthcare Life Science, US). The purification was performed according to the manufactures instructions. First the storage solution of the columns was removed and then the columns were equilibrated with sodium phosphate buffer containing 20 mM imidazole. Afterwards the lysate was applied to the column. Following, the columns were washed with sodium phosphate buffer containing 20 mM imidazole and the protein was eluted with sodium phosphate buffer containing 250 mM imidazole. The eluates were collected in 500 µl fractions and the concentration was measured with nano-drop using molecular weight and extinction-coefficient of the target protein. The columns were washed with sodium phosphate buffer and stored with 20 % ethanol. Samples of the lysate, flow-through, wash fraction and eluates were analyzed by an SDS-PAGE and coomassie-staining. Afterwards recombinant proteins were dialysed against PBS. The membrane was prepared according to manufactures instruction (6-8 kD Spectra/Por Dialysis membrane) and recombinant protein was loaded into dialysis tubing overnight at 4°C. The next day concentration of proteins was determined with Nanodrop 2000 (Thermo Scientific, USA).

5 Results

5.1 Differentiation

First, we investigated the impact of Grx2c on oligodendrocyte specific properties in A2B5[+]- and NG2^{+}-cells. In the following experiments Grx2 levels were up- or down regulated with different methods. It is important to note that the Grx2 siRNA and the Grx2 morpholino used in this study are not specific for the cytosolic isoform of Grx2 (Grx2c), while for example the treatment with recombinant protein or qRT-PCR analysis are specific for Grx2c.

5.1.1 Grx2c is regulated during oligodendrocyte differentiation

To investigate the regulation of Grx2c in differentiation of oligodendrocyte precursor cells A2B5-cells were differentiated for 5 days and Grx2c expression was analyzed by qRT-PCR after 0, 1, 3 and 5 days as described in *4.2.26*. In comparison to d0 (100 %; n=7) level of Grx2c increased on d1 to 171.8 % ± 66.88 before it decreased to 124.1 % ± 24.17 on d3 and to 72.31 % ± 15.2 on d5 (Fig. 5).
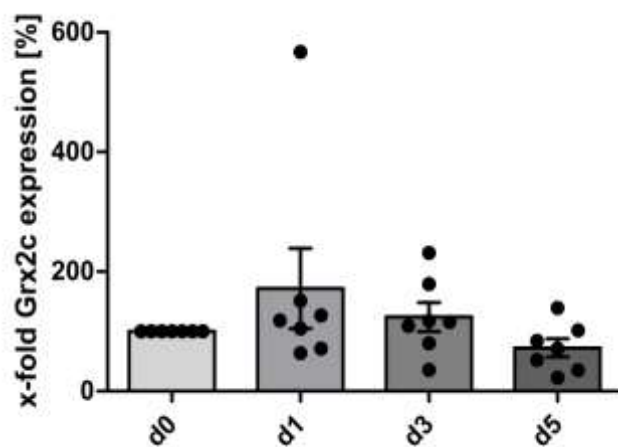
Figure 5: Grx2c is regulated during oligodendrocyte differentiation. 750,000 NG2-cells were differentiated for 5 days. Afterwards they were harvested, RNA was isolated by Trizol extraction and gene expression was quantified using qRT-PCR. Grx2c expression was quantified after 0d, 1d, 3d, and 5d and was normalized to GAPDH expression. n=7

5.1.2 Grx2c is taken up by NG2^{+}-cells

To investigate the effect of Grx2c on A2B5[+]- and NG2^{+}-cells recombinant Grx2c protein was expressed and purified as described in *4.2.30 and 4.2.31* for the following experiments. It was describe before by our group that Grx2c is taken up by A2B5[+]-cells (Lepka et al., 2017). To examine, if recombinant Grx2c is also taken up by NG2^{+}-cells we treated NG2^{+}-cells for 24 h and 2 h with 2 µM Grx2c, which was labeled with a Flag-tag. Afterwards an acidic wash was performed as described in *4.2.9* to remove the protein from the cell surface before the cells were harvested and western blot was performed as described in *4.2.21*.

Untreated NG2^{+}-cells (ctrl: 0.000 RU) showed no signal after using the anti-Flag antibody, while treated cells showed signal (+2μM Grx2c: 0.0037 RU), which was increased after acidic wash (+ acidic wash: 0.0065 RU) (Fig. 6).
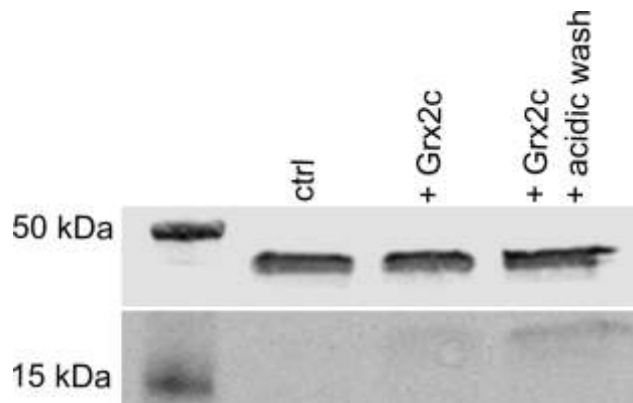
Figure 6: Grx2c is taken up by NG2^{+}-cells. 750,000 NG2^{+}-cells were treated for 24 h and 2 h with 2μM recombinant Grx2c with a Flag-tag. Acidic wash was performed and cells were harvested afterwards for western blot. Membrane was stained with anti-Flag and anti-actin antibodies.

5.1.3 Grx2c blocks differentiation of oligodendrocyte precursor cells in the NG2-state

To shed light on the effect of Grx2c expression on differentiation of oligodendrocyte precursor cells (OPCs), primary NG2^{+}-cells were isolated as described in *4.2.1* and differentiated afterwards by changing to differentiation medium containing T3 and T4. Cells were either treated with 2 μM Grx2c or were kept untreated as control. Afterwards cells were differentiated for 1, 3 or 5 days before immunocytochemistry was performed using antibodies against NG2, CNPase and MBP. Nuclei were visualized by DAPI and amount of NG2^{+}-, CNPase[+]- and MBP[+]-cells was calculated normalized to the total cell number (Fig. 7A).

In untreated control cells the amount of NG2^{+}-cells decreased after day 1 from 53.76 % ± 1.6 (n=5) to 33.31 % ± 6.26 (n=5) after 3 days and further to 15.48 % ± 6.55 (n=3) after 5 days. In contrast the number of CNPase[+]-cells increased with ongoing differentiation from 10.63 % ± 4.22 (day1; n=5) to 14.81 % ± 4.52 (day 3; n=5) to 21.35 % ± 2.22 (day 5; n=3). Also the amount of MBP[+]-cells increased from 2.28 % ± 2.23 at day 1 (n=5) to 8.33 % ± 6.4 at day 3 (n=5) before it decreased again to 6.9 % ± 4.99 at day 5 (n=3). In comparison treatment with 2 μM Grx2c showed higher amounts of NG2+-cells at all timepoints. Here number of NG2^{+}-cells decreased from 60.42 % ± 10.07 (n=5) at day 1 to 49.55 % ± 5.74 (n=5) at day 3 before it decreased to 27.9 % ± 3.68 (n=3) at day 5 of differentiation. The amount of CNPase[+]-cells was constant over time when treated with Grx2c, but lower at day 3 and day 5 compared to the control group (day 1: 15.16 % ± 9.54, n=5; day 3: 13.16 % ± 3.59, n=5; day 5: 13.33 % ± 4.84, n=3). The number of MBP[+]-cells increased from 5.5 % ± 4.05 (day1; n=5) to 6.29 % ± 4.76 (day 3; n=5) before it decreased again to 1.88 % ± 0.87 (day 5; n=3).

To sum up after 5 days of differentiation cells treated with Grx2c showed 12.42 % more NG2^{+}-cells, but 8.02 % less CNPase[+]- as well as 5.02 % less MBP[+]-cells compared to control (Fig. 7B).
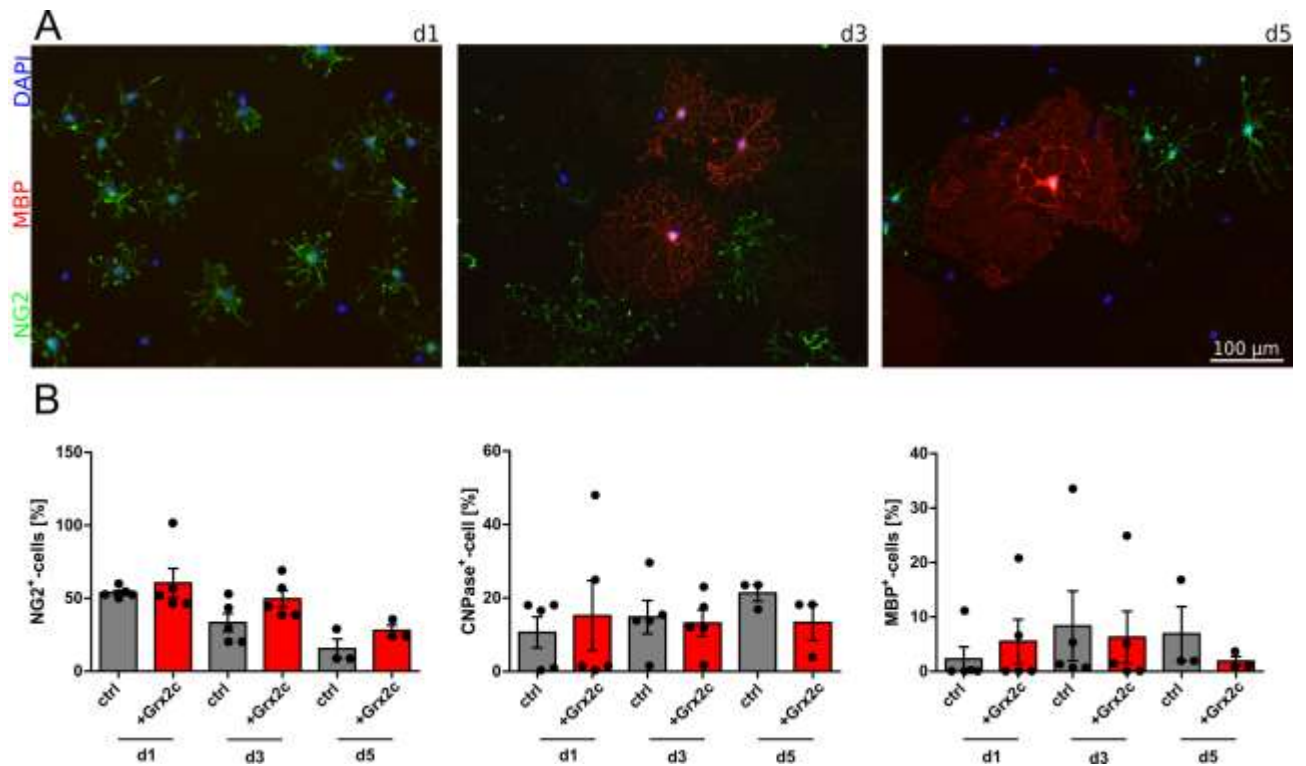
Figure 7: Grx2c blocks differentiation of oligodendrocyte precursor cells in the NG2-state. Primary NG2⁺-cells were isolated and afterwards 30,000 cells were differentiated for 3 or 5 days before immunocytochemistry was performed using antibodies against NG2, CNPase and MBP. Nuclei were visualized by DAPI. Scale bar represents 100 µm (**A**). Cells were either treated with 2 µM Grx2c or were kept untreated as control. Number of NG2+-, CNPase+- and MBP+-cells was calculated normalized to the total cell number (**B**). Statistical significance was determined using the two-tailed student's t-test, shown with mean and ± SEM. There were no statistically significant differences between control and Grx2c treatment. d1, d3 n=5; d5 n=3

5.1.4 Grx2 knock-down increases number and size of CNPase⁺- and MBP⁺-cells in differentiating OPCs

Next the effect of Grx2 knockdown on the number of NG2⁺-, CNPase⁺- and MBP⁺-cells in primary oligodendrocytes was investigated. Therefore NG2⁺-cells were either treated with control or Grx2 siRNA before differentiation was induced for up to 3 days. Treatment with Grx2 siRNA decreased Grx2c level to 22.36 % ± 0.315 in NG2⁺-cells in comparison to control (100 %).

In control as well as in Grx2 knockdown group number of NG2⁺-cells decreased similar over time (ctrl siRNA: 48.7 % ± 4.02 (d 1), 39.85 % ± 2.72 (d 2), 34.39 % ± 10.8 (d 3); n=3; Grx2 siRNA: 42.84 % ± 2.59 (d 1; p=0.6941), 39.92 % ± 3.36 (d 2; p=0.6867), 34.78 % ± 6.60 (d 3; p=0.9695); n=3). In control cells the number of CNPase⁺-cells increased from 23.08 % ± 3.88 (d 1) to 37.62 % ± 3.77 (d 2) before it decreased to 10.99 % ± 5.36 (d 3) (n=3). The number of MBP⁺-cells stayed constant at day 1 (1.76 % ± 1.03) and day 2 (1.77 % ± 0.55) before it increased to 10.17 % ± 6.18 at day 3 (n=3). In contrast Grx2 knockdown increased number of CNPase⁺- and MBP⁺-cells in comparison to control group. In Grx2 knockout cells number of CNPase⁺-cells increased from 27.79

% ± 3.63 (d 1) to 35.01 % ± 4.28 (d 2) before it decreased to 21.2 % ± 5.24 (d 3) (n=3). Number of MBP⁺-cells increased from 2.36 % ± 1.5 (d 1) to 7.74 % ± 1.38 (d 2) to 9.71 % ± 4.08 (d 3) (n=3). To sum up after 3 days compared to control the number of CNPase⁺-cells was 10.21 % higher when Grx2 was knocked down, while after 2 days the amount of MBP⁺-cells was 5.97 % higher (Fig. 8A). In the next step we repeated the differentiation experiment with primary A2B5⁺-cells isolated from Grx2 knock-out mice. This Grx2-lacZ mouse strain was established together with Dr. Marcus Conrad (Helmholz Zentrum München, Munich, Germany). As mentioned in *4.2.16* in this mouse strain a *lacZ* gene replaces the *Glrx2* gene. Primary A2B5⁺-cells isolated from homozygous mice show a knock-down of Grx2c expression to 1.325 % ± 0.4911 (n=3; p<0.0001) compared to control cells isolated from C57BL/6J mice.

As described in *5.1.3* cells were differentiated for 1, 3 or 5 days before immunocytochemistry was performed using antibodies against NG2, CNPase and MBP. Nuclei were visualized by DAPI and amount of NG2⁺-, CNPase⁺- and MBP⁺-cells was calculated normalized to the total cell number.

Control as well as Grx2 knock-out cells showed a decrease of NG2⁺-cells over time. In control cells it decreased from 34.33 % ± 3.01 at day 1 to 29.31 % ± 2.17 at day 3 to 21.84 % ± 1.22 at day 5. Number of CNPase positive cells decreased from 10.41 % ± 2.21 at day 1 to 8.98 % ± 0.99 at day 3 of differentiation before it incresaed to 12.65 % ± 1.15 at day 5. The number of MBP positive cells increased from 0.06 % ± 0.02 at day 1 to 4.98 % ± 0.62 at day 3 to 7.43 % ± 0.82 at day 5. In comparison in Grx2 knock-out cells the amount of NG2⁺-cells decreased from 26.17 % ± 2.57 (p=0.0429) at day 1 to 26.03 % ± 2.51 at day 3 to 20.63 % ± 1.53 at day 5. Number of CNPase positive cells decreased from 18.75 % ± 2.93 (p=0.0259) at day 1 to 14.75 % ± 0.90 (p<0.0001) at day 3 before it slightly increased to 17.79 % ± 1.21 (p=0.0029) at day 5. In contrast number of MBP⁺-cells increased from 3.46 % ± 1.00 (p=0.0011) at day 1 to 8.41 % ± 0.74 (p=0.0007) at day 3 and 11.98 % ± 0.92 (p=0.0004) at day 5. In conclusion the number of NG2⁺-cells was lower in the Grx2 knock-out cells, while the number of CNPase⁺- and MBP⁺-cells was higher in Grx2 knock-out cells on all three timepoints compared to control (Fig. 8B).

Furthermore, the size of CNPase⁺- and MBP⁺-cells after 3 days of differentiation was determined. Grx2 knock-out cells did not only show a higher amount of CNPase⁺- and MBP⁺-cells compared to control, the cells were also bigger in size indicating an earlier start of differentiation. Compared to control they showed an increase in size to 169.5 % ± 9.44 for CNPase⁺-cells (ctrl: 100 ± 5.52; p<0.0001) and 176.3 % ± 11.12 for MBP⁺-cells (ctrl: 100 ± 6.90; p<0.0001) (Fig. 8C).
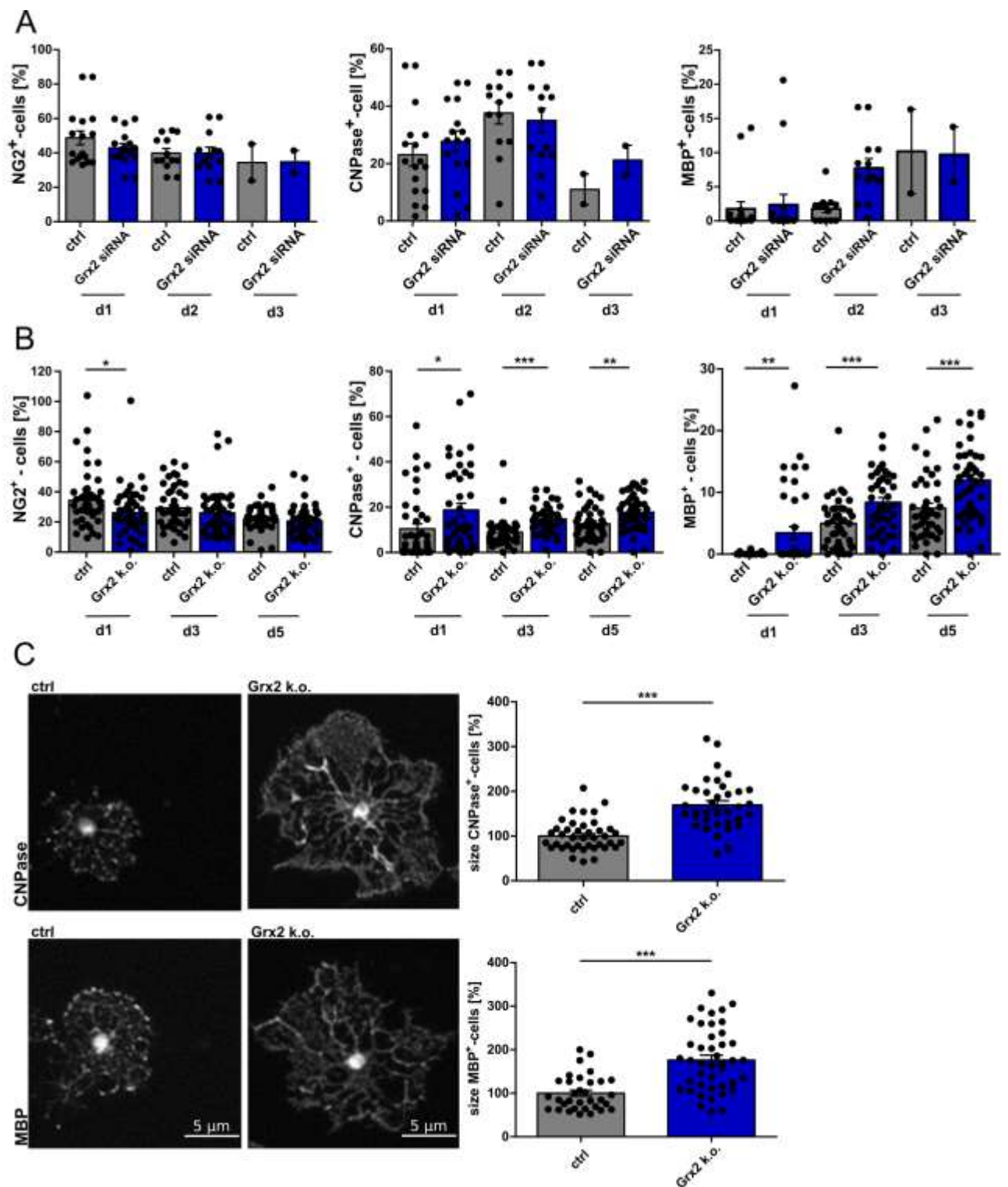
Figure 8: Grx2 knock-down affects differentiation of A2B5⁺-cells and NG2⁺-cells. Primary A2B5⁺- or NG2⁺-cells were isolated and afterwards 30,000 cells were differentiated for up to 5 days before immunocytochemistry was performed using antibodies against NG2, CNPase and MBP. Nuclei were visualized by DAPI. NG2⁺-cells were either treated with ctrl or Grx2 siRNA, n=3 (**A**). Primary A2B5⁺-cells were isolated from Grx2 knock-out (k.o.) or C57BL/6J (ctrl) mice, n=4 (**B**). Number of NG2+-, CNPase+- and MBP+-cells was calculated normalized to the total cell number (**A, B**). Furthermore, the size of CNPase+- and MBP+-cells was determined after 3 days of differentiation. Scale bar represents 5 µm (**C**). Statistical significance was determined using the two-tailed student's t-test, shown with mean and ± SEM. *: $p < 0.05$; **: $p < 0.01$; ***: $p < 0.001$

5.1.5 Grx2 knock-down leads to loss of visual function in mice

To investigate if this effect of Grx2 on differentiation of OPCs *in vitro* also affects functional myelination *in vivo* optomotor response (OMR) and optical coherence tomography (OCT) were performed. The retina is part of the CNS and contains retinal ganglion cells, the neurons of the optic nerve. The functional and structural evaluation of the visual pathway is relatively easy, little time-consuming and non-invasive and can provide insight to the mechanisms occurring during myelination. Therefore, optomotor response (OMR) and optical coherence tomography (OCT) were performed to analyze the influence of Grx2 knock-out on visual function and thickness of retinal layers of mice. Here visual function is evaluated by spatial frequency by OMR and neuroaxonal damage is assessed as total retinal thickness (TRT) and inner retinal layer (IRL) thinning by OCT. Therefore, measurements were performed with C57BL/6J (ctrl) and Grx2-lacZ (Grx2 knock-out) mice every week from the age of 3 to 13 weeks. OCT measurements and OMR analysis were performed at the same time points.

OMR reveals a decreased visual acuity of Grx2 knock-out animals to 67.5 % ± 4.06 over 13 weeks in comparison to control (100 %). OMR measurements were analyzed using AUC compared by generalized estimating equations (GEE) with an exchangeable correlation matrix to adjust for intrasubject inter-eye correlations using SPSS (Fig. 9A).

Further OCT analysis detected an increase of the total retinal thickness (TRT) and a thinning of the inner retinal layer (IRL) in control as well as in Grx2 knock-out mice. There were no significant differences between the two groups (Fig. 9B).
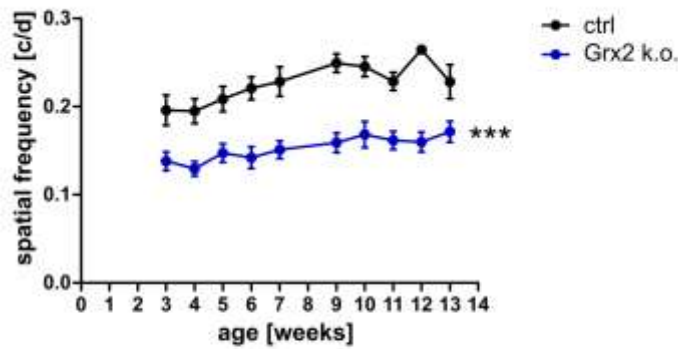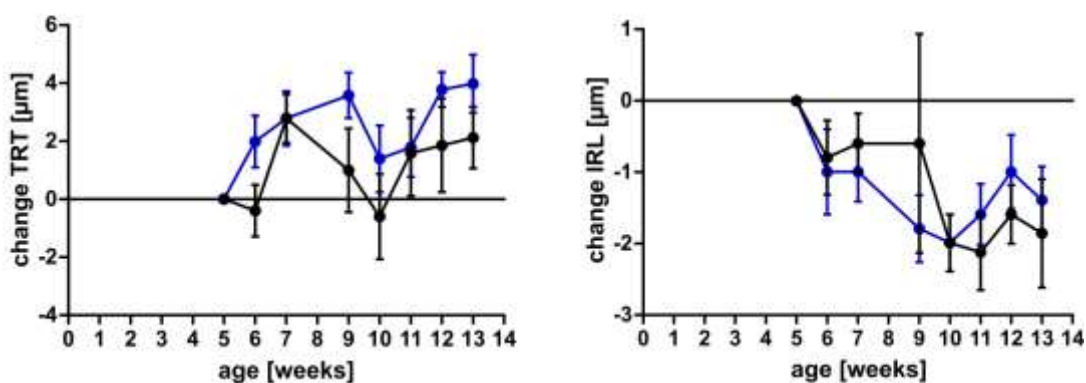
Figure 9: Grx2 knock-down mice show loss of visual function and retinal layer thinning. Optomotor response (OMR) **(A)** and optical coherence tomography (OCT) **(B)** were performed over 11 weeks to analyze visual function and retinal layer thickness of C57BL/6J (ctrl) and Grx2-lacZ (Grx2 k.o.) mice. The graphs represent the mean and standard error of the mean of at least 3 animals per group.

5.1.6 Grx2c promotes migration of A2B5⁺- and NG2⁺-cells

5.1.6 Grx2c promotes migration of A2B5$^+$- and NG2$^+$-cells

Afterwards, the impact of Grx2c on migration of A2B5$^+$- and NG2$^+$-cells was investigated. First, we performed a transwell-migration assay as described in *4.2.6*. A2B5$^+$- or NG2$^+$-cells in proliferation medium were plated in the upper compartment, while the complete well contained either control medium without treatment or medium containing 2 µM wt Grx2c or inactive Grx2c C37S mutant. Furthermore, a Grx2 knockdown was performed in A2B5$^+$- as well as in NG2$^+$-cells. After 24 h migrated cells were visualized with Hoechst and quantified.

In both cell types treatment with 2 µM Grx2c increased the number of migrated cells to 169.4.30 % ± 12.58 in A2B5$^+$-cells (p<0.0001; N=4, n=21) and to 211.4 % ± 13.80 in NG2$^+$-cells (p<0.0001; N=6, n=29) in comparison to the control group (A2B5: 100 % ± 8.30; NG2: 100 % ± 8.09). In contrast treatment with the inactive Grx2c C37S mutant did not alter migration abilities of A2B5$^+$- (91.01 % ± 9.74; N=4, n=18) or NG2$^+$-cells (104.5 % ± 9.55; N=6, n=20). Treatment with Grx2 siRNA decreased Grx2c level to 19.8 % ± 2.896 in A2B5$^+$- and 22.36 % ± 0.315 in NG2$^+$-cells in comparison

to control (100 %). This knockdown of Grx2 decreased migration of both cell types to 66.93 % ± 9.35 (p=0.0203; N=3, n=6) in A2B5$^+$- and to 75.17 % ± 5.44 (p=0.0023; N=3, n=6) in NG2$^+$-cells in comparison to cells treated with ctrl siRNA (A2B5: 100 % ± 7.51; NG2: 100 % ± 4.17) (Fig. 10).
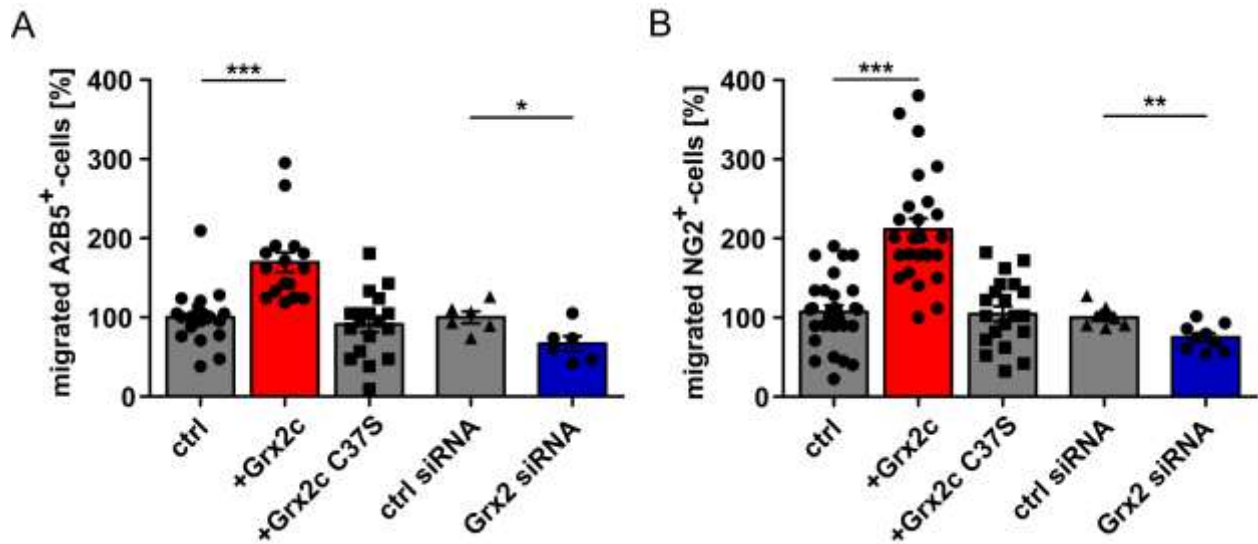
Figure 10: Grx2c level affects migration of A2B5$^+$- and NG2$^+$-cells. Transwell-migration assay was performed with 50,000 A2B5$^+$- (**A**) or NG2$^+$-cells (**B**). Cells were either kept untreated as control, were treated with 2 µM Grx2c or 2 µM Grx2c C37S (inactive mutant) (A2B5: n=4; NG2: n=6). Grx2 knockdown was performed using siRNA (A2B5: n=3; NG2: n=3). After 24 h migrated cells were visualized using Hoechst and quantified. Statistical significance was determined using the two-tailed student's t-test, shown with mean and ± SEM. *: p <0.05; **: p <0.01; ***: p < 0.001

5.1.7 Grx2 knock-down reduces number of migrated Olig2$^-$-, ClaudinK$^+$- and MBP$^+$-cells, while Grx2 overexpression increases number of migrated Olig2$^+$-cells in zebrafish

To shed light on the effect of Grx2 expression on differentiation and migration abilities *in vivo* zebrafish experiments were conducted. Therefore, Grx2 expression in zebrafish was down regulated by morpholino injection as described in *4.2.13* or Grx2 overexpressing zebrafish were used for analysis. 3 days (Olig2$^+$, ClaudinK$^+$) or 4 days (MBP$^+$) after fertilization and morpholino injection fish were sorted and prepared for Two-Photon microscopy. For quantitative analysis spinal cord was imaged and within 4 hemisegments of the spinal cord dorsally migrated Olig2$^-$-, ClaudinK$^+$- and MBP$^+$-cells were counted.

Knockdown of Grx2 decreased number of migrated Olig2$^+$-cells to 10.38 ± 2.418 (control: 24.44 ± 1.493; p<0.0001; N=4, n=16), number of migrated ClaudinK$^+$-cells to 9.6 ± 2.296 (control: 16.89 ± 1.585; p=0.0205; N=4, n=10) and MBP$^+$-cells to 2.1 ± 0.722 (control: 12.50 ± 1,302; p<0.0001; N=4, n=10) (Fig. 11A). In line, Grx2 overexpression increased number of migrated Olig2$^+$-cells to 16.54 ± 1.111 (p=0.0150; n=28) in comparison to control (13.07 ± 0.8304). However, number of migrated

ClaudinK[+]-cells was not altered by Grx2 overexpression (14.33 ± 1.441; control: 17.95 ± 1.629; p=0.1036; N=3, n=21) (Fig. 11B). Unfortunately, data concerning migrated MBP[+]-cells in Grx2 overexpressing zebrafish are missing, because all zebrafish died after fertilization.
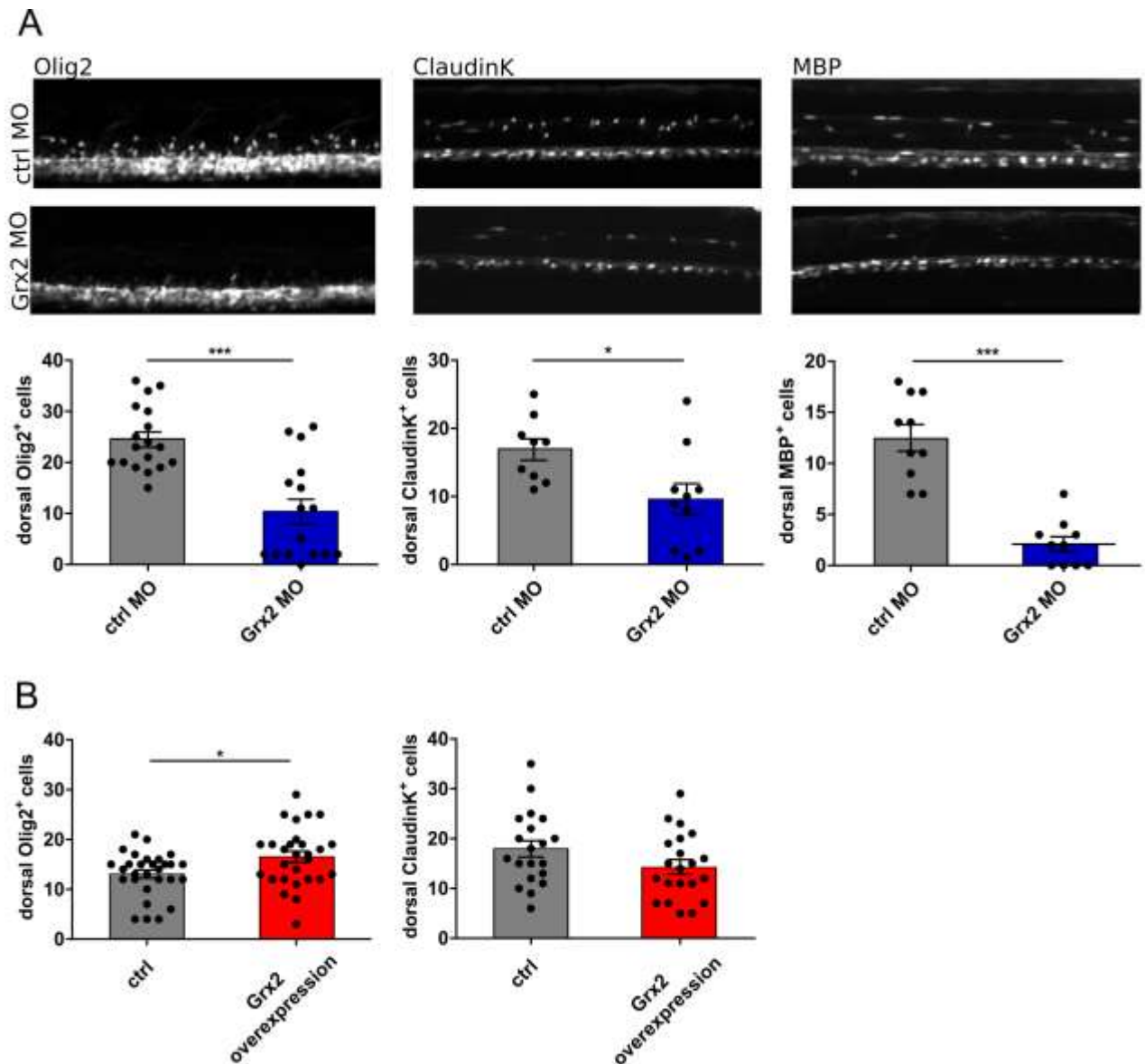

Figure 11: Grx2 level influences number of migrated Olig2+-, ClaudinK+- and MBP+-cells in zebrafish. Zebrafish with modulated expression of Grx2 (down regulation via morpholino injection), n=4 (**A**), Grx2 overexpression, n=3 (**B**) were used for analysis. 3 days (Olig2+, ClaudinK+) or 4 days (MBP+) after fertilization respectively after morpholino injection fish were sorted and prepared for 2-Photon microscopy. For analysis spinal cord was imaged and within 4 hemisegments of the spinal cord dorsally migrated Olig2+-, ClaudinK+- and MBP+-cells were counted. Statistical significance was determined using the two-tailed student's t-test, shown with mean and ± SEM. *: p <0.05; **: p <0.01; ***: p < 0.001

5.2 Dedifferentiation

Next, we investigated the impact of Grx2c on dedifferentiation under pathological conditions like cancer and endometriosis.

5.2.1 NG2 expression is up regulated in Grx2c overexpressing HeLa-cells

First, we determined the impact of Grx2c overexpression on NG2 expression in HeLa-cells, taking advantage of already existing Grx2c overexpressing HeLa-cells (HeLaGrx2c). Therefore, qRT-PCR was performed using HeLa wt or HeLaGrx2c cells. NG2 expression was normalized to GAPDH expression. In comparison to HeLa wildtype (106.1 % ± 46.28; n=8) HeLaGrx2c cells showed increased NG2 expression (451.9 % ± 115.7; p=0.0149; n=8) (Fig. 12).
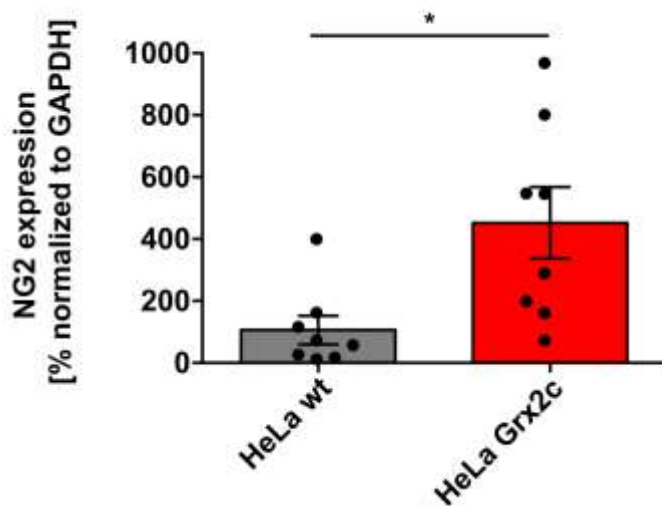
Figure 12: NG2 expression in HeLa wildtype and HeLaGrx2c cells. 10^6 HeLa wt or HeLaGrx2c cells were seeded and cultivated for 24h. Afterwards they were harvested, RNA was isolated by Trizol extraction and gene expression was quantified using qRT-PCR. NG2 expression was normalized to GAPDH expression. Statistical significance was determined using the two-tailed student's t-test, shown with mean and ± SEM. *: p <0.05; **: p <0.01; ***: p < 0.001; n=8

5.2.2 Grx2 knockdown in glioblastoma cells decreases NG2 expression, while Grx2 overexpression increases NG2 expression

Next, we investigated the impact of Grx2 amount on NG2 expression in the glioblastoma models, U343-MGA and GBM18. Therefore qRT-PCR was performed. Grx2 was knocked down using siRNA in U343-MGA- and GBM18-cells and stable Grx2 overexpressing U343-MGA-cells (pExpress Grx2) were generated as described in *4.2.10.* Cells were cultivated for 24 h, RNA was isolated by Trizol extraction and gene expression was quantified using qRT-PCR. Grx2c and NG2 expression were normalized to GAPDH expression. In comparison to control (100 %; n=5) Grx2c knockdown to 33.6 % ± 14.4 in GBM18-cells showed decreased NG2-expression (66.81 % ± 9.849; n=5). In contrast this could not be shown for Grx2c knockdown (30.68 % ± 24.03) in U343-MGA-cells (ctrl siRNA: 100 %; Grx2 siRNA: 224.4 % ± 61.9; n=6). However, overexpression of Grx2c (151.6 % ± 21.07) increased NG2 expression up to 740.7 % ± 503.0 (n=5) (Fig. 13A).

Furthermore, to confirm the impact of Grx2 on NG2 expression immunocytochemistry was performed. Therefore, spheres of U343-MGA-cells were generated as described in *4.2.7* and afterwards ICC was performed to stain for NG2 positive cells. All cells that migrated out of the sphere were positive for NG2, but spheres with decreased levels of Grx2 showed less NG2 positive cells within the center of the sphere. In contrast spheres with an increased amount of Grx2 showed no difference in number and distribution of NG2 positive cells in comparison to the control group (Fig. 13B).
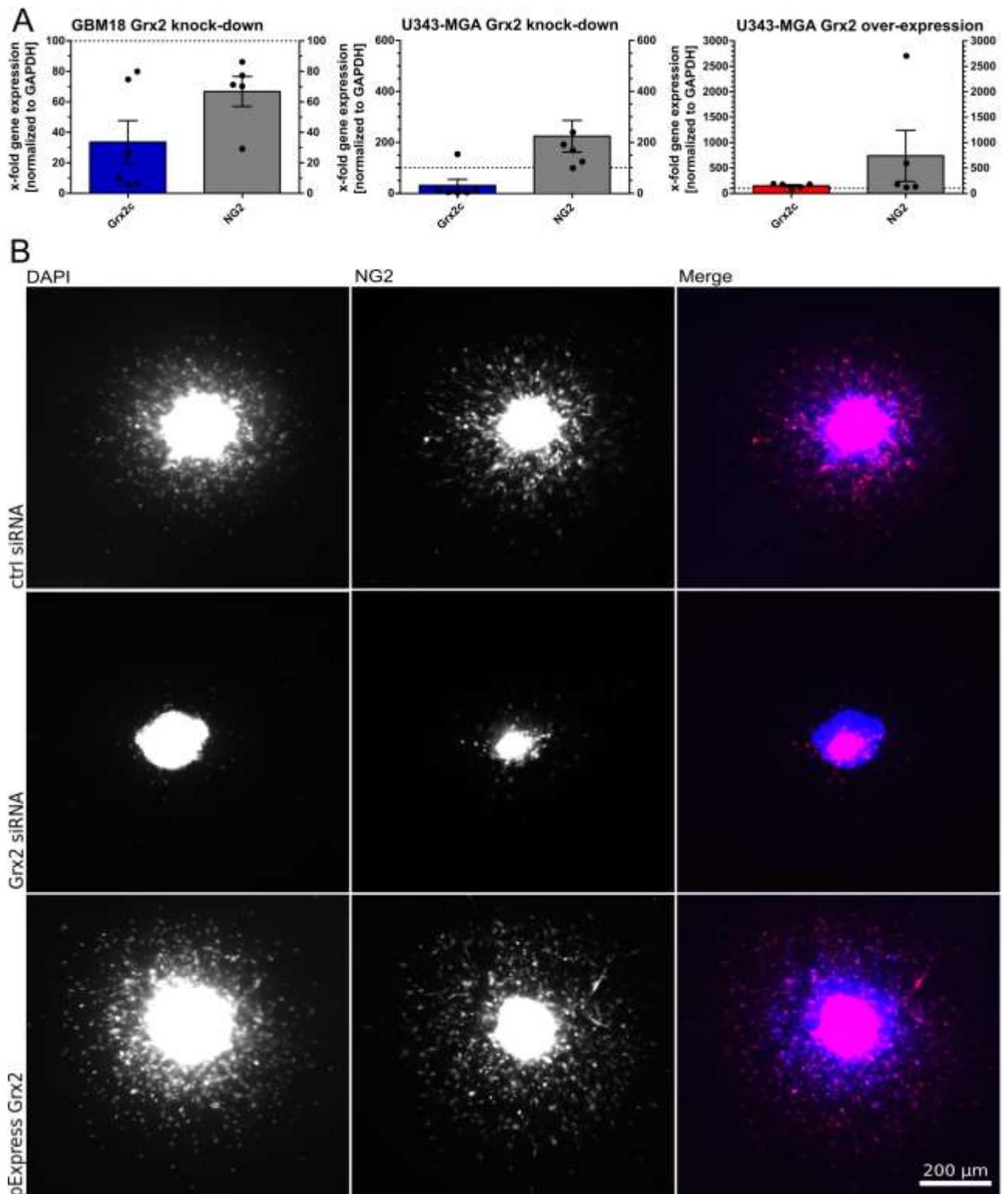
Figure 13: Grx2 amount influences NG2 expression in U343-MGA- and GBM18-cells. 10^6 GBM18- (ctrl siRNA, Grx2 siRNA) and 10^6 U343-MGA-cells (ctrl siRNA, Grx2 siRNA, pExpress Grx2) were harvested for qRT-PCR. RNA was isolated by Trizol extraction and gene expression was quantified using qRT-PCR. Grx2c and NG2 expression were normalized to GAPDH expression; n=5/6 (**A**). Furthermore, U343-MGA spheres were generated and Grx2 was knocked down using siRNA or Grx2 was overexpressed (pExpress Grx2). Spheres were stained using anti-NG2 antibodies und nuclei were visualized by DAPI. Scale bar represents 200 μm; n=3 (**B**).

5.2.3 Grx2c does not influence proliferation of GBM18- and U343-MGA-cells, but increases migration of glioblastoma cells, while knockdown decreases migration

To shed light on the effect of Grx2c on proliferation of glioblastoma cells a BrdU assay as described in *4.2.8* was performed with U343-MGA and GBM18-cells. Therefore, cells were treated either with 2 μM Grx2c or were kept as control without treatment. Proliferating cells were visualized by BrdU incorporation and all cells were counterstained using anti-H3 antibodies and percentage of proliferating cells was determined. In both cell lines presence of 2 μM Grx2c did not influence percentage of proliferating cells (GBM18: ctrl: 20.90 % ± 1.137; + Grx2c: 24.21 % ± 2.529; p=0.226; n=3) (U343-MGA: ctrl: 92.18 % ± 0.8830; + Grx2c. 91.37 % ± 1.541; p=0.6518; n=3) (Fig. 14A).

The impact of Grx2c on migration and invasion of glioblastoma cells was investigated using a transwell-migration assay and a 3D spheroid assay. Transwell-migration assay was performed as described in *4.2.6* and GBM18, GBM1- and U343-MGA-cells were either kept untreated as control or treated with 2 μM Grx2c. In U343-MGA-cells also a Grx2 knockdown with siRNA was performed. After 48 h migrated cells were visualized with DAPI and quantified. In comparison to control (100 % ± 10.48; n=5) treatment with 2 μM Grx2c increased migration of GBM18-cells to 280.4 % ± 39.57 (p=0.0004; n=5). Also, number of migrated GBM1-cells was increased by Grx2c treatment to 231.3 % ± 25.94 (p=0.0002; n=5) in comparison to control (100 % ± 11.25; n=5). In contrast number of migrated U343-MGA-cells was not influenced by treatment with Grx2c (ctrl: 100 % ± 12.2; + Grx2: 74.76 % ± 9.242; p=0.2978; n=5). However, Grx2c knockdown (6.84 % ± 3.91) decreased number of migrated U343-MGA-cells to 37.00 ± 3.148 (ctrl: 87.27 % ± 5.626; p<0.0001; n=5) (Fig. 14B).

To examine the effect of Grx2 on invasion of glioblastoma cells in a 3D model, a 3D spheroid assay was conducted as described in *4.2.7*. Therefore, Grx2c knockdown in GBM18- (13.46 % ± 2.51) and U343-MGA-cells (4.96 % ± 1.1) was performed as well as Grx2 overexpression in U343-MGA-cells (pExpress Grx2: 165.6 % ± 22.19) as described in *4.2.10*. After 72 h the invasion area of migrated cells was quantified. Grx2 knockdown decreased area of migrated GBM18-cells to 0.8174 square pixel ± 0.095 (ctrl: 2.244 square pixel ± 0.4953; p=0.0015; n=4), as well as area of migrated U343-MGA-cells to 1.124 square pixel ± 0.148 (ctrl: 3.709 square pixel ± 0.26; p<0.0001; n=3). Moreover, Grx2 overexpression increased area of migrated U343-MGA-cells to 6.612 square pixel ± 0.778 (p=0.0158; n=3) (Fig. 14C, D).
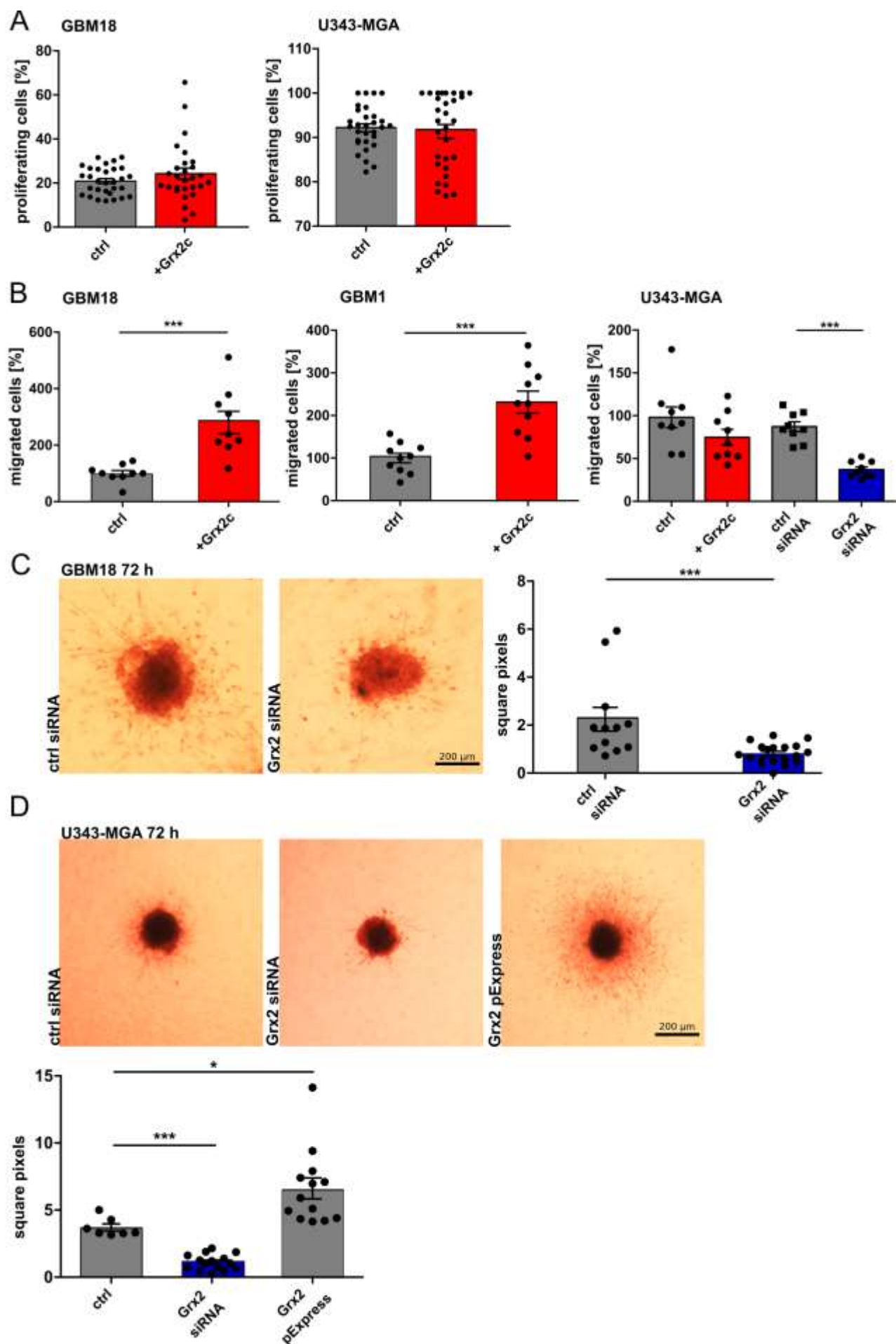
A

GBM18

proliferating cells [%]

ctrl   +Grx2c

U343-MGA

proliferating cells [%]

ctrl   +Grx2c

B

GBM18

migrated cells [%]

***

ctrl   +Grx2c

GBM1

migrated cells [%]

***

ctrl   + Grx2c

U343-MGA

migrated cells [%]

***

ctrl   + Grx2c   ctrl   Grx2
                   siRNA   siRNA

C

GBM18 72 h

ctrl siRNA

Grx2 siRNA

200 µm

square pixels

***

ctrl   Grx2
siRNA   siRNA

D

U343-MGA 72 h

ctrl siRNA

Grx2 siRNA

Grx2 pExpress

200 µm

square pixels

*

***

ctrl   Grx2   Grx2
        siRNA   pExpress

Figure 14: Grx2c does not influence proliferation but increases migration and invasion ability of glioblastoma cells. 30,000 human glioblastoma cells (U343-MGA, GBM18, GBM1) were seeded either untreated as control or treated with 2 µM Grx2c and BrdU assay was performed. Proliferating cells were visualized by anti BrdU-antibodies and all cells were counterstained using anti-H3 antibodies. Number of proliferating cells was calculated (n=3) (**A**). Transwell-migration assay was conducted with 50,000 untreated control cells or cells treated with 2 µM Grx2c. After 48 h cells were visualized using DAPI and quantified (n=5) (**B**). For 3D spheroid assay U343-MGA- and GBM18-cells were embedded into a collagen matrix. Grx2 was knocked down with siRNA or was overexpressed (pExpress Grx2). After 72 h invasion area with migrated cells was quantified (GBM18: n=4; U343-MGA: n=3). Scale bar represents 200 µM (**C, D**). Statistical significance was determined using the two-tailed student's t-test, shown with mean and ± SEM. *: p <0.05; **: p <0.01; ***: p < 0.001

5.2.4 Grx2 expression does not affect morphology of GBM18- and U343-MGA-cells

To investigate if the expression of Grx2 also affects the morphology of GBM18- and U343-MGA-cells Grx2 knockdown was performed using siRNA in GBM18- and U343-MGA-cells. In U343-MGA-cells Grx2 was also overexpressed (Grx2 pExpress). Cells were plated on glasses for microscopy and immunocytochemistry was performed as described in *4.2.4*. Nuclei were visualized by DAPI and actin was stained using Phalloidin. Pictures were taken using the TCS SP8 Confocal Microscope (Leica, Germany) at 40x magnification.

Different expression of Grx2 did not change the morphology neither in GBM18- nor in U343-MGA-cells (Fig. 15).
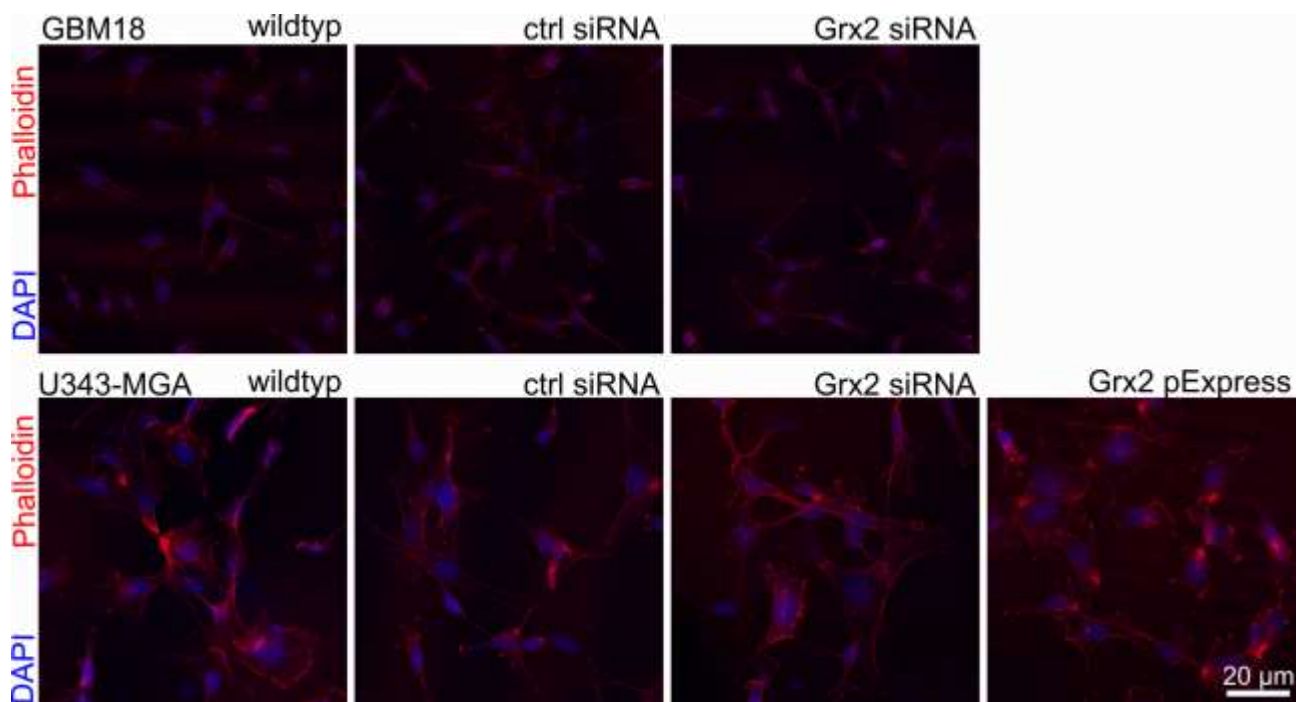
Figure 15: Grx2 expression does not affect morphology of GBM18- and U343-MGA-cells. Grx2 was knocked down using siRNA or Grx2 was overexpressed (pExpress Grx2) in GBM18- and U343-MGA-cells. 30,000 cells were plated on glasses for microscopy and immunocytochemistry was performed. Nuclei were visualized by DAPI and actin was stained using Phalloidin. Pictures were taken using the TCS SP8 Confocal Microscope (Leica, Germany) at 40x magnification. Scale bar represents 20 µm; n=1

5.2.5 Grx2 knockdown reduces outgrowth of glioblastoma cells (U343-MGA) as well as number and length of protrusions in zebrafish

To investigate the impact of Grx2 on migration and invasion of glioblastoma cells *in vivo* U343-MGA-cells were injected into blastula-stage zebrafish embryos as described in *4.2.14*. Cells were either treated with ctrl or Grx2 siRNA. Grx2c expression was decreased to 0.7 % after transfection in comparison to control. After injection embryos were screened for successful transplantation and 24 h post fertilization (hpf) embryos were imaged for another 24 h using 2-photon-microscopy. For analysis number of protrusions was counted and length of protrusions was measured. Knockdown of Grx2 decreased migration and invasion of U343-MGA-cells in zebrafish. The number of protrusions was nearly 4-fold decreased to 2.3 ± 1.2 in comparison to control (8.3 ± 0.8; p=0.0158; N=1, n=3). Furthermore, also the length of protrusions was decreased after Grx2 knockdown to 158.3 µm ± 87.00 (ctrl: 870.0 µm ± 219.3; p=0.0393; N=1, n=3) (Fig. 16).
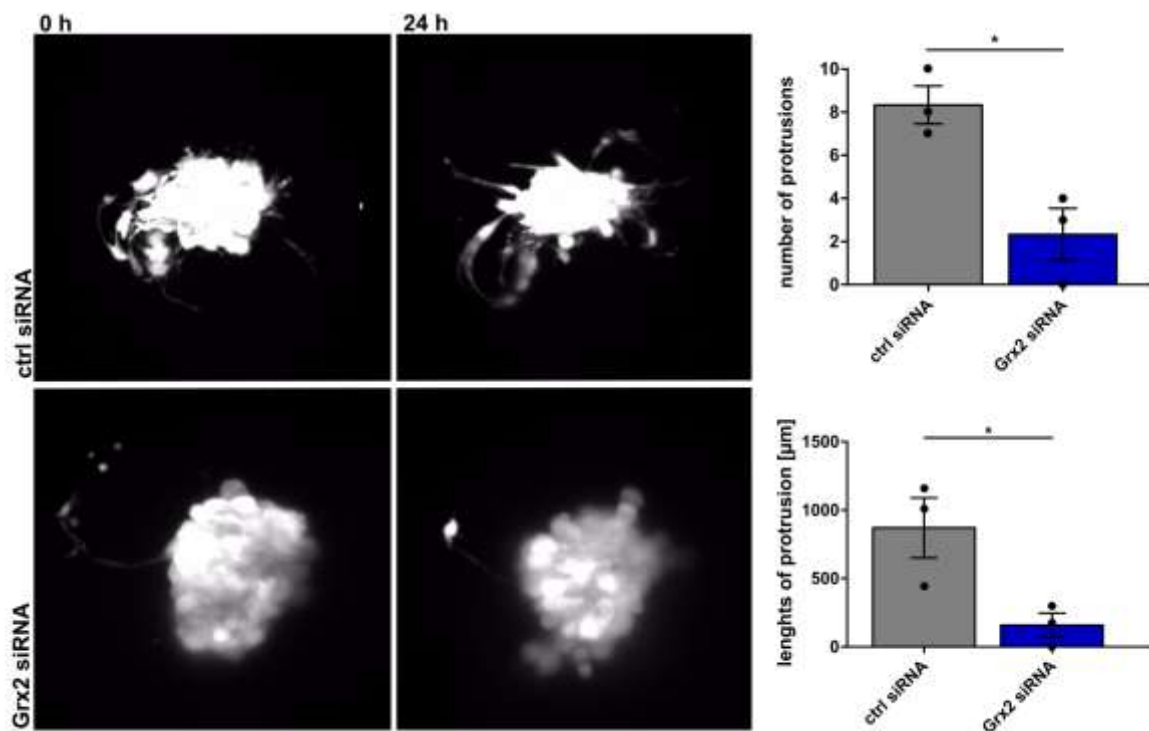
Figure 16: Grx2 knockdown reduces invasion of glioblastoma cells in zebrafish and reduces number as well as length of tumor protrusions. 10^6 U343-MGA-cells were treated with ctrl or Grx2 siRNA. Approximately 100 tumor cells were injected into 1k-cell stage of zebrafish embryos. Embryos with brain tumors were sorted 24 h post fertilization (hpf) and then imaged for 24 h using 2-photon-microscopy. For analysis number of protrusions was counted and length of protrusions was measured. Statistical significance was determined using the two-tailed student's t-test, shown with mean and ± SEM. *: p <0.05; **: p <0.01; ***: p < 0.001; N=1; n=3

5.2.6 Expression of Grx2c and NG2 correlates in glioblastoma patient samples

To investigate if there is a correlation between Grx2c expression and NG2 expression in glioblastoma patient samples qRT-PCR was conducted using glioblastoma patient samples kindly provided by Prof. Dr. Guido Reifenberger (Neuropathology, Heinrich-Heine-University, Dusseldorf, Germany). RNA was isolated by Trizol extraction and Grx2c and NG2 transcripts were normalized to GAPDH expression. Human total RNA (Takara, Japan) was used as healthy control.

15 patient samples (GB3742, GB3746, GB3839, GB3847, GB3783, GB1224, GB3039, GB1208, GB1246, GB1215, GB1172, GBM1174, GB1191, GB1245, and GB3037, all WHO grade IV) were tested for Grx2c and NG2 expression. All 15 patient samples showed an increase in NG2 expression compared to healthy control, while some tumors showed an increased and some a decreased Grx2c expression. Patient samples displayed a correlation between Grx2c and NG2 expression. Tumors with a high expression of Grx2c also displayed a high expression of NG2 (Fig. 17).
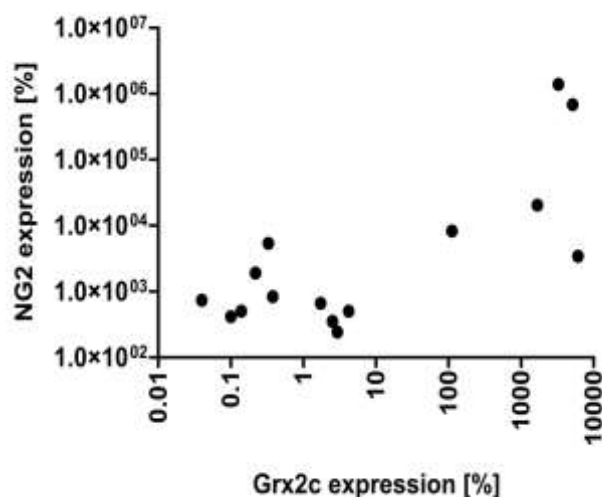
Figure 17: Grx2c expression and NG2 expression correlate in glioblastoma patient samples. Glioblastoma patient samples were kindly provided by Prof. Dr. Reifenberger. RNA was isolated by Trizol extraction and gene expression was quantified using qRT-PCR. Grx2c and NG2 expression were normalized to GAPDH expression. Human total RNA (Takara, Japan) was used as a healthy control. N=3, n=15

5.2.7 Grx2c promotes migration (in vitro) and invasion (in vivo) of melanoma cells

To examine if the influence of Grx2c on migration and invasion is specific for the brain and glioblastoma cells we wanted to conduct migration experiments with other type of tissue and cancer cells. Therefore, we decided to shed light on the effect of Grx2c on the migration and invasion ability of melanoma cells.

In the following three human melanoma cell lines, 1205LU-GFP, Skmel2 and WM3734, were kept untreated as control or were treated with 2 µM Grx2c and transwell-migration assay was performed as described in *4.2.6*. After 48 h migrated cells were visualized with DAPI and quantified. In comparison to control (1205LU-GFP: 100 % ± 51.04; Skmel2: 100 % ± 17.57; WM3734: 100 % ± 30.21; n=4) treatment with 2 µM Grx2c increased migration of 1205LU-GFP-cells to 140.1 % ±

69.48 (p=0.6585; n=4), 145.6 % ± 16.21 (p=0.1048; n=4) in Skmel2-cells and 148.8 % ± 48.26 (p=0.4241; n=4) in WM3734-cells (Fig. 18A).

Invasion and metastatic ability of melanoma cells *in vivo* was investigated in zebrafish. Therefore, Skmel2-cells were injected into the yolk of zebrafish embryos 48 hpf as described in *4.2.14*. Cells were either kept untreated as control or were treated with 2 µM Grx2c. After injection embryos were screened for successful transplantation and were imaged after 2 days. Control melanoma cells showed distribution just into the yolk, while in zebrafish that were injected with Grx2c-treated melanoma cells melanoma cells were found in different organs, such as the spinal cord and even in the blood producing area in the tail. So Grx2c increased metastatic ability of melanoma cells. 0 out of 11 zebrafish injected with control melanoma cells showed metastasis, while the injection of Grx2c-treated cells led to metastasis in 4 out of 12 zebrafish (N=3, n=12) (Fig. 18B).
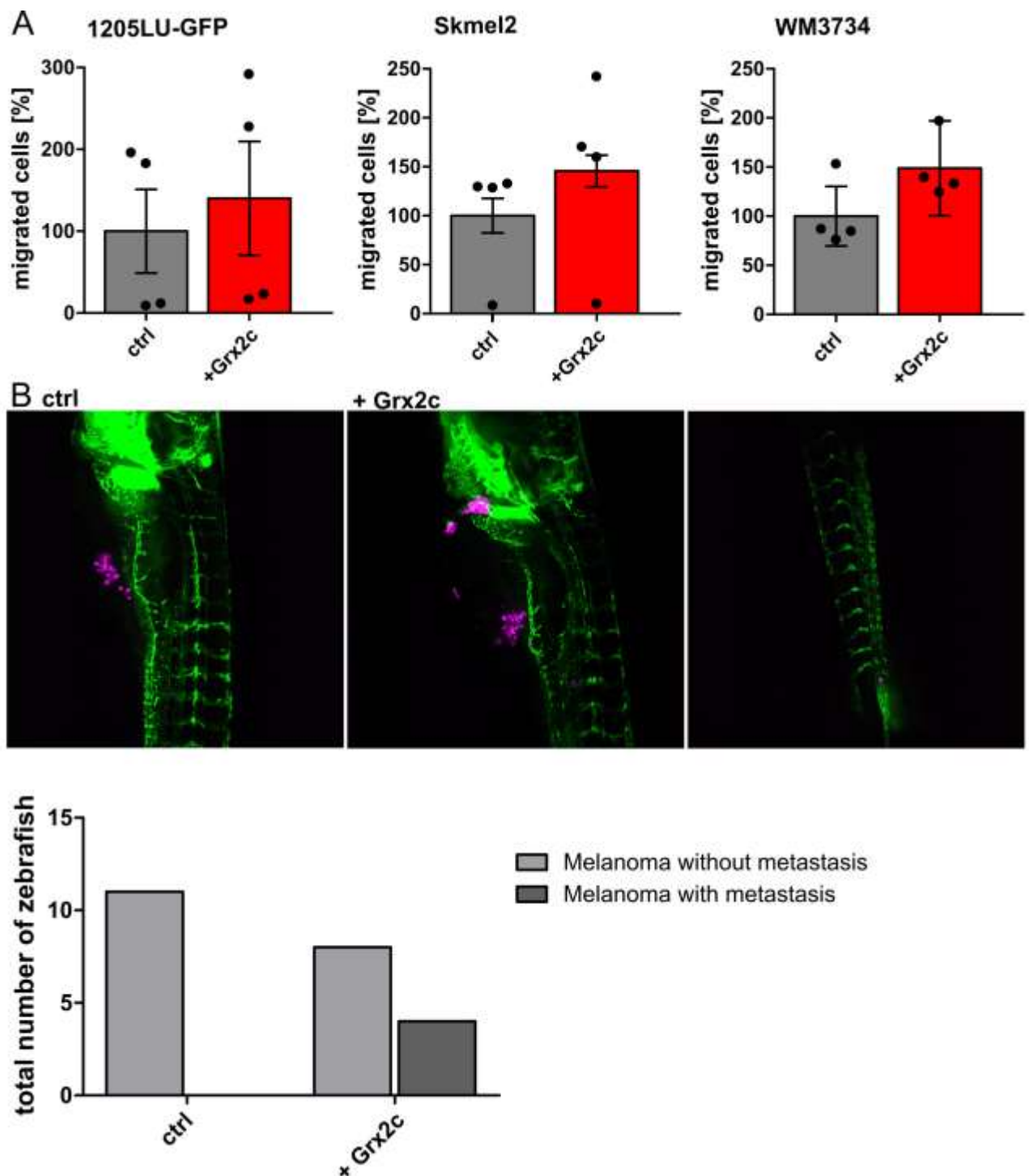
Figure 18: Grx2c promotes migration and metastic ability of melanoma cells. Transwell-migration assay was conducted with 50,000 untreated control cells or cells treated with 2 µM Grx2c. After 48 h cells were visualized using DAPI and quantified; n=4. Statistical significance was determined using the two-tailed student's t-test, shown with mean and ± SEM. There were no statistically significant differences between control and Grx2 treatment **(A).** 10^6 Skmel2-cells were kept untreated as control or were treated with 2 µM Grx2c. Approximately 100 tumor cells were injected 24 h post fertilization (hpf) into the yolk of zebrafish embryos. Embryos with tumors were sorted after 24 h and then imaged for another 24 h. For analysis number of zebrafish with metastasis was determined. (N=3, n=12) **(B)**.

5.2.8 Grx2c amount does not influence proliferation and migration of endometric Z12-cells

The previous data showed, that Grx2c is able to increase migration and invasion in different cancer cells. To investigate if this is also true for other diseases characterized by unbalanced migration proliferation and migration assays were conducted with endometric Z12-cells, a model of endometriosis.

To analyze the effect of Grx2c on proliferation of endometric cells a BrdU assay was performed with Z12-cells. Therefore, percentage of proliferating cells was determined comparing untreated control cells and cells treated with 2 μM Grx2c, ctrl siRNA or Grx2 siRNA. Neither the treatment with 2 μM Grx2c (47.68 % ± 1.828; ctrl: 47.19 % ± 2.255; p=0.8673; n=3), nor the knockdown of Grx2 via siRNA (47.91 % ± 3.605; ctrl siRNA: 47.53 % ± 2.659; p=0.9333; n=3) changed the percentage of proliferating cells (Fig. 19A).

The impact of Grx2c on migration and invasion of endometric cells was investigated using a transwell-migration assay and a 3D spheroid assay. Transwell-migration assay was performed using Z12-cells with or without treatment with 2 μM Grx2c or siRNA (ctrl, Grx2). After transfection with Grx2 siRNA, Grx2c expression was decreased to 3.70 % ± 2.08 (n=3) compared to cells treated with ctrl siRNA. After 72 h migrated cells were visualized with DAPI and quantified. In comparison to control (203.8 % ± 14.65; n=3) treatment with 2 μM Grx2c decreased number of migrated Z12-cells to 180.8 % ± 25.92 (p=4576; n=3) whereas Grx2 knockdown did not affect number of migrated endometric cells (ctrl siRNA: 208.7 % ± 18.20; Grx2 siRNA: 193.7 % ± 15.41; p=0.5435; n=3) (Fig. 19B).

To investigate the effect of Grx2 on invasion of endometric cells a 3D spheroid assay was conducted. Therefore, Grx2 knockdown was performed in Z12-cells using siRNA. After 48 h the invasion area with migrated cells was quantified. However, Grx2 knockdown did not affect the invasion ability of Z12-cells (area with migrated cells, ctrl siRNA: 4.344 square pixel ± 0.3322; Grx2 siRNA: 4.457 square pixel ± 0.4113; p=0.8155; n=4) (Fig. 19C).
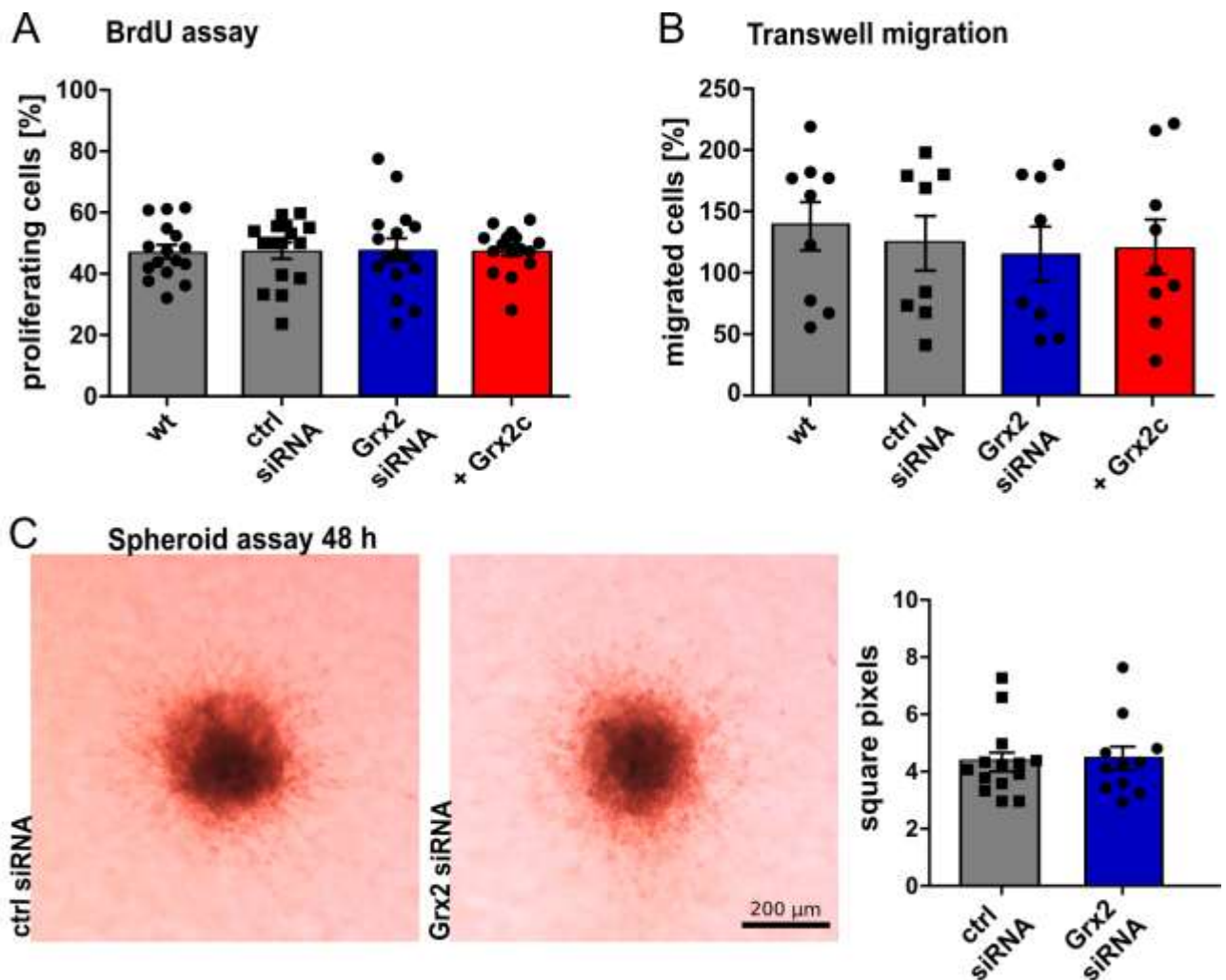
Figure 19: Grx2c does not affect proliferation and migration of endometric Z12-cells. 30,000 Z12-cells were seeded either untreated as control, were treated with 2 µM Grx2c or siRNA (ctrl, Grx2) and BrdU assay was performed. Proliferating cells were visualized by anti BrdU-antibodies and all cells were counterstained using anti-H3 antibodies. Number of proliferating cells was calculated (n=3) (**A**). Transwell-migration assay was conducted with 50,000 untreated control cells, cells treated with 2 µM Grx2c or siRNA (ctrl, Grx2). After 48 h cells were visualized using DAPI and quantified (n=3) (**B**). For 3D spheroid assay Z12-cells were embedded into a collagen matrix. Grx2 was knocked down using siRNA. After 48 h invasion area with migrated cells was quantified (n=4). Scale bar represents 200 µM (**C**). Statistical significance was determined using the two-tailed student's t-test, shown with mean and ± SEM. There were no statistically significant differences between control and Grx2 treatment.

5.2.9 Grx2 expression does not affect morphology of endometric Z12-cells

To examine if the expression of Grx2 affects the morphology of Z12-cells Grx2 knockdown was performed using siRNA. Cells were plated on glasses for microscopy and immunocytochemistry was performed as described in *4.2.4*. Nuclei were visualized by DAPI and actin was stained using Phalloidin. Pictures were taken using the TCS SP8 Confocal Microscope (Leica, Germany) at 40x magnification.

Knockdown of Grx2 does not change the morphology of Z12-cells (Fig. 20).
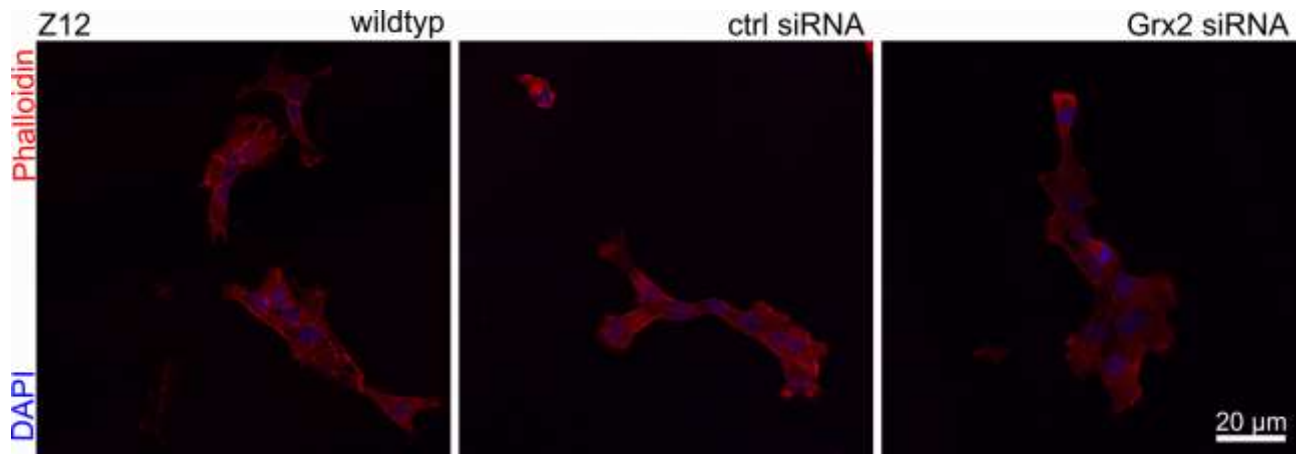
Figure 20: Grx2 expression does not affect morphology of Z12-cells. Grx2 was knocked down using siRNA in Z12-cells. 30,000 cells were plated on glasses for microscopy and imunocytochemistry was performed. Nuclei were visualized by DAPI and actin was stained using Phalloidin. Pictures were taken using the TCS SP8 Confocal Microscope (Leica, Germany) at 40x magnification. Scale bar represents 20 µm; n=1

5.2.10 NG2 expression and amount of Grx2c does not correlate in endometric Z12-cells

To shed light on the correlation between Grx2c and NG2 expression in endometric Z12-cells RNA was isolated by Trizol extraction, qRT-PCR was conducted and Grx2c and NG2 expression were normalized to GAPDH expression in cells after Grx2 knockdown with siRNA.

The obtained results show no correlation between amounts of Grx2c and NG2 (Fig. 21).
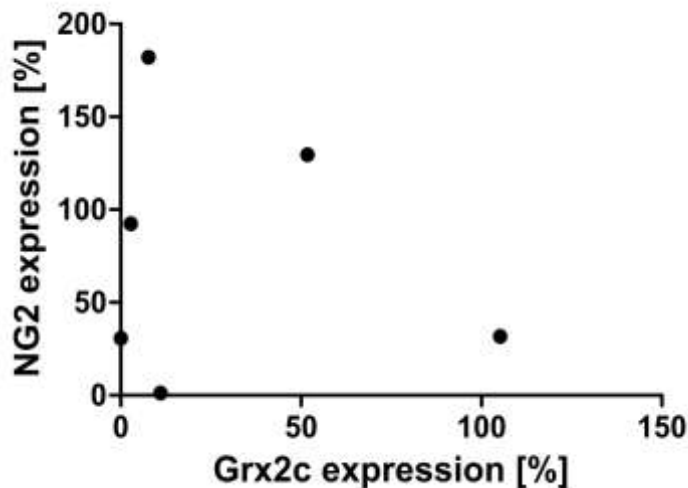
Figure 21: NG2 expression and amount of Grx2c do not correlate in endometric Z12-cells. Grx2 knockdown was performed in 10^6 endometric Z12-cells using siRNA. RNA was isolated by Trizol extraction and gene expression was quantified using qRT-PCR. Grx2c and NG2 expression were normalized to GAPDH expression. n=6

5.3 Molecular mechanism underlying Grx2 impact on NG2 expression in differentiation and dedifferentiation

The previous experiments showed that an increased amount of Grx2c increased NG2 expression in different cell types and therefore promotes migration under physiological as well as under pathological conditions. In the next part of this study, we want to shed light on the molecular mechanism of Grx2-regulated NG2 expression. NG2 expression is influenced by different transcription factors, like C/EBP, p300, CBP and Sp1 (Ampofo et al., 2017). Since Sp1 seemed most promising to play a crucial role in the regulation of NG2 gene expression we decided to examine the interaction between Grx2 and Sp1.

5.3.1 Sp1 interacts with Grx2

To identify potential interaction partners of Grx2 an intermediate trapping was performed as described at *4.2.23*. Here a mutant form of Grx2 (C37S) was used, which is unable to release substrates after binding because of the missing second cysteine at the active site. Thereby, all substrates are irreversible bound and can be eluated afterwards.

Eluates were given to Dr. Gereon Poschmann (Institute for Molecular Medicine I, Heinrich-Heine-University, Dusseldorf, Germany) for mass spectrometry and furthermore, western blot was performed. Both methods identified Sp1 in the eluate and therefore as interaction partner of Grx2 (Fig. 22).
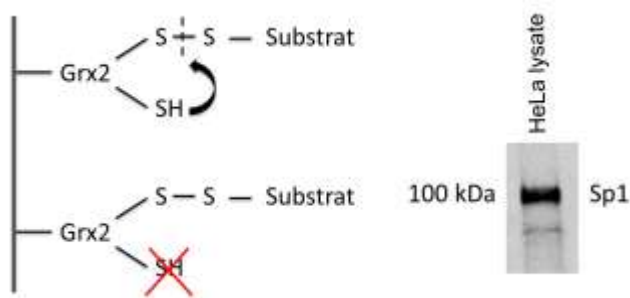
Figure 22: Sp1 is a substrate for Grx2. Intermediate trapping was performed with Grx2 C37S mutant, which is unable to release substrates after binding. Therefore all substrates are irreversible bound and can be eluate afterwards. Western bot was performed with eluates and membrane was stained against Sp1.

5.3.2 Establishment of electrophoretic mobility shift assay (EMSA)

To examine the redox-regulated binding of Sp1 at the CSPG4 promoter an electrophoretic mobility shift assay (EMSA) was conducted. Therefore, two different duplex DNA probes with predicted Sp1 binding sites were designed: one sequence from the CSPG4 promoter region (probe 1) and one from the CSPG4 enhancer region (probe 2). In the following, different conditions were tested in cells to optimize the EMSA and evaluate its specificity.

61

First the effect of electroporation on Sp1 binding was tested. Therefore, an EMSA was conducted as described in *4.2.22* with wildtype untreated HeLa-cells and HeLa-cells that were transfected without any siRNA, with ctrl siRNA or with Grx2 siRNA. The result showed that the electroporation itself without siRNA decreased the binding of Sp1 to the CSPG4 promoter. The binding was comparable to ctrl siRNA and could be further decreased after transfection with Grx2 siRNA. Therefore, we decided to only compare ctrl siRNA and Grx2 siRNA in the following experiments (Fig. 23A). Moreover, we tested the effect of fractionation into whole cell lysate and organelle fraction as described in *4.2.18.* In another EMSA we compared whole lysate ctrl siRNA and Grx2 siRNA against organelle fraction ctrl siRNA and Grx2 siRNA. For whole lysate samples Grx2 knockdown showed a small decrease in binding to the CSPG4 promoter in comparison to the control, but the decrease in binding could be increased when comparing organelle fractions. Therefore, we decided to fractionate the samples in the next experiments to enrich the nuclei and therefore also Sp1 in our samples (Fig. 23B).
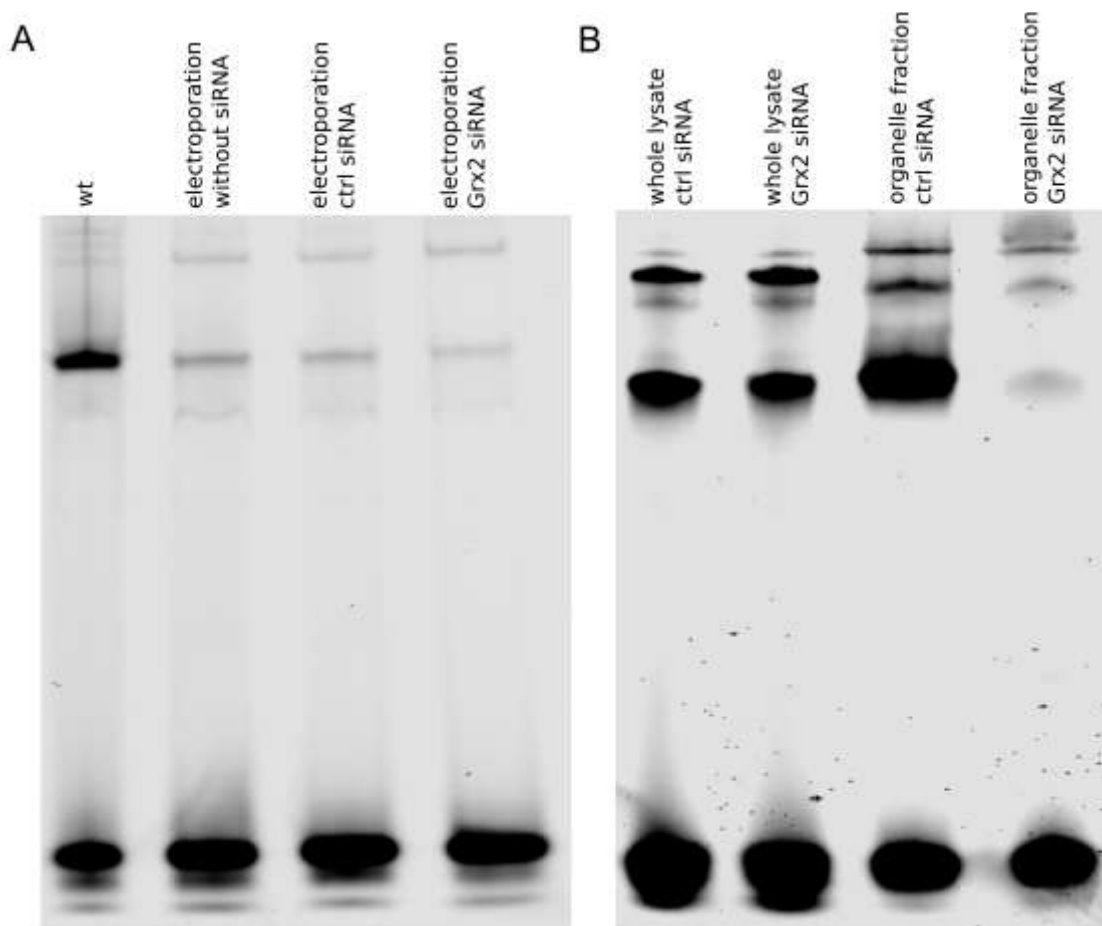
Figure 23: Establishment of electrophoretic mobility shift assay (EMSA) in HeLa-cells. EMSA was performed with untreated wildtype HeLa-cells and HeLa-cells transfected without siRNA, with ctrl siRNA or Grx2 siRNA (**A**). Furthermore, an EMSA was performed after fractionation to compare whole lysate ctrl siRNA and Grx2 siRNA to organelle fraction ctrl siRNA and Grx2 siRNA (**B**).

5.3.3 Grx2 knockdown decreases binding of Sp1 to the CSPG4 promoter in HeLa-cells.

Due to the establishment of the EMSA the following experiments were conducted with fractionated cell lysate and ctrl siRNA and Grx2 siRNA were compared. HeLa-cells transfected with Grx2 siRNA showed a decrease in Grx2c transcripts (23.30 % ± 15.36, p = 0.0075) as well as a decrease in CSPG4 transcripts (16.89 % ± 9.01, p = 0.0008) compared to control (100%). Furthermore, the Sp1-CSPG4 binding (normalized to the amount of Sp1) was decreased to 43.80 % ± 21.13 (p = 0.0564) in Grx2 knockdown cells compared to control (100 %; n=3) (Fig. 24).
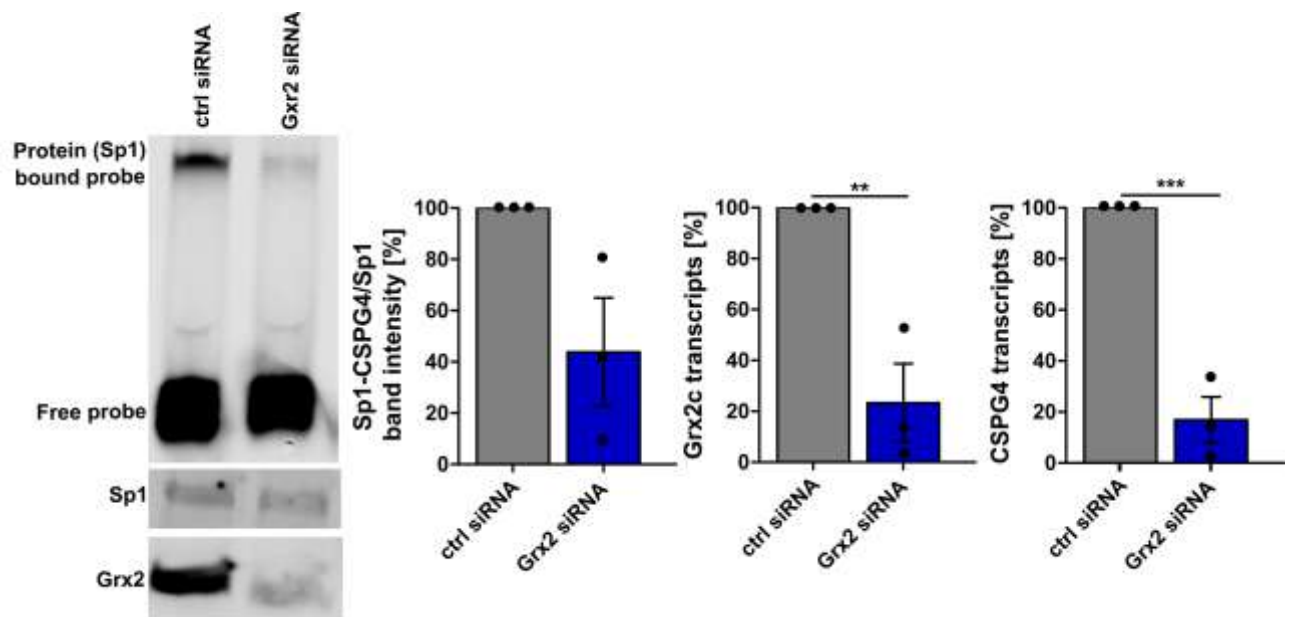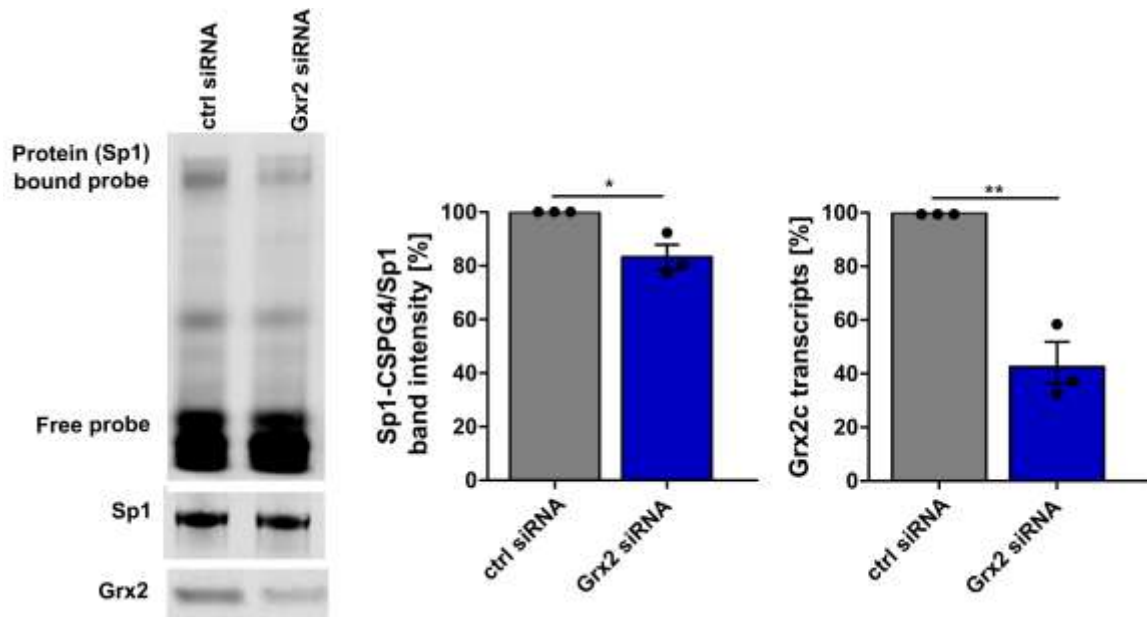

Figure 24: Grx2 knockdown decreases binding of Sp1 to the CSPG4 promoter in HeLa-cells. Electrophoretic mobility shift assay (EMSA) was performed with HeLa-cells transfected with ctrl or Grx2 siRNA. Sp1-CSPG4 binding was quantified normalized to amount of Sp1. Grx2c and CSPG4 expression was investigated by qRT-PCR. Statistical significance was determined using the two-tailed student's t-test, shown with mean and ± SEM. *: p <0.05; **: p <0.01; ***: p < 0.001. n=3

Next, we designed two different CSPG4 probes as mentioned above to test the specificity of Sp1 binding and compared both probes in an EMSA with HeLa-cells which were transfected with ctrl siRNA or Grx2 siRNA. Both probes showed a decrease in binding after Grx2 knockdown and both showed the same pattern of bands (Fig. 25A).

To shed light on the specificity of redox-regulated binding of Sp1 to the CSPG4 promoter we blocked all cysteine in untreated HeLa lysate with 100 mM NEM. This lack of free thiols decreased the binding of Sp1 to the CSPG4 promoter (Fig. 25B).
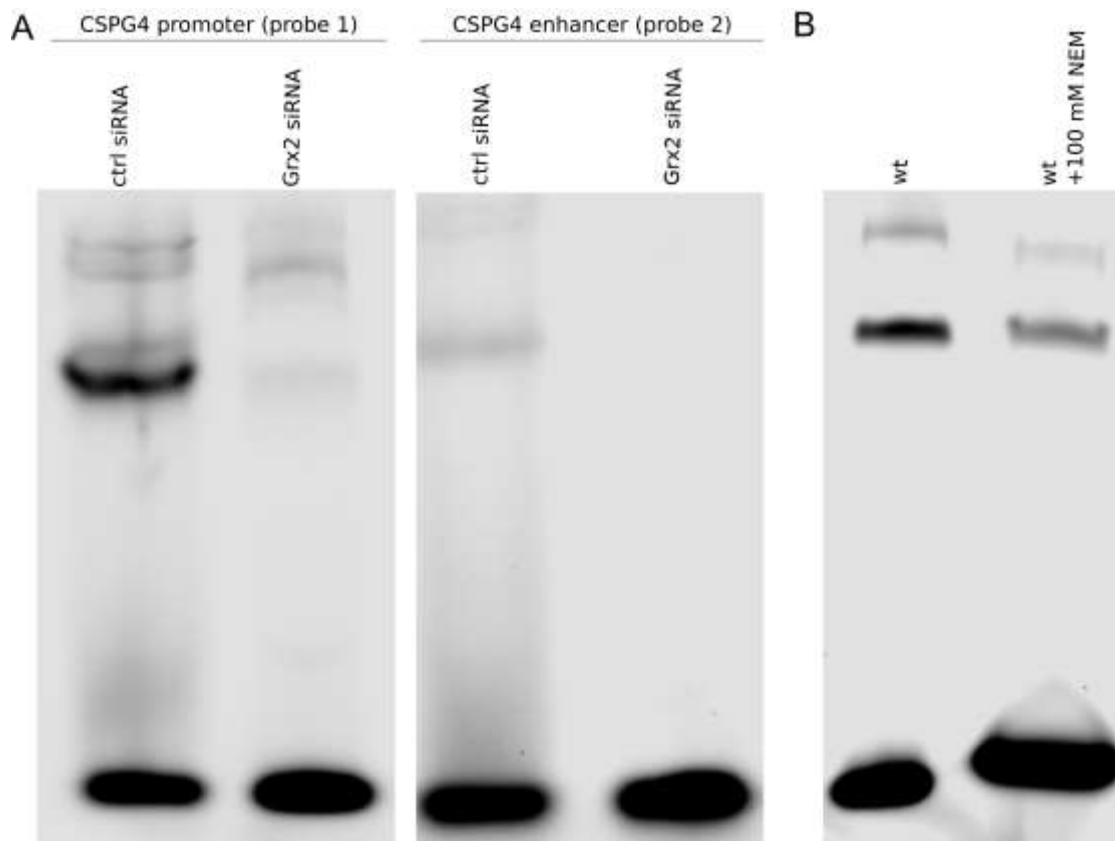
Figure 25: Grx2 knockdown as well as blocking of free thiols decrease binding of Sp1 to the CSPG4 promoter and enhancer in HeLa-cells. Ctrl siRNA and Grx2 siRNA were compared in two different CSPG4 probes: one from the promoter region (probe 1) and one from the enhancer region (probe 2) (**A**). Moreover, HeLa wildtype lysate was treated with 100 mM NEM to block free thiols and compared to untreated lysate (**B**).

5.3.4 Grx2 knockdown decreases binding of Sp1 to the CSPG4 promoter in GBM18-cells

In the next step GBM18-cells were transfected with ctrl or Grx2 siRNA. GBM18-cells transfected with Grx2 siRNA showed a decrease in Grx2c transcripts to 42.55 % ± 7.89, p = 0.0018 compared to control (100%) as shown by western blot and qRT-PCR. Furthermore, also here the Sp1-CSPG4 binding (normalized to the amount of Sp1) was decreased to 83.31 % ± 4.54, p = 0.0214 in Grx2 knockdown cells compared to control (100 %; n=3) (Fig. 26).

Figure 26: Grx2 knockdown decreases binding of Sp1 to the CSPG4 promoter in GBM18-cells. Electrophoretic mobility shift assay (EMSA) was performed with GBM18-cells transfected with ctrl or Grx2 siRNA. Sp1-CSPG4 binding was quantified normalized to amount of Sp1. Grx2c expression was investigated by qRT-PCR. Statistical significance was determined using the two-tailed student's t-test, shown with mean and $\pm$ SEM. *: $p < 0.05$; **: $p < 0.01$; ***: $p < 0.001$. n=3

5.3.5 Increase of Grx2 expression enhances Sp1 binding to the CSPG4 promoter

Previous experiments showed that in HeLa- and GBM18-cells a decrease in Grx2 expression results in a decrease in Sp1 binding to the CSPG4 promoter (Fig. 24, 26). Further experiments with HeLa-, GBM18- and U343-MGA cells showed that there is a correlation between the amount of Grx2 and the binding of Sp1 to the CSPG4 promoter. For example, an overexpression of Grx2 in HeLa-cells to 119 % increased the binding of Sp1 to the CSPG4 promoter to 128 % in comparison to control. Also, in U343-MGA cells an increase of Grx2 to 182.2 % enhanced the binding of Sp1 to the CSPG4 promoter to 116 % (Fig. 27).
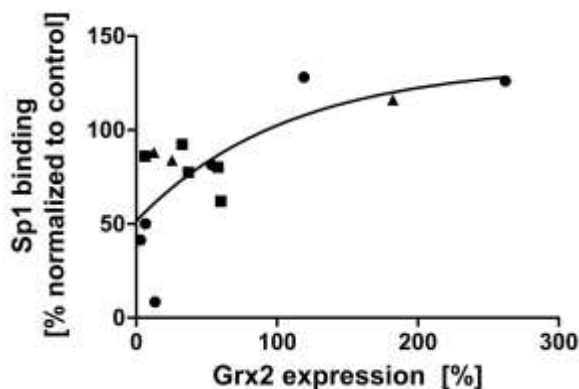
Figure 27: HeLa-, GBM18- and U343-MGA-cells show a correlation between Grx2 expression and Sp1 binding. EMSA was performed with HeLa-, GBM18- and U343-MGA-cells after Grx2 knockdown or overexpression. Sp1 binding to the CSPG4 was quantified and Grx2 amount was estimated using western blot or qRT-PCR. ●: HeLa, ■: GBM18, ▲: U343-MGA; n=14 nonlinear regression, one-phase association, R^2: 0.5427

5.3.6 Grx2c can not rescue inhibitory effects on migration when Sp1 is inhibited by Mithramycin A

To confirm that Grx2´s impact on migration depends on the function of Sp1 we analyzed the impact of Grx2c on migration of GBM18- and GBM1-cells in the presence of an Sp1 inhibitor. Therefore we choose the gene-selective Sp1 inhibitor Mithramycin A (MitA), which binds to GC rich DNA sequences displacing Sp1 transcription factors, inhibiting their expression (Sleiman et al., 2011).

We first determined a non-lethal MitA concentration performing a celltiter blue survival assay. Here 5 nM (97.36 % ± 1.12) and 10 nM MitA (94.83 % ± 1.12) showed a tolerable impact on survival of GBM18-cells compared to untreated control cells (100 % ± 1.28). 25 nM MitA decreased survival of GBM18-cells considerable to 76.85 % ± 1.35, so that we choose concentrations of 5 nM and 10 nM MitA for the following transwell-migration assay (Fig. 28A).

Moreover, we investigated the effect of Sp1 inhibition on NG2 expression. We treated GBM18-cells with 10 or 25 nM MitA for 48 h. Afterwards cells were harvested, RNA was isolated by Trizol extraction and gene expression was quantified using qRT-PCR. NG2 expression was normalized to GAPDH expression. In comparison to untreated control (100 %) 10 nM MitA decreased NG2 expression to 47.7 % ± 15.45. Treatment with 25 nM MitA further decreased NG2 expression to 12.83 % ± 6.54 (Fig. 28B).

Transwell-migration assay was performed with GBM18- and GBM1-cells in the presence of Grx2c or MitA alone or in combination. As seen before Grx2c could increase migration of GBM18-cells to 289.2 % ± 45.66 in comparison to control (100 % ± 1.57; $p = 0.0010$). 5 nM MitA decreased migration of GBM18-cells to 83.94 % ± 6.26. 10 nM MitA decreased migration to 41.26 % ± 4.56. An additional treatment with Grx2c could not rescue the inhibitory effect of MitA on migration (5 nM MitA, +Grx2: 76.53 % ± 4.63; 10 nM MitA, +Grx2: 53.89 % ± 4.43) (Fig. 28C).

Also, in GBM1-cells Grx2c increased migration to 175.5 % ± 27.49 in comparison to control (100% ± 5.12; $p = 0.027$). 5 nM MitA decreased migration of GBM1-cells to 69.99 % ± 3.14, while 10 nM MitA further decreased migration to 53.41 % ± 6.58. Also here an additional treatment with Grx2c could not rescue the inhibitory effect of MitA on migration (5 nM MitA, +Grx2: 51.73 % ± 7.55; 10 nM MitA, +Grx2: 33.21 % ± 3.65) (Fig. 28D).
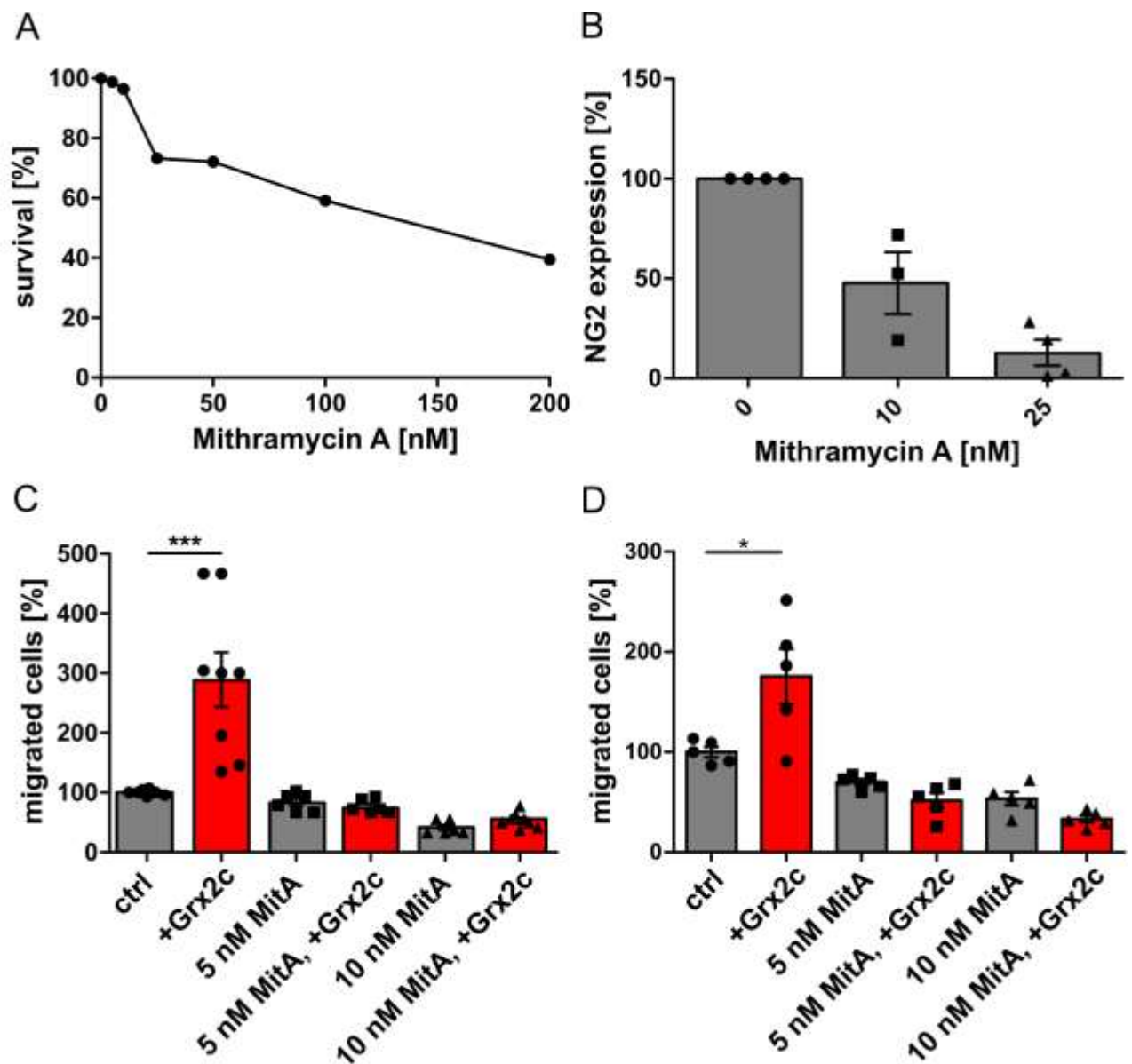
Figure 28: MithramycinA (MitA) decrease NG2 expression and migration in GBM18- and GBM1-cells, which can not be rescued by additional Grx2c. Celltiter blue survival assay was performed with 10,000 GBM18-cells and 5 nM, 10 nM, 25 nM, 50 nM, 100 nM and 200 nM MitA (n=3) (**A**). 10^6 GBM18-cells were treated with 10 nM or 25 nM MitA for 48 h. Afterwards they were harvested, RNA was isolated by Trizol extraction and NG2 expression was quantified using qRT-PCR. NG2 expression was normalized to GAPDH expression (ctrl, 25 nM MitA n=4; 10 nM MitA n=3) (**B**). Transwell-migration assay was conducted with 50,000 GBM18- (**C**) and GBM1-cells (**D**). Cells were kept untreated as control or cells were treated with 2 μM Grx2c, 5 nM MitA, 10 nM MitA or Grx2c and MitA in combination. After 48 h cells were visualized using DAPI and quantified (GBM18: ctrl, +Grx2, 10 nM MitA + Grx2 n=8; 5 nM MitA, 5 nM MitA + Grx2, 10 nM MitA n=6; GBM1: n=3**).** Statistical significance was determined using the two-tailed student's t-test, shown with mean and ± SEM. *: p <0.05; **: p <0.01; ***: p < 0.001.

6   Discussion

The aim of the present study was to gain insights into the role of Grx2 in differentiation and dedifferentiation concerning NG2/CSPG4 expression and the redox-regulated molecular mechanism behind that. In terms of this, we investigated the impact of Grx2 on oligodendrocytes as well as on glioblastoma, melanoma and endometric cells in the context of migration, differentiation and dedifferentiation using *in vitro* and *in vivo* models. For *in vitro* experiments different cell lines as well as primary cells were used in cellular assays like migration assays. Further molecular methods like qRT-PCR, western blot or EMSA were used. For *in vivo* experiments mouse and zebrafish were used as model organisms. The zebrafish has become an important model organism to study myelination during development as well as remyelination of the adult CNS (Ej et al., 2012). The general dynamic behavior of OPCs and the ability to generate myelinating oligodendrocytes is conserved between zebrafish and rodents (Lyons and Talbot, 2015). In zebrafish and rodent embryos oligodendrocytes arise from the same region of the ventral spinal cord that earlier generated motor neurons and migrate to new positions (Park et al., 2002). The genome of zebrafish is fully sequenced and encodes for two dithiol Grxs. The zebrafish Grx2 (ZfGrx2) lacks a mitochondrial target sequence and is most closely related to hGrx2c. ZfGrx2 possesses the common Grx active site motif C-P-Y-C and two conserved extra structural cysteines. Furthermore, Bräutigam et al. confirmed that its activity is comparable to mammalian Grx2 and it is ubiquitously distributed in zebrafish embryos throughout development (Bräutigam et al., 2011).

6.1   Redox-regulation of oligodendrocyte functions

6.1.1 Differentiation

We found that during differentiation of oligodendrocyte precursor cells Grx2 is first up- and then down regulated. Furthermore, we could show that Grx2 affects differentiation of oligodendrocytes promoting a progenitor state. An increase of Grx2 level increased the amount of NG2$^+$-cells, while the amount of more mature oligodendrocytes, e.g. CNPase$^+$- and MBP$^+$-cells, was decreased. In contrast transient knockdown of Grx2 via siRNA increased the amount of CNPase$^+$- and MBP$^+$-cells. We confirmed this result in Grx2 knock-out mice. In addition, we found an increase in size of CNPase$^+$- and MBP$^+$-cells compared to control OPCs after differentiation.

Different studies have demonstrated that ROS act as a regulator of several physiological processes, particularly in different aspects of nervous system development. Neuronal differentiation of stem cells is determined by a change toward oxidative metabolism, increased levels of mitochondrial ROS as well as increased activity of NADPH oxidase enzymes, decreased levels of nuclear factor erythroid

2–related factor 2 (Nrf2) and differential regulation of redoxins (Olguín-Albuerne and Morán, 2018). In neuronal stem cells from the subventricular zone, exogenous hydrogen peroxide induces neuronal differentiation and oligodendrocyte differentiation by up regulation of the histone deacetylase sirtuin 2 (Olguín-Albuerne and Morán, 2018). In OPCs the redox state of cells determines the balance between proliferation and differentiation. Here OPCS with high levels of ROS, meaning more oxidized cells, are differentiated to a greater extent than OPCs with low levels of ROS, meaning more reduced cells (Noble et al., 2005; Olguín-Albuerne and Morán, 2018). These findings are in line with our observations. Moreover, antioxidant treatment results in a decrease of differentiated cells, while pro-oxidant treatment increased number of differentiated cells. This indicates a modulation of the differentiation process by the redox state of the cell rather than being a consequence of the differentiation process (Olguín-Albuerne and Morán, 2018).

6.1.2 Migration

Additionally to the effect of Grx2 on differentiation of OPCs we could also show that Grx2 affects migration of OPCs. Increased levels of Grx2 enhanced migration of A2B5[+]- as well as NG2^{+}-cells significantly, while Grx2 knock-down via siRNA decreased migration. Due to the intracellular effect of Grx2 on differentiation and migration of oligodendrocyte precursor cells, demonstrated by siRNA experiments, we shed light on the intracellular uptake of recombinant Grx2. Previous studies of our group confirmed that A2B5[+]-cells are able to take up recombinant Grx2 (Lepka et al., 2017). In line, our findings in this study show that also NG2^{+}-cells can take up recombinant Grx2.

Using zebrafish, we found that the amount of Grx2 affects migration of progenitor cells *in vivo*. Therefore, Grx2 expression in zebrafish was modulated by morpholino injection or overexpression and dorsally migrated Olig2^{+}-, ClaudinK[+]- and MBP[+]-cells were analyzed. *Olig2*-expressing cells exist in the adult zebrafish brain functioning as progenitor cells, although their functions have not been fully explored (Lyons and Talbot, 2015). In contrast ClaudinK is a myelin-associated protein in zebrafish associated with early stages of wrapping and myelin formation in zebrafish development and adult regeneration (Ej et al., 2012). For this study we choose Olig2 as a marker for migrating progenitor cells, ClaudinK for an early stage of myelinating oligodendrocytes and MBP for fully matured myelinating oligodendrocytes. We found that knockdown of Grx2 in zebrafish decreased number of dorsally migrated Olig2^{+}-, ClaudinK[+]- and MBP[+]-cells. In contrast overexpression of Grx2 increased at least number of dorsally migrated Olig2^{+}-cells. To evaluate if this effect is just based on a decrease of migrating OPCs or if there is also an effect on differentiation of progenitor cells further experiments have to be conducted.

Cytoskeletal dynamics, especially cell migration are essential for fundamental biological processes, starting at embryonic development and proceeding with regeneration, tissue repair, inflammatory immune response and also cancer metastasis and age related disorders like atherosclerosis (Gellert et al., 2015). Thiol and methionyl switches play an essential role in the regulation of cytoskeletal dynamics, which are indispensible for cell differentiation and all developmental processes (Gellert et al., 2015). Grx2c has been identified as essential for vertebrate development influencing formation of the cardiovascular system as well as the brain. Here, axon formation, vessel outgrowth and migration of cardiac neural crest cells are regulated by reversible thiol redox modifications of sirtuin 1, actin and CRMP2 (Berndt et al., 2014; Bräutigam et al., 2013, 2011). It was shown that for example a dithiol-disulfide switch in CRMP2 controls protein's function during neuronal development (Gellert et al., 2013, p. 2). Gellert et al. showed that CRMP2 is regulated by Grx2c through a redox switch that controls the phosphorylation state of the protein (Gellert et al., 2020). CRMP2 is essential for brain development, involved in the regulation of cytoskeletal dynamics and an effector protein of the semaphorin/plexin pathway controlling axon branching and guidance. The switch in CRMP2 is triggered during neuronal differentiation and controls axonal outgrowth (Gellert et al., 2013, p. 2). Moreover, Gellert et al displayed that cell lines expressing Grx2c showed dramatic alterations in morphology and migrated two-fold faster (Gellert et al., 2020).

Bräutigam et al. demonstrated that embryonic brain development in zebrafish depends on the oxidoreductase activity of cytosolic Grx2 (Bräutigam et al., 2011). Zebrafish embryos with silenced Grx2 expression lost virtually all types of neurons by apoptosis and the ability to develop an axonal scaffold. The diminished number of neurons, *i.e.* secondary motor neurons, dopaminergic neurons and glutamatergic excitatory interneurons, resulted in behavioral changes of embryos. In contrast to wild-type embryos zebrafish lacking zfGrx2 showed no stereotypical fast escape response upon mechanical stimuli but swam away slowly in an uncoordinated, circlewise manner. Moreover, not only axonal length and number of branching points of the existing axons were significantly reduced also the number of neurons was diminished in embryos lacking Grx2 and neuronal networks did not mature (Bräutigam et al., 2011). This demonstrates the essential role of Grx2 for vertebrate embryonic development. Bräutigam et al. further demonstrated that this control of axonal outgrowth by Grx2 is regulated via thiol redox regulation of CRMP2 (Bräutigam et al., 2011).

6.1.3 Functional Analysis

Due to the effects of Grx2 on differentiation and migration of oligodendrocytes we decided to investigate a potential effect of Grx2 on functional myelination. In this study we choose optomotor

response (OMR) and optical coherence tomography (OCT) analysis as a functional readout to examine visual function and retinal layer thickness of Grx2 knock-out mice compared to control mice. We found that knock-out of Grx2 led to a decreased visual acuity in comparison to control. There were no significant differences between the two groups concerning the retinal thickness. To evaluate if this deficiency is due to hypomyelination we will perform electron microscopy of the optic nerve and the brain in the future to analyze the myelin structure. To investigate if knock-out of Grx2 in mice leads to further cognitive and motor disfunctions or if it is just affecting the visual system further experiments have to be conducted. Behavioural tests like the grid walk test and water maze test are planned to investigate the effect of Grx2 knock-out on motor function and learning. Electron microscopy as well as behavioural tests are planned in cooperation with Prof. Dr. Charlotte von Gall (Institute for anatomy II, Heinrich-Heine-University, Dusseldorf, Germany).

Due to daily exposure to UV light, high metabolic activities and oxygen tension the eye is constantly exposed to oxidative stress (Upadhyaya et al., 2015). Upadhyaya et al. were able to show that Grx2 is present in all ocular tissues (cornea, lens, ciliary body, retina, optic nerve) except the vitreous humor. Here, gene expression, protein level and enzyme activity correlates with the amount of mitochondria and vasculature within the tissue (Upadhyaya et al., 2015). They also investigated whether *Glrx2* gene deletion could induce faster age-related cataract formation and lens opacity. They found that *Glrx2* gene deletion produces a phenotype of early onset and faster progression in cataract formation during aging. In Grx2 knock-out mice lens opacity began at 5 months, 3 months sooner than in control mice. Lenses of Grx2 knock-out mice further contained lower levels of protein thiols and GSH and accumulation of S-glutathionylated proteins (Wu et al., 2014). In line with these results primary lens epithelial cells isolated from knock-out mice exhibited unusual sensitivity to oxidation, which could be rescued by imported recombinant Grx2 protein (Wu et al., 2011). Until now there are no data available concerning the effect of Grx2 on cognitive functioning. However, unpublished data indicate, that Grx2 overexpressing zebrafish show improved learning and memory (unpublished).

6.2 Redox-regulated dedifferentiation

6.2.1 Glioblastoma

In this study we were able to show that Grx2 not just increases migration of OPCs but also increases migration of glioblastoma cells. Here, altered Grx2 levels did not affect proliferation and morphology of the cells. *In vivo* experiments revealed that Grx2 knockdown decreases number as well as lengths of protrusions of tumors in zebrafish. We found that in Grx2c overexpressing HeLa-cells NG2

expression is increased in comparison to wildtype HeLa-cells. Also in glioblastoma cell lines we found a correlation between the level of Grx2 and NG2 expression. In GBM18-cells a knockdown of Grx2 led to a decrease in NG2 expression. RT-qPCR showed that in U343-MGA-cells Grx2 knockdown did not decrease NG2 expression, but Grx2 overexpression increased NG2 expression compared to wildtype. In contrast immunocytochemistry demonstrated that Grx2 knockdown in U343-MGA spheres also reduces the amount of $NG2^+$-cells within the spheres. These different outcomes may be due to the poor correlation between transcript and protein levels in most tissues and cells (Schiffer et al., 2018). Furthermore, we observed a correlation between Grx2c and NG2 expression in glioblastoma patient samples. Tumors with a high expression of Grx2c displayed a high expression of NG2. This high expression negatively correlates with the survival of patients. In cooperation with Dr. Nan Quin (Pediatric Neuro-Oncogenomics, Heinrich-Heine-University Dusseldorf, Germany) we searched in different databanks for the expression levels of Grx2 and CSPG4 in glioblastoma patient samples. Kaplan-Meier plots from two independent cohorts (Gravendeel et al., 2009; Kawaguchi et al., 2013) of glioma samples revealed, that patients with a high expression of Grx2 display a significantly shorter survival rate compared to patients with low expression of Grx2 (Fig. 29). In our glioblastoma patient samples we found an up regulation of CSPG4, while some tumors showed an increased and some a decreased Grx2c expression in comparison to healthy control tissue. This may be due to the two isoforms of Grx2. While data available online always include Grx2a as well as Grx2c we specifically measured Grx2c. Other factors could be the grade of the tumor as well as the selected area within the tumor and the amount of healthy tissue within the tumor sample due to the surgical extraction method.
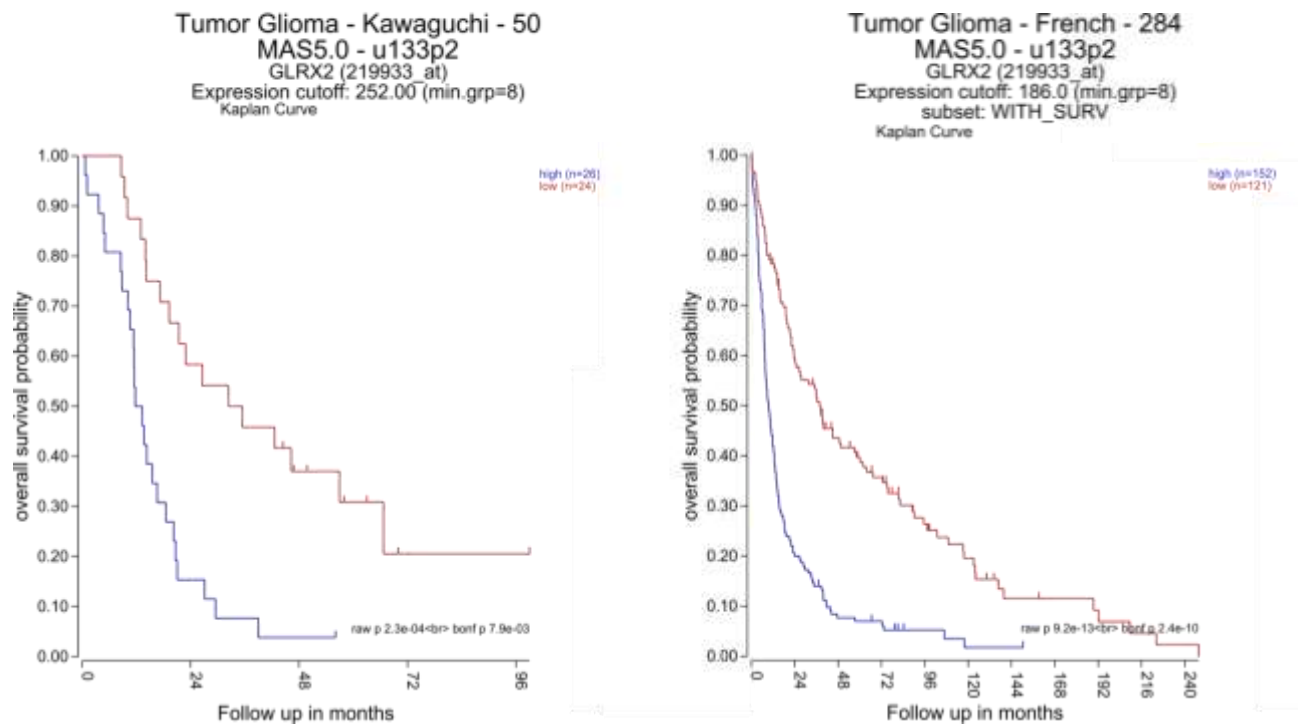
Figure 29: Survival rate of glioblastoma patients with high *Glrx2* expression is decreased. Kaplan-Meier plots from two independent cohorts of glioma samples showing survival rate of patients due to high or low *Glrx2* expression. Data taken from (Gravendeel et al., 2009; Kawaguchi et al., 2013).

Cancer cell spreading is linked to pathological cell migration (Gellert et al., 2015). Metastasis is associated with the expression of sirtuin 1 (Byles et al., 2012; Kunimoto et al., 2014) and cellular nucleoside diphosphate kinase (NDPK) (Almgren et al., 2004), whose activity is regulated by redox modification of a single cysteine (Gellert et al., 2015). While NDPK suppress tumor metastasis via the redox state of Cys109 which is reduced by the Trx system (Lee et al., 2009), sirtuin 1 activity is modulated by Grx2(c)-dependent reversible S-glutathionylation of Cys204 (Bräutigam et al., 2013). Both, NDPK and sirtuin1 regulate the activity of the transcription factor FOXO-1 and thereby the release of vascular endothelial growth factor-C (VEGF-C). Enhanced release of VEGF-C positively regulates cell migration and metastasis, connecting redox-modulated pathways with cancer cell migration (Li et al., 2005). Gellert et al. provide evidence that Grx2c does not only control axonal outgrowth and guidance, but may also promote motility and invasiveness of non-neuronal cells by controlling cell adhesion and cytoskeletal dynamics (Gellert et al., 2020). They revealed Grx2c-mediated alterations at the level of protein phosphorylation leading to increased (CDK5, ERK2, GSK3β, MK14/p38α, PAK1) and decreased (EGFR, FAK1, MET) activity of kinases, which are involved in the regulation of cell adhesion or actin cytoskeleton dynamics (Gellert et al., 2020). Furthermore, activation of CDK5, ERK2, GSK3β and PAK1 are also associated with the development and progression of various cancers (Gellert et al., 2020). Additionally pathways that are

associated with tumor invasion and metastasis are affected by altered phosphorylation, for example MARCS, vimentin, STMN1, MAP4 and MCM7 (Gellert et al., 2020).

Lönn et al. provided in 2008 the first evidence for potential roles of Grx2 in cellular dedifferentiation and tumor progression, when Grx2c, was found to be exclusively expressed in testis and transformed cells that encode cytosolic/nuclear proteins (Lönn et al., 2008). Overexpression of Grx2a and Grx2c in HeLa-cells provided protection from apoptosis induced by the anti-cancer agents doxorubicin/adriamycin and 2-deoxy-D-glucose indicating a major role of Grx2 in cell survival (Lönn et al., 2008). Gellert et al. demonstrated the presence of Grx2c in tumor samples of clear cell renal cell carcinoma. Further they were able to proof a negative correlation with cancer-specific survival, supporting a role of Grx2 and especially Grx2c in tumor progression and cancer-specific survival (Gellert et al., 2020) .

Also other proteins of the thioredoxin family have been shown to be upregulated in different cancers. Overexpression of Trx1 has been observed in various types of cancers and has a negative correlation with survival in squamous cell carcinoma of the tongue, gastric cancer, gallbladder carcinoma, non-small cell lung cancer and colorectal cancer (Fernandes et al., 2009; Mollbrink et al., 2014). In hepatocellular carcinoma and colorectal carcinoma liver metastases also Trx1, Trx2, Grx3 and Grx5 were upregulated (Mollbrink et al., 2014). In hepatocellular carcinoma Trx1 correlated with cell proliferation and increased micro-vascular invasion (Mollbrink et al., 2014). Furthermore, high levels of Trx1 haven been linked to chemotherapeutic resistance (Fernandes et al., 2009). In general various different cancer types displayed an overexpression of Trx1, Trx2, Grx2, Grx3 and Grx5 which correlates with a poor prognosis for patients (Fernandes et al., 2009; Mollbrink et al., 2014). Moreover, also PRDX-1 was found to be upregulated in GBM biopsies in patients with shortest survival. Here knockdown of PRDX-1 slowed tumor growth and further sensitized tumors to ionizing radiation *in vivo* (Svendsen et al., 2011).

But not just proteins of the thioredoxin family are overexpressed in various cancer types correlating with poor prognosis for the patients also NG2 is associated with both. It was not just shown that NG2 promotes tumor growth and angiogenesis in animal models. Svendsen et al. further demonstrated that increased expression of NG2 by tumor cells in GBM biopsies was associated with shorter patient survival and increased the risk of death by 155%. This correlation was independent of age, clinical treatment and MGMT promoter hypermethylation status (Svendsen et al., 2011). NG2 does not only show an aberrant expression on cancer cells, but also on angiogenic vasculature, which is associated with an aggressive disease course in several malignancies including glioblastoma and melanoma. NG2 overexpression in GBM cell lines resulted in increased growth rate, angiogenesis and vascular permeability while NG2 knockdown reduced melanoma proliferation and increased apoptosis and

necrosis (Wang et al., 2011). Also, Grx2 plays an essential role concerning vascular development and angiogenesis. Bräutigam et al. showed that knockdown of Grx2 in zebrafish resulted in a delayed and disordered blood vessel network. Formation of a functional vascular system requires Grx2-dependent reversible S-glutathionylation of the deacetylase sirtuin 1 (Bräutigam et al., 2013).

6.2.2 Melanoma

To investigate the specificity of these findings for brain tissue or glioblastoma we conducted migration experiments with melanoma cells. We discovered that Grx2 increased migration ability of melanoma cells *in vitro* and *in vivo*. Grx2 promotes metastasis of melanoma cells in zebrafish. Moreover, the human protein atlas displays also in melanoma a negative correlation between the amount of Grx2 and the survival of patients. All patients suffering from melanoma with high Grx2 expression die before 3 years, whereas all patients with low Grx2 expression survive more than 5 years (Fig. 30).
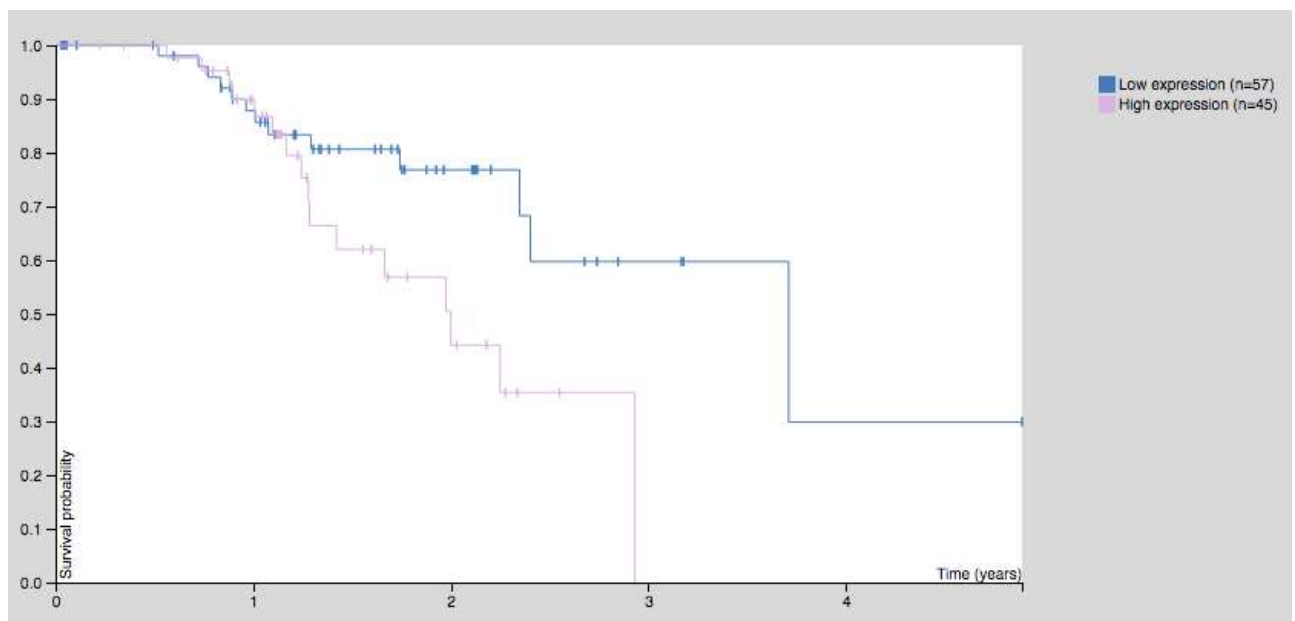
Figure 30: Survival rate of patients with melanoma. Patients with melanoma expressing high levels of Grx2 have a lower survival rate, than patients with melanoma expressing low levels of Grx2 (adapted from the human protein atlas). https://www.proteinatlas.org/ENSG00000023572-GLRX2/pathology/melanoma

It has been demonstrated that in melanoma high NG2 expression occurs in 95% of uveal melanomas increasing metastic potential and poor prognosis (Wang et al., 2011). In contrast disruption of NG2 function resulted in reduced proliferation, increased apoptosis and immune infiltration (Wang et al., 2011). ROS and RNS play a central role in all aspects of melanoma pathophysiology, due to the high number of somatic mutations in the melanoma genome associated with UV radiation (Obrador et al., 2019). Su et al. found for example that the antioxidant genes *PRDX5, PRDX3, GPX4* and *GLRX2* are

up regulated in different melanoma cell lines (Su et al., 2009). Furthermore, it has been shown, that PRDX-2 represses melanoma metastasis by increasing E-cadherin/β-catenin complexes in adherens junctions, while PRDX-6, which is overexpressed in most melanoma cells, can trigger melanoma cell growth by increasing arachidonic acid-dependent lipid signaling (Obrador et al., 2019).

6.2.3 Endometriosis

Endometriosis and cancer share many characteristics, like the altered proliferation and migration of cells, chronic inflammation and the increased production of ROS. In this study we investigated the effect of Grx2 on proliferation, migration and morphology of endometric cells. In contrast to glioblastoma and melanoma cells we found that Grx2 does not affect proliferation, migration or morphology of endometric cells. This may be due to the fact that Grx2 seems not to affect NG2 expression in endometric cells in contrast to cancer cells. Unfortunately until now there are no studies concerning the expression of NG2 in endometriosis and as a result invasion of endometric cells. Until today there is little known about the role of proteins of the thioredoxin family in endometriosis. While there is nothing known about Grxs in endometriosis there are a few studies concerning Trxs. Seo at el. showed that there were no differences in Trx mRNA levels but for TBP-2, a negative regulator of Trx function, mRNA levels in the endometrium were lower and the Trx to TBP-2 ratio was higher in patients with endometriosis than in the control group. In normal endometrium Trx mRNA levels correlated with TBP-2 mRNA levels, while in women with endometriosis there was no correlation, suggesting that Trx and TBP-2 play a crucial role in the homeostasis of the normal endometrium. Furthermore, IHC studies revealed a decreased TBP-2 immunoreactivity in patients with endometriosis (Seo et al., 2010). Zeitvogel et al. showed that in peritoneal fluid of patients with endometriosis the number of activated macrophages as well as the chemotactic activity of cells of the immune system and the levels of cytokines, growth factors and prostaglandins is increased in comparison to females without the disease (Zeitvogel et al., 2001). Furthermore, oxidative stress-induced SOD2 expression is increased in patients with endometriosis regardless of the menstrual cycle (Chen et al., 2019). Recent data provide evidence that oxidative stress and redox imbalance may have an impact on malignant transformation of endometriosis (Shigetomi et al., 2014). Clinicopathological studies have suggested a malignant transformation of ovarian endometriosis to endometrioid, clear cell carcinomas, Müllerian-type tumors and sarcomas. It is assumed that the heme- and iron-mediated oxidative stress, occurring from repeated hemorrhage, could modify genomic DNA and induce DNA damage leading to adaptation of cells to oxidative stress and their survival. While overproduction of ROS causes cell death in endometriosis, antioxidants may be able

to slow down the ROS-induced cell death, leading to endometriosis-associated ovarian carcinogenesis. It has been shown that antioxidant enzymes have been overexpressed in a variety of cancers offering a proliferation-permissive environment and give cells an advantage for survival and growth, thus promoting carcinogenesis (Iwabuchi et al., 2015).

Taken together, Grx2 affects differentiation as well as dedifferentiation by increasing migration and invasion of different cell types. For differentiation as well as dedifferentiation, the expression of NG2/CSPG4 plays a crucial role. Unfortunately until now little is known about the mechanisms regulating NG2 expression (Ampofo et al., 2017).

6.3 Molecular mechanism of redox-regulated NG2/CSPG4 expression

In this study we investigated the redox-regulated NG2/CSPG4 expression through the transcription factor Sp1. Sp1 was identified by western blot and mass spectrometry as interaction partner of Grx2 using trapping mutant forming stable disulfides between Grx2 and its substrates. We found that in HeLa-cells as well as in GBM18-cells Grx2 knockdown decreases binding of Sp1 to the CSPG4 promoter. Electrophoretic mobility shift assays with three different cell lines displayed that there is a positive correlation between Grx2 expression and Sp1 binding to the CSPG4 promoter. In addition, Grx2 was not able to rescue the inhibitory effect of MithramycinA, a Sp1 inhibitor, decreasing NG2-expression in glioblastoma cells as well as migration. Therefore, we claim that the redox-regulation of NG2 expression is mediated by Sp1.

It seems that Sp1 plays a crucial role in the regulation of NG2 gene expression, acting either as a transcriptional activator or repressor of NG2 depending on its additional post-transcriptional modifications (Ampofo et al., 2017). Sp1 is a transcription factor belonging to the Specificity protein/Krüppel-like factor (Sp/KLF) family of transcription factors, which has currently 26 members. A highly conserved DNA binding domain near to the C-terminus recognizing GC and GT/CACC boxes characterizes this protein family. The DNA binding domain consists of three enclosed Cys2His2-type zinc fingers with exactly 81 amino acids. According to the structure at the N-terminus the Sp/KLF family can be subdivided into KLF-like transcription factors and Sp-like transcription factors (Sp1-9), which can be further grouped into Sp1-4 and Sp5-9 (O'Connor et al., 2016). While Sp-like transcription factors function as an activator of transcription, the KLF-like subgroup can act as an activator as well as a repressor of gene expression (O'Connor et al., 2016). Sp1 itself is a 785-amino-acid, 100- to 110-kDa nuclear transcription factor, which is ubiquitously expressed in mammalian tissues (Tan and Khachigian, 2009; Wu et al., 1996). However, expression

levels of Sp1 seem to vary in different cell types and different stages of development (O'Connor et al., 2016). Sp1 is essential for normal mouse embryogenesis and *Sp1*-knockout embryos die around day 11 of gestation. They display a broad range of phenotypic abnormalities and are retarded in development, indicating a general function of Sp1 in many cell types (Suske, 1999). Sp1 binds to DNA sites with different affinities and regulates expression of genes associated with a wide range of cellular processes in mammalian cells via multiple mechanisms (O'Connor et al., 2016; Tan and Khachigian, 2009; Wu et al., 1996). In the human genome there are at least 12,000 Sp1 binding sites (O'Connor et al., 2016).

The transcriptional activity and stability of Sp1 can be influenced by posttranslational modifications, like phosphorylation, acetylation, sumoylation, ubiquitylation and glycosylation (Tan and Khachigian, 2009). In addition, gene expression and the activity of transcription factors can be modulated by redox regulation (Bloomfield et al., 2003). It has been demonstrated for a range of transcription factors that redox regulation occurs through reversible oxidation of key cysteine sulfhydryl groups (Wu et al., 1996). Zinc finger transcriptions factors are prone to redox regulation due to their cysteine residues as part of the DNA-binding zinc fingers (Wu et al., 1996). Ammendola et al. displayed that DNA binding activity of Sp1 is decreased in nuclear extracts from aged rat tissue. This phenomenon could be reversed by adding the reducing agent dithiothreitol (DTT). In contrast adding H_2O_2 to extracts from young rats decreased binding efficiency, which could be reversed again by addition of DTT (Ammendola et al., 1994). Furthermore, Wu et al. showed that Sp1 appears to contain redox-sensitive thiol groups and therefore display a high sensitivity to redox regulation *in vitro* and *in vivo* (Wu et al., 1996). Additionally, the reversible loss of zinc finger binding by oxidizing agents *in vitro* provides evidence that Sp1-dependent transcription is sensitive to oxidation (Wu et al., 1996). Furthermore, it was shown that the regulation of the DNA binding activity of Sp1 is redox-dependent by Trx. Using EMSAs Bloomfield et al. showed that Trx can increase Sp1 DNA binding activity *in vitro* and therefore regulate the DNA binding activity of Sp1 redox-dependent (Bloomfield et al., 2003). Myelinating glia cells express Sp1, Sp2, Sp3 and Sp4 and expression levels slightly decrease over time during differentiation (Wegener et al., 2017). Concerning differentiation and myelination in oligodendrocytes and Schwann cells Sp1 has been shown to remove Nkx2.2 as an inhibitory factor from the MBP promoter and therefore activate MBP expression in cooperation with Sox10 (Wegener et al., 2017). Wegener et al. further investigated the effect of Sp1 and Sp3 in oligodendrocytes and found no difference in number of differentiating oligodendrocytes, onset of myelin gene expression and myelin maintenance in adult oligodendrocytes in Sp1and Sp3 knockout mice. Even Sp1 and Sp3 double mutants showed no defects in differentiation (Wegener et al., 2017). This may lead to the conclusion that Sp1 and Sp3 may not play an essential role during

oligodendrocyte differentiation and myelin gene expression (Wegener et al., 2017)

Due to its role in various cellular pathways and processes, it is not surprising, that Sp1 is associated with numerous diseases. Maybe the best-studied example is cancer. Sp1 regulates genes, that are involved in proliferation, immortality, evasion of apoptosis, angiogenesis, tissue invasion and metastasis which are all characteristic for cancer (Black et al., 2001; O'Connor et al., 2016). Alterations in the expression of Sp/KLF family members were found in multiple tumor types and Sp1 is overexpressed in numerous cancer cell types (Black et al., 2001; O'Connor et al., 2016). Here, Sp1 overexpression correlates with tumor stage and a poor prognosis (Li and Davie, 2010). In cancer cell lines (breast, kidney, pancreatic, lung and colon cancers) knockdown of Sp1 decreased survival of cancer cells and inhibited cell growth and migration. Also in mouse xenograft models Sp1 knockdown decreased tumor formation and metastasis (Hedrick et al., 2016). Therefore, it is not surprising that several effective anticancer agents in clinical use, like Mithramycin A, Tolfenomic and Anthracyclines act by inhibiting Sp1 action and binding (O'Connor et al., 2016). Moreover, it is suggested that modulation of ROS scavengers by Sp1 increases cancer malignancy and resistance to chemotherapy. Here the resistance against temozolomide (TMZ), a frequently used chemotherapeutic agent, is for example a major factor leading to the failure of glioblastoma treatment. Chang et al. showed that TMZ-resistant cells showed increased expression of SOD2 as well as Sp1, which is associated with reduced ROS accumulation and revealed Sp1 as a critical transcriptional activator that enhances SOD2 gene expression protecting the GBM and resulting in TMZ tolerance (Chang et al., 2017). Sp1 also seems to play a role in neurodegenerative diseases. Huntington's disease for example is a dominantly inherited neurodegenerative disorder caused by expansion of a polyglutamine tract in the Huntingtin (Htt) protein. Htt binds to Sp1 and TAFII130 and inhibits DNA. Overexpression of both factors lead to an improvement of symptoms (Dunah et al., 2002). Another study showed that Sp1 is overexpressed in brains of transgenic mouse models of Huntington's disease and that inhibition or knockdown of Sp1 led to an improvement of toxicity of Htt and increased survival of the mice (Qiu et al., 2006). Inhibition of Sp1 with Mithramycin A in a mouse model led to further memory impairment and an increase of Amyloidβ peptides indicating an important role of Sp1 in Alzheimer's disease (Citron et al., 2015). Also, in the development of multiple sclerosis Sp1 is implicated. Due to polymorphisms in the *IRF5* and *CD24* genes Sp1 binding is increased, increasing the risk of MS (Kristjansdottir et al., 2008; Wang et al., 2012).

7   Conclusion and Outlook

To sum up, in this study we were able to shed light on the influence of Grx2 on oligodendrocytes under physiological conditions as well as on cancer cells under pathological conditions. We found that Sp1 is a substrate of Grx2. Higher Grx2 levels enhance binding of Sp1 to the CSPG4 promoter, acting as an activator of gene expression. This activation of gene expression leads to an increase of NG2/CSPG4 protein level, which affects differentiation of oligodendrocytes promoting a progenitor state and enhances migration as well as invasion of cells. Favoring a migrating progenitor state of different cell types Grx2 plays an essential role concerning differentiation of oligodendrocytes as well as dedifferentiation of cancer cells. In the future Grx2 could be helpful as a diagnostic marker as well as a therapeutic target. Here, up regulation of Grx2 would be beneficial for example in neurodegenerative diseases like multiple sclerosis to promote migration of OPCs. Previous studies of our group indicated that Grx2 is also beneficial for wound healing (Wilms, 2017). Here further experiments regarding the effect of Grx2 on regeneration and (re-)myelination should be conducted taking advantage of the Grx2 knock-out mouse. On the other hand, in invasive diseases like cancer a down regulation would be beneficial to inhibit migration as well as invasion and metastasis. The future approach and challenge would be to generate therapeutic agents, which are able to modulate Grx2 levels in a disease specific manner.
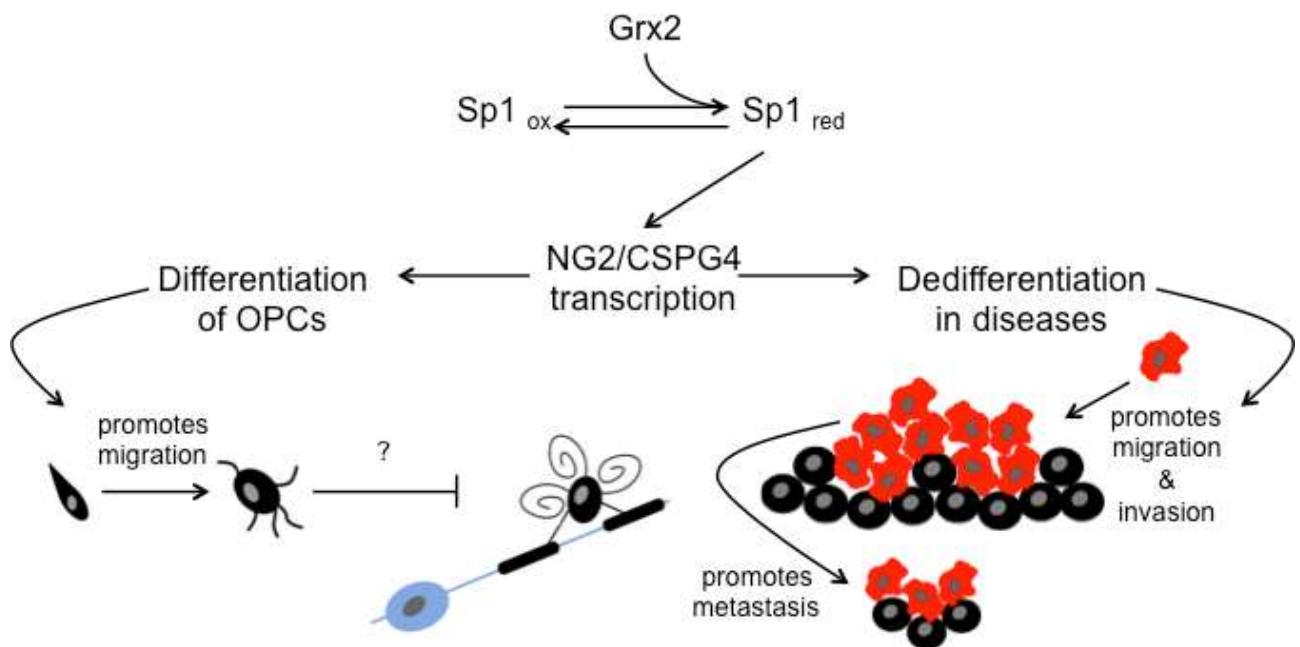
Figure 31: Grx2 regulates NG2/CSPG4 expression via Sp1. Grx2 is able to reduce Sp1 promoting binding of Sp1 to the NG2/CSPG4 promoter. Increased NG2/CSPG4 expression favors progenitor state of oligodendrocytes and promotes migration of oligodendrocytes as well as invasion and metastasis of cancer cells.

8   References

Adams, C.W., Poston, R.N., Buk, S.J., 1989. Pathology, histochemistry and immunocytochemistry of lesions in acute multiple sclerosis. J. Neurol. Sci. 92, 291–306. https://doi.org/10.1016/0022-510x(89)90144-5

Aktas, O., Ullrich, O., Infante-Duarte, C., Nitsch, R., Zipp, F., 2007. Neuronal Damage in Brain Inflammation. Arch. Neurol. 64, 185–189. https://doi.org/10.1001/archneur.64.2.185

Almeida, R.G., Czopka, T., Ffrench-Constant, C., Lyons, D.A., 2011. Individual axons regulate the myelinating potential of single oligodendrocytes in vivo. Dev. Camb. Engl. 138, 4443–4450. https://doi.org/10.1242/dev.071001

Almgren, M., Kc, H., J, F., Cl, C., 2004. Nucleoside diphosphate kinase A/nm23-H1 promotes metastasis of NB69-derived human neuroblastoma [WWW Document]. Mol. Cancer Res. MCR. URL https://pubmed.ncbi.nlm.nih.gov/15280446/ (accessed 4.20.21).

Ammendola, R., Mesuraca, M., Russo, T., Cimino, F., 1994. The DNA-binding efficiency of Sp1 is affected by redox changes. Eur. J. Biochem. 225, 483–489. https://doi.org/10.1111/j.1432-1033.1994.t01-1-00483.x

Amor, S., Puentes, F., Baker, D., van der Valk, P., 2010. Inflammation in neurodegenerative diseases. Immunology 129, 154–169. https://doi.org/10.1111/j.1365-2567.2009.03225.x

Ampofo, E., Schmitt, B.M., Menger, M.D., Laschke, M.W., 2017. The regulatory mechanisms of NG2/CSPG4 expression. Cell. Mol. Biol. Lett. 22, 4. https://doi.org/10.1186/s11658-017-0035-3

Arthur-Farraj, P.J., Latouche, M., Wilton, D.K., Quintes, S., Chabrol, E., Banerjee, A., Woodhoo, A., Jenkins, B., Rahman, M., Turmaine, M., Wicher, G.K., Mitter, R., Greensmith, L., Behrens, A., Raivich, G., Mirsky, R., Jessen, K.R., 2012. c-Jun reprograms Schwann cells of injured nerves to generate a repair cell essential for regeneration. Neuron 75, 633–647. https://doi.org/10.1016/j.neuron.2012.06.021

Attar, E., Bulun, S.E., 2006. Aromatase and other steroidogenic genes in endometriosis: translational aspects. Hum. Reprod. Update 12, 49–56. https://doi.org/10.1093/humupd/dmi034

Bae, Y.S., Kang, S.W., Seo, M.S., Baines, I.C., Tekle, E., Chock, P.B., Rhee, S.G., 1997. Epidermal growth factor (EGF)-induced generation of hydrogen peroxide. Role in EGF receptor-mediated tyrosine phosphorylation. J. Biol. Chem. 272, 217–221.

Berndt, C., Lillig, C.H., 2017. Glutathione, Glutaredoxins, and Iron. Antioxid. Redox Signal. 27, 1235–1251. https://doi.org/10.1089/ars.2017.7132

Berndt, C., Poschmann, G., Stühler, K., Holmgren, A., Bräutigam, L., 2014. Zebrafish heart development is regulated via glutaredoxin 2 dependent migration and survival of neural crest cells. Redox Biol. 2, 673–678. https://doi.org/10.1016/j.redox.2014.04.012

Bin, L., Kim, B.E., Hall, C.F., Leach, S.M., Leung, D.Y., 2011. Inhibition of Transcription Factor Specificity Protein 1 Alters the Gene Expression Profile of Keratinocytes Leading to Up-regulation of Kallikrein-related Peptidases and TSLP. J. Invest. Dermatol. 131, 2213–2222. https://doi.org/10.1038/jid.2011.202

Binamé, F., Sakry, D., Dimou, L., Jolivel, V., Trotter, J., 2013. NG2 regulates directional migration of oligodendrocyte precursor cells via Rho GTPases and polarity complex proteins. J. Neurosci. Off. J. Soc. Neurosci. 33, 10858–10874. https://doi.org/10.1523/JNEUROSCI.5010-12.2013

Black, A.R., Black, J.D., Azizkhan-Clifford, J., 2001. Sp1 and krüppel-like factor family of transcription factors in cell growth regulation and cancer. J. Cell. Physiol. 188, 143–160. https://doi.org/10.1002/jcp.1111

Bloomfield, K.L., Osborne, S.A., Kennedy, D.D., Clarke, F.M., Tonissen, K.F., 2003. Thioredoxin-mediated redox control of the transcription factor Sp1 and regulation of the thioredoxin gene promoter. Gene 319, 107–116. https://doi.org/10.1016/s0378-1119(03)00799-6

Bradl, M., Lassmann, H., 2010. Oligodendrocytes: biology and pathology. Acta Neuropathol. (Berl.)

119, 37–53. https://doi.org/10.1007/s00401-009-0601-5

Bräutigam, L., Jensen, L.D.E., Poschmann, G., Nyström, S., Bannenberg, S., Dreij, K., Lepka, K., Prozorovski, T., Montano, S.J., Aktas, O., Uhlén, P., Stühler, K., Cao, Y., Holmgren, A., Berndt, C., 2013. Glutaredoxin regulates vascular development by reversible glutathionylation of sirtuin 1. Proc. Natl. Acad. Sci. U. S. A. 110, 20057–20062. https://doi.org/10.1073/pnas.1313753110

Bräutigam, L., Schütte, L.D., Godoy, J.R., Prozorovski, T., Gellert, M., Hauptmann, G., Holmgren, A., Lillig, C.H., Berndt, C., 2011. Vertebrate-specific glutaredoxin is essential for brain development. Proc. Natl. Acad. Sci. U. S. A. 108, 20532–20537. https://doi.org/10.1073/pnas.1110085108

Brigelius-Flohé, R., Flohé, L., 2011. Basic principles and emerging concepts in the redox control of transcription factors. Antioxid. Redox Signal. 15, 2335–2381. https://doi.org/10.1089/ars.2010.3534

Bruner-Tran, K.L., Mokshagundam, S., Herington, J.L., Ding, T., Osteen, K.G., 2018. Rodent Models of Experimental Endometriosis: Identifying Mechanisms of Disease and Therapeutic Targets. Curr. Womens Health Rev. 14, 173–188. https://doi.org/10.2174/1573404813666170921162041

Buday, K., Conrad, M., 2021. Emerging roles for non-selenium containing ER-resident glutathione peroxidases in cell signaling and disease. Biol. Chem. 402, 271–287. https://doi.org/10.1515/hsz-2020-0286

Buffo, A., Rossi, F., 2013. Origin, lineage and function of cerebellar glia. Prog. Neurobiol. 109, 42–63. https://doi.org/10.1016/j.pneurobio.2013.08.001

Byles, V., L, Z., Jd, L., Lk, C., J, W., Dv, F., Y, D., 2012. SIRT1 induces EMT by cooperating with EMT transcription factors and enhances prostate cancer cell migration and metastasis [WWW Document]. Oncogene. https://doi.org/10.1038/onc.2011.612

Calabrese, V., Raffaele, R., Cosentino, E., Rizza, V., 1994. Changes in cerebrospinal fluid levels of malondialdehyde and glutathione reductase activity in multiple sclerosis. Int. J. Clin. Pharmacol. Res. 14, 119–123.

Chang, K.-Y., Hsu, T.-I., Hsu, C.-C., Tsai, S.-Y., Liu, J.-J., Chou, S.-W., Liu, M.-S., Liou, J.-P., Ko, C.-Y., Chen, K.-Y., Hung, J.-J., Chang, W.-C., Chuang, C.-K., Kao, T.-J., Chuang, J.-Y., 2017. Specificity protein 1-modulated superoxide dismutase 2 enhances temozolomide resistance in glioblastoma, which is independent of O6-methylguanine-DNA methyltransferase. Redox Biol. 13, 655–664. https://doi.org/10.1016/j.redox.2017.08.005

Chari, D.M., 2007. Remyelination in multiple sclerosis. Int. Rev. Neurobiol. 79, 589–620. https://doi.org/10.1016/S0074-7742(07)79026-8

Chen, C., Zhou, Y., Hu, C., Wang, Y., Yan, Z., Li, Z., Wu, R., 2019. Mitochondria and oxidative stress in ovarian endometriosis. Free Radic. Biol. Med. 136, 22–34. https://doi.org/10.1016/j.freeradbiomed.2019.03.027

Choi, Y.S., Cho, S., Seo, S.K., Park, J.H., Kim, S.H., Lee, B.S., 2015. Alteration in the intrafollicular thiol-redox system in infertile women with endometriosis. Reprod. Camb. Engl. 149, 155–162. https://doi.org/10.1530/REP-14-0438

Citron, B.A., Saykally, J.N., Cao, C., Dennis, J.S., Runfeldt, M., Arendash, G.W., 2015. Transcription factor Sp1 inhibition, memory, and cytokines in a mouse model of Alzheimer's disease. Am. J. Neurodegener. Dis. 4, 40–48.

Costa, C., Martínez-Sáez, E., Gutiérrez-Franco, A., Eixarch, H., Castro, Z., Ortega-Aznar, A., Ramón Y Cajal, S., Montalban, X., Espejo, C., 2015. Expression of semaphorin 3A, semaphorin 7A and their receptors in multiple sclerosis lesions. Mult. Scler. Houndmills Basingstoke Engl. 21, 1632–1643. https://doi.org/10.1177/1352458515599848

Covacu, R., Danilov, A.I., Rasmussen, B.S., Hallén, K., Moe, M.C., Lobell, A., Johansson, C.B., Svensson, M.A., Olsson, T., Brundin, L., 2006. Nitric oxide exposure diverts neural stem cell fate from neurogenesis towards astrogliogenesis. Stem Cells Dayt. Ohio 24, 2792–2800.

https://doi.org/10.1634/stemcells.2005-0640

Dickinson, B.C., Peltier, J., Stone, D., Schaffer, D.V., Chang, C.J., 2011. Nox2 redox signaling maintains essential cell populations in the brain. Nat. Chem. Biol. 7, 106–112. https://doi.org/10.1038/nchembio.497

Dietrich, M., Hecker, C., Hilla, A., Cruz-Herranz, A., Hartung, H.-P., Fischer, D., Green, A., Albrecht, P., 2019. Using Optical Coherence Tomography and Optokinetic Response As Structural and Functional Visual System Readouts in Mice and Rats. J. Vis. Exp. JoVE. https://doi.org/10.3791/58571

Dimou, L., Gallo, V., 2015. NG2-glia and their functions in the central nervous system. Glia 63, 1429–1451. https://doi.org/10.1002/glia.22859

Dunah, A.W., Jeong, H., Griffin, A., Kim, Y.-M., Standaert, D.G., Hersch, S.M., Mouradian, M.M., Young, A.B., Tanese, N., Krainc, D., 2002. Sp1 and TAFII130 transcriptional activity disrupted in early Huntington's disease. Science 296, 2238–2243. https://doi.org/10.1126/science.1072613

Ej, M., K, S., B, O., E, K., Ea, B., V, K., Cg, B., C, B., A, W., T, B., 2012. Claudin K Is Specifically Expressed in Cells That Form Myelin During Development of the Nervous System and Regeneration of the Optic Nerve in Adult Zebrafish [WWW Document]. Glia. https://doi.org/10.1002/glia.21260

Ellwardt, E., Zipp, F., 2014. Molecular mechanisms linking neuroinflammation and neurodegeneration in MS. Exp. Neurol. 262 Pt A, 8–17. https://doi.org/10.1016/j.expneurol.2014.02.006

Enoksson, M., Fernandes, A.P., Prast, S., Lillig, C.H., Holmgren, A., Orrenius, S., 2005. Overexpression of glutaredoxin 2 attenuates apoptosis by preventing cytochrome c release. Biochem. Biophys. Res. Commun. 327, 774–779. https://doi.org/10.1016/j.bbrc.2004.12.067

Feng, X., Szulzewsky, F., Yerevanian, A., Chen, Z., Heinzmann, D., Rasmussen, R.D., Alvarez-Garcia, V., Kim, Y., Wang, B., Tamagno, I., Zhou, H., Li, X., Kettenmann, H., Ransohoff, R.M., Hambardzumyan, D., 2015. Loss of CX3CR1 increases accumulation of inflammatory monocytes and promotes gliomagenesis. Oncotarget 6, 15077–15094. https://doi.org/10.18632/oncotarget.3730

Fernandes, A.P., Capitanio, A., Selenius, M., Brodin, O., Rundlöf, A.-K., Björnstedt, M., 2009. Expression profiles of thioredoxin family proteins in human lung cancer tissue: correlation with proliferation and differentiation. Histopathology 55, 313–320. https://doi.org/10.1111/j.1365-2559.2009.03381.x

Franklin, R.J., Blakemore, W.F., 1997. To what extent is oligodendrocyte progenitor migration a limiting factor in the remyelination of multiple sclerosis lesions? Mult. Scler. Houndmills Basingstoke Engl. 3, 84–87.

Franklin, R.J.M., Ffrench-Constant, C., 2008. Remyelination in the CNS: from biology to therapy. Nat. Rev. Neurosci. 9, 839–855. https://doi.org/10.1038/nrn2480

Gellert, M., Hanschmann, E.-M., Lepka, K., Berndt, C., Lillig, C.H., 2015. Redox regulation of cytoskeletal dynamics during differentiation and de-differentiation. Biochim. Biophys. Acta 1850, 1575–1587. https://doi.org/10.1016/j.bbagen.2014.10.030

Gellert, M., Richter, E., Mostertz, J., Kantz, L., Masur, K., Hanschmann, E.-M., Ribback, S., Kroeger, N., Schaeffeler, E., Winter, S., Hochgräfe, F., Schwab, M., Lillig, C.H., 2020. The cytosolic isoform of glutaredoxin 2 promotes cell migration and invasion. Biochim. Biophys. Acta Gen. Subj. 1864, 129599. https://doi.org/10.1016/j.bbagen.2020.129599

Gellert, M., Venz, S., Mitlöhner, J., Cott, C., Hanschmann, E.-M., Lillig, C.H., 2013. Identification of a dithiol-disulfide switch in collapsin response mediator protein 2 (CRMP2) that is toggled in a model of neuronal differentiation. J. Biol. Chem. 288, 35117–35125. https://doi.org/10.1074/jbc.M113.521443

Gravendeel, L.A.M., Kouwenhoven, M.C.M., Gevaert, O., Rooi, J.J. de, Stubbs, A.P., Duijm, J.E., Daemen, A., Bleeker, F.E., Bralten, L.B.C., Kloosterhof, N.K., Moor, B.D., Eilers, P.H.C.,

Spek, P.J. van der, Kros, J.M., Smitt, P.A.E.S., Bent, M.J. van den, French, P.J., 2009. Intrinsic Gene Expression Profiles of Gliomas Are a Better Predictor of Survival than Histology. Cancer Res. 69, 9065–9072. https://doi.org/10.1158/0008-5472.CAN-09-2307

Greco, A., Minghetti, L., Sette, G., Fieschi, C., Levi, G., 1999. Cerebrospinal fluid isoprostane shows oxidative stress in patients with multiple sclerosis. Neurology 53, 1876–1879. https://doi.org/10.1212/wnl.53.8.1876

Hametner, S., Wimmer, I., Haider, L., Pfeifenbring, S., Brück, W., Lassmann, H., 2013. Iron and neurodegeneration in the multiple sclerosis brain. Ann. Neurol. 74, 848–861. https://doi.org/10.1002/ana.23974

Hanschmann, E.-M., Godoy, J.R., Berndt, C., Hudemann, C., Lillig, C.H., 2013a. Thioredoxins, glutaredoxins, and peroxiredoxins--molecular mechanisms and health significance: from cofactors to antioxidants to redox signaling. Antioxid. Redox Signal. 19, 1539–1605. https://doi.org/10.1089/ars.2012.4599

Hanschmann, E.-M., Godoy, J.R., Berndt, C., Hudemann, C., Lillig, C.H., 2013b. Thioredoxins, glutaredoxins, and peroxiredoxins--molecular mechanisms and health significance: from cofactors to antioxidants to redox signaling. Antioxid. Redox Signal. 19, 1539–1605. https://doi.org/10.1089/ars.2012.4599

Hedrick, E., Cheng, Y., Jin, U.-H., Kim, K., Safe, S., 2016. Specificity protein (Sp) transcription factors Sp1, Sp3 and Sp4 are non-oncogene addiction genes in cancer cells. Oncotarget 7, 22245–22256. https://doi.org/10.18632/oncotarget.7925

Hohlfeld, R., Dornmair, K., Meinl, E., Wekerle, H., 2016. The search for the target antigens of multiple sclerosis, part 2: CD8+ T cells, B cells, and antibodies in the focus of reverse-translational research. Lancet Neurol. 15, 317–331. https://doi.org/10.1016/S1474-4422(15)00313-0

Hudemann, C., Lönn, M.E., Godoy, J.R., Zahedi Avval, F., Capani, F., Holmgren, A., Lillig, C.H., 2009. Identification, expression pattern, and characterization of mouse glutaredoxin 2 isoforms. Antioxid. Redox Signal. 11, 1–14. https://doi.org/10.1089/ars.2008.2068

Hussain, S.P., Amstad, P., He, P., Robles, A., Lupold, S., Kaneko, I., Ichimiya, M., Sengupta, S., Mechanic, L., Okamura, S., Hofseth, L.J., Moake, M., Nagashima, M., Forrester, K.S., Harris, C.C., 2004. p53-induced up-regulation of MnSOD and GPx but not catalase increases oxidative stress and apoptosis. Cancer Res. 64, 2350–2356. https://doi.org/10.1158/0008-5472.can-2287-2

Hybertson, B.M., Gao, B., Bose, S.K., McCord, J.M., 2011. Oxidative stress in health and disease: the therapeutic potential of Nrf2 activation. Mol. Aspects Med. 32, 234–246. https://doi.org/10.1016/j.mam.2011.10.006

Idelchik, M.D.P.S., Begley, U., Begley, T.J., Melendez, J.A., 2017. Mitochondrial ROS control of cancer. Semin. Cancer Biol. 47, 57–66. https://doi.org/10.1016/j.semcancer.2017.04.005

Iwabuchi, T., Yoshimoto, C., Shigetomi, H., Kobayashi, H., 2015. Oxidative Stress and Antioxidant Defense in Endometriosis and Its Malignant Transformation. Oxid. Med. Cell. Longev. 2015. https://doi.org/10.1155/2015/848595

Jana, M., Pahan, K., 2005. Redox regulation of cytokine-mediated inhibition of myelin gene expression in human primary oligodendrocytes. Free Radic. Biol. Med. 39, 823–831. https://doi.org/10.1016/j.freeradbiomed.2005.05.014

Jones, D.P., Sies, H., 2015. The Redox Code. Antioxid. Redox Signal. 23, 734–746. https://doi.org/10.1089/ars.2015.6247

Juurlink, B.H., 1997. Response of glial cells to ischemia: roles of reactive oxygen species and glutathione. Neurosci. Biobehav. Rev. 21, 151–166. https://doi.org/10.1016/s0149-7634(96)00005-x

Kawaguchi, A., Yajima, N., Tsuchiya, N., Homma, J., Sano, M., Natsumeda, M., Takahashi, H., Fujii, Y., Kakuma, T., Yamanaka, R., 2013. Gene expression signature-based prognostic risk score in patients with glioblastoma. Cancer Sci. 104, 1205–1210. https://doi.org/10.1111/cas.12214

Koch, M.W., Ramsaransing, G.S.M., Arutjunyan, A.V., Stepanov, M., Teelken, A., Heersema, D.J., De Keyser, J., 2006. Oxidative stress in serum and peripheral blood leukocytes in patients with different disease courses of multiple sclerosis. J. Neurol. 253, 483–487. https://doi.org/10.1007/s00415-005-0037-3

Kocsis, J.D., Waxman, S.G., 2007. Schwann cells and their precursors for repair of central nervous system myelin. Brain 130, 1978–1980. https://doi.org/10.1093/brain/awm161

Kremer, D., Göttle, P., Hartung, H.-P., Küry, P., 2016. Pushing Forward: Remyelination as the New Frontier in CNS Diseases. Trends Neurosci. 39, 246–263. https://doi.org/10.1016/j.tins.2016.02.004

Kristjansdottir, G., Sandling, J.K., Bonetti, A., Roos, I.M., Milani, L., Wang, C., Gustafsdottir, S.M., Sigurdsson, S., Lundmark, A., Tienari, P.J., Koivisto, K., Elovaara, I., Pirttilä, T., Reunanen, M., Peltonen, L., Saarela, J., Hillert, J., Olsson, T., Landegren, U., Alcina, A., Fernández, O., Leyva, L., Guerrero, M., Lucas, M., Izquierdo, G., Matesanz, F., Syvänen, A.-C., 2008. Interferon regulatory factor 5 (IRF5) gene variants are associated with multiple sclerosis in three distinct populations. J. Med. Genet. 45, 362–369. https://doi.org/10.1136/jmg.2007.055012

Kunimoto, R., K, J., A, T., M, S., K, H., T, H., S, H., T, S., T, H., T, Y., Y, H., 2014. SIRT1 regulates lamellipodium extension and migration of melanoma cells [WWW Document]. J. Invest. Dermatol. https://doi.org/10.1038/jid.2014.50

Lambrinoudaki, I.V., Augoulea, A., Christodoulakos, G.E., Economou, E.V., Kaparos, G., Kontoravdis, A., Papadias, C., Creatsas, G., 2009. Measurable serum markers of oxidative stress response in women with endometriosis. Fertil. Steril. 91, 46–50. https://doi.org/10.1016/j.fertnstert.2007.11.021

Lawson, N.D., Weinstein, B.M., 2002. In vivo imaging of embryonic vascular development using transgenic zebrafish. Dev. Biol. 248, 307–318. https://doi.org/10.1006/dbio.2002.0711

Le Belle, J.E., Orozco, N.M., Paucar, A.A., Saxe, J.P., Mottahedeh, J., Pyle, A.D., Wu, H., Kornblum, H.I., 2011. Proliferative neural stem cells have high endogenous ROS levels that regulate self-renewal and neurogenesis in a PI3K/Akt-dependant manner. Cell Stem Cell 8, 59–71. https://doi.org/10.1016/j.stem.2010.11.028

Lee, E., J, J., Se, K., Ej, S., Sw, K., Kj, L., 2009. Multiple functions of Nm23-H1 are regulated by oxido-reduction system [WWW Document]. PloS One. https://doi.org/10.1371/journal.pone.0007949

Lepka, K., Berndt, C., Hartung, H.-P., Aktas, O., 2016. Redox Events As Modulators of Pathology and Therapy of Neuroinflammatory Diseases. Front. Cell Dev. Biol. 4, 63. https://doi.org/10.3389/fcell.2016.00063

Lepka, K., Volbracht, K., Bill, E., Schneider, R., Rios, N., Hildebrandt, T., Ingwersen, J., Prozorovski, T., Lillig, C.H., van Horssen, J., Steinman, L., Hartung, H.-P., Radi, R., Holmgren, A., Aktas, O., Berndt, C., 2017. Iron-sulfur glutaredoxin 2 protects oligodendrocytes against damage induced by nitric oxide release from activated microglia. Glia 65, 1521–1534. https://doi.org/10.1002/glia.23178

Lepka, K.M., n.d. Iron-sulfur cluster coordinating Glutaredoxins in neuroinflammatory degeneration and regeneration. Dissertation, Düsseldorf, Heinrich-Heine-Universität, 2017.

Li, J., E, W., F, R., K, D., 2005. Upregulation of VEGF-C by androgen depletion: the involvement of IGF-IR-FOXO pathway [WWW Document]. Oncogene. https://doi.org/10.1038/sj.onc.1208693

Li, L., Davie, J.R., 2010. The role of Sp1 and Sp3 in normal and cancer cell biology. Ann. Anat. Anat. Anz. Off. Organ Anat. Ges. 192, 275–283. https://doi.org/10.1016/j.aanat.2010.07.010

Lillig, C.H., Berndt, C., 2013. Glutaredoxins in thiol/disulfide exchange. Antioxid. Redox Signal. 18, 1654–1665. https://doi.org/10.1089/ars.2012.5007

Lillig, C.H., Berndt, C., Holmgren, A., 2008. Glutaredoxin systems. Biochim. Biophys. Acta 1780, 1304–1317. https://doi.org/10.1016/j.bbagen.2008.06.003

Lillig, C.H., Berndt, C., Vergnolle, O., Lönn, M.E., Hudemann, C., Bill, E., Holmgren, A., 2005. Characterization of human glutaredoxin 2 as iron-sulfur protein: a possible role as redox sensor. Proc. Natl. Acad. Sci. U. S. A. 102, 8168–8173. https://doi.org/10.1073/pnas.0500735102

Lönn, M.E., Hudemann, C., Berndt, C., Cherkasov, V., Capani, F., Holmgren, A., Lillig, C.H., 2008. Expression pattern of human glutaredoxin 2 isoforms: identification and characterization of two testis/cancer cell-specific isoforms. Antioxid. Redox Signal. 10, 547–557. https://doi.org/10.1089/ars.2007.1821

Lopez Juarez, A., He, D., Richard Lu, Q., 2016. Oligodendrocyte progenitor programming and reprogramming: Toward myelin regeneration. Brain Res. 1638, 209–220. https://doi.org/10.1016/j.brainres.2015.10.051

Lundberg, M., Fernandes, A.P., Kumar, S., Holmgren, A., 2004. Cellular and plasma levels of human glutaredoxin 1 and 2 detected by sensitive ELISA systems. Biochem. Biophys. Res. Commun. 319, 801–809. https://doi.org/10.1016/j.bbrc.2004.04.199

Lyons, D.A., Talbot, W.S., 2015. Glial Cell Development and Function in Zebrafish. Cold Spring Harb. Perspect. Biol. 7. https://doi.org/10.1101/cshperspect.a020586

Macedo, G.S., Lisbôa da Motta, L., Giacomazzi, J., Netto, C.B.O., Manfredini, V., Vanzin, C.S., Vargas, C.R., Hainaut, P., Klamt, F., Ashton-Prolla, P., 2012. Increased oxidative damage in carriers of the germline TP53 p.R337H mutation. PloS One 7, e47010. https://doi.org/10.1371/journal.pone.0047010

Mirsky, R., Jessen, K.R., 1996. Schwann cell development, differentiation and myelination. Curr. Opin. Neurobiol. 6, 89–96.

Mollbrink, A., Jawad, R., Vlamis-Gardikas, A., Edenvik, P., Isaksson, B., Danielsson, O., Stål, P., Fernandes, A.P., 2014. Expression of thioredoxins and glutaredoxins in human hepatocellular carcinoma: correlation to cell proliferation, tumor size and metabolic syndrome. Int. J. Immunopathol. Pharmacol. 27, 169–183. https://doi.org/10.1177/039463201402700204

Münzel, E.J., Schaefer, K., Obirei, B., Kremmer, E., Burton, E.A., Kuscha, V., Becker, C.G., Brösamle, C., Williams, A., Becker, T., 2012. Claudin k is specifically expressed in cells that form myelin during development of the nervous system and regeneration of the optic nerve in adult zebrafish. Glia 60, 253–270. https://doi.org/10.1002/glia.21260

Nishiyama, A., Boshans, L., Goncalves, C.M., Wegrzyn, J., Patel, K.D., 2016. Lineage, fate, and fate potential of NG2-glia. Brain Res. 1638, 116–128. https://doi.org/10.1016/j.brainres.2015.08.013

Noble, M., Mayer-Pröschel, M., Pröschel, C., 2005. Redox regulation of precursor cell function: insights and paradoxes. Antioxid. Redox Signal. 7, 1456–1467. https://doi.org/10.1089/ars.2005.7.1456

Obrador, E., Liu-Smith, F., Dellinger, R.W., Salvador, R., Meyskens, F.L., Estrela, J.M., 2019. Oxidative stress and antioxidants in the pathophysiology of malignant melanoma. Biol. Chem. 400, 589–612. https://doi.org/10.1515/hsz-2018-0327

O'Connor, L., Gilmour, J., Bonifer, C., 2016. The Role of the Ubiquitously Expressed Transcription Factor Sp1 in Tissue-specific Transcriptional Regulation and in Disease. Yale J. Biol. Med. 89, 513–525.

Olguín-Albuerne, M., Morán, J., 2018. Redox Signaling Mechanisms in Nervous System Development. Antioxid. Redox Signal. 28, 1603–1625. https://doi.org/10.1089/ars.2017.7284

Pacher, P., Beckman, J.S., Liaudet, L., 2007. Nitric oxide and peroxynitrite in health and disease. Physiol. Rev. 87, 315–424. https://doi.org/10.1152/physrev.00029.2006

Park, H.-C., Mehta, A., Richardson, J.S., Appel, B., 2002. olig2 is required for zebrafish primary motor neuron and oligodendrocyte development. Dev. Biol. 248, 356–368. https://doi.org/10.1006/dbio.2002.0738

Pérez Estrada, C., Covacu, R., Sankavaram, S.R., Svensson, M., Brundin, L., 2014. Oxidative stress increases neurogenesis and oligodendrogenesis in adult neural progenitor cells. Stem Cells

Dev. 23, 2311–2327. https://doi.org/10.1089/scd.2013.0452

Petratos, S., Azari, M.F., Ozturk, E., Papadopoulos, R., Bernard, C.C.A., 2010. Novel therapeutic targets for axonal degeneration in multiple sclerosis. J. Neuropathol. Exp. Neurol. 69, 323–334. https://doi.org/10.1097/NEN.0b013e3181d60ddb

Price, M.A., Colvin Wanshura, L.E., Yang, J., Carlson, J., Xiang, B., Li, G., Ferrone, S., Dudek, A.Z., Turley, E.A., McCarthy, J.B., 2011. CSPG4, a potential therapeutic target, facilitates malignant progression of melanoma. Pigment Cell Melanoma Res. 24, 1148–1157. https://doi.org/10.1111/j.1755-148X.2011.00929.x

Qiu, Z., Norflus, F., Singh, B., Swindell, M.K., Buzescu, R., Bejarano, M., Chopra, R., Zucker, B., Benn, C.L., DiRocco, D.P., Cha, J.-H.J., Ferrante, R.J., Hersch, S.M., 2006. Sp1 is up-regulated in cellular and transgenic models of Huntington disease, and its reduction is neuroprotective. J. Biol. Chem. 281, 16672–16680. https://doi.org/10.1074/jbc.M511648200

Radeff-Huang, J., Seasholtz, T.M., Chang, J.W., Smith, J.M., Walsh, C.T., Brown, J.H., 2007. Tumor necrosis factor-alpha-stimulated cell proliferation is mediated through sphingosine kinase-dependent Akt activation and cyclin D expression. J. Biol. Chem. 282, 863–870. https://doi.org/10.1074/jbc.M601698200

Rastrelli, M., Tropea, S., Rossi, C.R., Alaibac, M., 2014. Melanoma: epidemiology, risk factors, pathogenesis, diagnosis and classification. Vivo Athens Greece 28, 1005–1011.

Reardon, D.A., Ligon, K.L., Chiocca, E.A., Wen, P.Y., 2015. One size should not fit all: advancing toward personalized glioblastoma therapy. Discov. Med. 19, 471–477.

Robinson, S., Miller, R.H., 1999. Contact with central nervous system myelin inhibits oligodendrocyte progenitor maturation. Dev. Biol. 216, 359–368. https://doi.org/10.1006/dbio.1999.9466

Rudick, R.A., Mi, S., Sandrock, A.W., 2008. LINGO-1 antagonists as therapy for multiple sclerosis: in vitro and in vivo evidence. Expert Opin. Biol. Ther. 8, 1561–1570. https://doi.org/10.1517/14712598.8.10.1561

Salazar-Ramiro, A., Ramírez-Ortega, D., Pérez de la Cruz, V., Hérnandez-Pedro, N.Y., González-Esquivel, D.F., Sotelo, J., Pineda, B., 2016. Role of Redox Status in Development of Glioblastoma. Front. Immunol. 7, 156. https://doi.org/10.3389/fimmu.2016.00156

Salzano, S., Checconi, P., Hanschmann, E.-M., Lillig, C.H., Bowler, L.D., Chan, P., Vaudry, D., Mengozzi, M., Coppo, L., Sacre, S., Atkuri, K.R., Sahaf, B., Herzenberg, L.A., Herzenberg, L.A., Mullen, L., Ghezzi, P., 2014. Linkage of inflammation and oxidative stress via release of glutathionylated peroxiredoxin-2, which acts as a danger signal. Proc. Natl. Acad. Sci. U. S. A. 111, 12157–12162. https://doi.org/10.1073/pnas.1401712111

Sawcer, S., Hellenthal, G., Pirinen, M., Spencer, C.C.A., Patsopoulos, N.A., Moutsianas, L., Dilthey, A., Su, Z., Freeman, C., Hunt, S.E., Edkins, S., Gray, E., Booth, D.R., Potter, S.C., Goris, A., Band, G., Oturai, A.B., Strange, A., Saarela, J., Bellenguez, C., Fontaine, B., Gillman, M., Hemmer, B., Gwilliam, R., Zipp, F., Jayakumar, A., Martin, R., Leslie, S., Hawkins, S., Giannoulatou, E., D'alfonso, S., Blackburn, H., Boneschi, F.M., Liddle, J., Harbo, H.F., Perez, M.L., Spurkland, A., Waller, M.J., Mycko, M.P., Ricketts, M., Comabella, M., Hammond, N., Kockum, I., McCann, O.T., Ban, M., Whittaker, P., Kemppinen, A., Weston, P., Hawkins, C., Widaa, S., Zajicek, J., Dronov, S., Robertson, N., Bumpstead, S.J., Barcellos, L.F., Ravindrarajah, R., Abraham, R., Alfredsson, L., Ardlie, K., Aubin, C., Baker, A., Baker, K., Baranzini, S.E., Bergamaschi, L., Bergamaschi, R., Bernstein, A., Berthele, A., Boggild, M., Bradfield, J.P., Brassat, D., Broadley, S.A., Buck, D., Butzkueven, H., Capra, R., Carroll, W.M., Cavalla, P., Celius, E.G., Cepok, S., Chiavacci, R., Clerget-Darpoux, F., Clysters, K., Comi, G., Cossburn, M., Cournu-Rebeix, I., Cox, M.B., Cozen, W., Cree, B.A.C., Cross, A.H., Cusi, D., Daly, M.J., Davis, E., de Bakker, P.I.W., Debouverie, M., D'hooghe, M.B., Dixon, K., Dobosi, R., Dubois, B., Ellinghaus, D., Elovaara, I., Esposito, F., Fontenille, C., Foote, S., Franke, A., Galimberti, D., Ghezzi, A., Glessner, J., Gomez, R., Gout, O., Graham, C., Grant, S.F.A., Guerini, F.R., Hakonarson, H., Hall, P., Hamsten, A., Hartung, H.-P.,

Heard, R.N., Heath, S., Hobart, J., Hoshi, M., Infante-Duarte, C., Ingram, G., Ingram, W., Islam, T., Jagodic, M., Kabesch, M., Kermode, A.G., Kilpatrick, T.J., Kim, C., Klopp, N., Koivisto, K., Larsson, M., Lathrop, M., Lechner-Scott, J.S., Leone, M.A., Leppä, V., Liljedahl, U., Bomfim, I.L., Lincoln, R.R., Link, J., Liu, J., Lorentzen, Å.R., Lupoli, S., Macciardi, F., Mack, T., Marriott, M., Martinelli, V., Mason, D., McCauley, J.L., Mentch, F., Mero, I.-L., Mihalova, T., Montalban, X., Mottershead, J., Myhr, K.-M., Naldi, P., Ollier, W., Page, A., Palotie, A., Pelletier, J., Piccio, L., Pickersgill, T., Piehl, F., Pobywajlo, S., Quach, H.L., Ramsay, P.P., Reunanen, M., Reynolds, R., Rioux, J.D., Rodegher, M., Roesner, S., Rubio, J.P., Rückert, I.-M., Salvetti, M., Salvi, E., Santaniello, A., Schaefer, C.A., Schreiber, S., Schulze, C., Scott, R.J., Sellebjerg, F., Selmaj, K.W., Sexton, D., Shen, L., Simms-Acuna, B., Skidmore, S., Sleiman, P.M.A., Smestad, C., Sørensen, P.S., Søndergaard, H.B., Stankovich, J., Strange, R.C., Sulonen, A.-M., Sundqvist, E., Syvänen, A.-C., Taddeo, F., Taylor, B., Blackwell, J.M., Tienari, P., Bramon, E., Tourbah, A., Brown, M.A., Tronczynska, E., Casas, J.P., Tubridy, N., Corvin, A., Vickery, J., Jankowski, J., Villoslada, P., Markus, H.S., Wang, K., Mathew, C.G., Wason, J., Palmer, C.N.A., Wichmann, H.-E., Plomin, R., Willoughby, E., Rautanen, A., Winkelmann, J., Wittig, M., Trembath, R.C., Yaouanq, J., Viswanathan, A.C., Zhang, H., Wood, N.W., Zuvich, R., Deloukas, P., Langford, C., Duncanson, A., Oksenberg, J.R., Pericak-Vance, M.A., Haines, J.L., Olsson, T., Hillert, J., Ivinson, A.J., De Jager, P.L., Peltonen, L., Stewart, G.J., Hafler, D.A., Hauser, S.L., McVean, G., Donnelly, P., Compston, A., 2011. Genetic risk and a primary role for cell-mediated immune mechanisms in multiple sclerosis. Nature 476, 214–219. https://doi.org/10.1038/nature10251

Schafer, F.Q., Buettner, G.R., 2001. Redox environment of the cell as viewed through the redox state of the glutathione disulfide/glutathione couple. Free Radic. Biol. Med. 30, 1191–1212.

Schiffer, D., Mellai, M., Boldorini, R., Bisogno, I., Grifoni, S., Corona, C., Bertero, L., Cassoni, P., Casalone, C., Annovazzi, L., 2018. The Significance of Chondroitin Sulfate Proteoglycan 4 (CSPG4) in Human Gliomas. Int. J. Mol. Sci. 19. https://doi.org/10.3390/ijms19092724

Scutiero, G., Iannone, P., Bernardi, G., Bonaccorsi, G., Spadaro, S., Volta, C.A., Greco, P., Nappi, L., 2017. Oxidative Stress and Endometriosis: A Systematic Review of the Literature. Oxid. Med. Cell. Longev. 2017, 7265238. https://doi.org/10.1155/2017/7265238

Sellers, D.L., Maris, D.O., Horner, P.J., 2009. Postinjury Niches Induce Temporal Shifts in Progenitor Fates to Direct Lesion Repair after Spinal Cord Injury. J. Neurosci. 29, 6722–6733. https://doi.org/10.1523/JNEUROSCI.4538-08.2009

Seo, S.K., Yang, H.I., Lee, K.E., Kim, H.Y., Cho, S., Choi, Y.S., Lee, B.S., 2010. The roles of thioredoxin and thioredoxin-binding protein-2 in endometriosis. Hum. Reprod. Oxf. Engl. 25, 1251–1258. https://doi.org/10.1093/humrep/deq027

Shigetomi, S., T, S., K, S., C, U., Y, T., S, K., K, N., Y, Y., N, K., H, K., 2014. Inhibition of cell death and induction of G2 arrest accumulation in human ovarian clear cells by HNF-1β transcription factor: chemosensitivity is regulated by checkpoint kinase CHK1 [WWW Document]. Int. J. Gynecol. Cancer Off. J. Int. Gynecol. Cancer Soc. https://doi.org/10.1097/IGC.0000000000000136

Shin, J., Park, H.-C., Topczewska, J.M., Mawdsley, D.J., Appel, B., 2003. Neural cell fate analysis in zebrafish using olig2 BAC transgenics. Methods Cell Sci. Off. J. Soc. Vitro Biol. 25, 7–14. https://doi.org/10.1023/B:MICS.0000006847.09037.3a

Sies, H., Cadenas, E., 1985. Oxidative stress: damage to intact cells and organs. Philos. Trans. R. Soc. Lond. B. Biol. Sci. 311, 617–631. https://doi.org/10.1098/rstb.1985.0168

Sleiman, S.F., Langley, B.C., Basso, M., Berlin, J., Xia, L., Payappilly, J.B., Kharel, M.K., Guo, H., Marsh, J.L., Thompson, L.M., Mahishi, L., Ahuja, P., MacLellan, W.R., Geschwind, D.H., Coppola, G., Rohr, J., Ratan, R.R., 2011. Mithramycin Is a Gene-Selective Sp1 Inhibitor That Identifies a Biological Intersection between Cancer and Neurodegeneration. J. Neurosci. 31, 6858–6870. https://doi.org/10.1523/JNEUROSCI.0710-11.2011

Socha, K., Kochanowicz, J., Karpińska, E., Soroczyńska, J., Jakoniuk, M., Mariak, Z., Borawska, M.H., 2014. Dietary habits and selenium, glutathione peroxidase and total antioxidant status in the serum of patients with relapsing-remitting multiple sclerosis. Nutr. J. 13, 62. https://doi.org/10.1186/1475-2891-13-62

Sock, E., Wegner, M., 2019. Transcriptional control of myelination and remyelination. Glia 67, 2153–2165. https://doi.org/10.1002/glia.23636

Su, D.M., Zhang, Q., Wang, X., He, P., Zhu, Y.J., Zhao, J., Rennert, O.M., Su, Y.A., 2009. Two types of human malignant melanoma cell lines revealed by expression patterns of mitochondrial and survival-apoptosis genes: implications for malignant melanoma therapy. Mol. Cancer Ther. 8, 1292–1304. https://doi.org/10.1158/1535-7163.MCT-08-1030

Suske, G., 1999. The Sp-family of transcription factors. Gene 238, 291–300. https://doi.org/10.1016/s0378-1119(99)00357-1

Svendsen, A., Verhoeff, J.J.C., Immervoll, H., Brøgger, J.C., Kmiecik, J., Poli, A., Netland, I.A., Prestegarden, L., Planagumà, J., Torsvik, A., Kjersem, A.B., Sakariassen, P.Ø., Heggdal, J.I., Van Furth, W.R., Bjerkvig, R., Lund-Johansen, M., Enger, P.Ø., Felsberg, J., Brons, N.H.C., Tronstad, K.J., Waha, A., Chekenya, M., 2011. Expression of the progenitor marker NG2/CSPG4 predicts poor survival and resistance to ionising radiation in glioblastoma. Acta Neuropathol. (Berl.) 122, 495–510. https://doi.org/10.1007/s00401-011-0867-2

Tan, M., Li, S., Swaroop, M., Guan, K., Oberley, L.W., Sun, Y., 1999. Transcriptional activation of the human glutathione peroxidase promoter by p53. J. Biol. Chem. 274, 12061–12066. https://doi.org/10.1074/jbc.274.17.12061

Tan, N.Y., Khachigian, L.M., 2009. Sp1 phosphorylation and its regulation of gene transcription. Mol. Cell. Biol. 29, 2483–2488. https://doi.org/10.1128/MCB.01828-08

Thorburne, S.K., Juurlink, B.H., 1996. Low glutathione and high iron govern the susceptibility of oligodendroglial precursors to oxidative stress. J. Neurochem. 67, 1014–1022. https://doi.org/10.1046/j.1471-4159.1996.67031014.x

Trapp, B.D., Nave, K.-A., 2008. Multiple sclerosis: an immune or neurodegenerative disorder? Annu. Rev. Neurosci. 31, 247–269. https://doi.org/10.1146/annurev.neuro.30.051606.094313

Trotter, J., Karram, K., Nishiyama, A., 2010. NG2 cells: properties, progeny and origin. Brain Res. Rev. 63, 72–82. https://doi.org/10.1016/j.brainresrev.2009.12.006

Upadhyaya, B., Tian, X., Wu, H., Lou, M.F., 2015. Expression and distribution of thiol-regulating enzyme glutaredoxin 2 (GRX2) in porcine ocular tissues. Exp. Eye Res. 130, 58–65. https://doi.org/10.1016/j.exer.2014.12.004

van Horssen, J., Witte, M.E., Schreibelt, G., de Vries, H.E., 2011. Radical changes in multiple sclerosis pathogenesis. Biochim. Biophys. Acta 1812, 141–150. https://doi.org/10.1016/j.bbadis.2010.06.011

Viganò, F., Dimou, L., 2016. The heterogeneous nature of NG2-glia. Brain Res. 1638, 129–137. https://doi.org/10.1016/j.brainres.2015.09.012

Wang, J., Svendsen, A., Kmiecik, J., Immervoll, H., Skaftnesmo, K.O., Planagumà, J., Reed, R.K., Bjerkvig, R., Miletic, H., Enger, P.Ø., Rygh, C.B., Chekenya, M., 2011. Targeting the NG2/CSPG4 Proteoglycan Retards Tumour Growth and Angiogenesis in Preclinical Models of GBM and Melanoma. PLoS ONE 6. https://doi.org/10.1371/journal.pone.0023062

Wang, L., Liu, R., Li, D., Lin, S., Fang, X., Backer, G., Kain, M., Rammoham, K., Zheng, P., Liu, Y., 2012. A hypermorphic SP1-binding CD24 variant associates with risk and progression of multiple sclerosis. Am. J. Transl. Res. 4, 347–356.

Wegener, A., Küspert, M., Sock, E., Philipsen, S., Suske, G., Wegner, M., 2017. Sp2 is the only glutamine-rich specificity protein with minor impact on development and differentiation in myelinating glia. J. Neurochem. 140, 245–256. https://doi.org/10.1111/jnc.13908

Wilms, C., 2017. Regulation of oligodendrocyte differentiation and migration via Glutaredoxin 2.

Wu, H., Lin, L., Giblin, F., Ho, Y.-S., Lou, M.F., 2011. Glutaredoxin 2 knockout increases sensitivity to oxidative stress in mouse lens epithelial cells. Free Radic. Biol. Med. 51, 2108–2117.

https://doi.org/10.1016/j.freeradbiomed.2011.09.011

Wu, H., Yu, Y., David, L., Ho, Y.-S., Lou, M.F., 2014. Glutaredoxin 2 (Grx2) gene deletion induces early onset of age-dependent cataracts in mice. J. Biol. Chem. 289, 36125–36139. https://doi.org/10.1074/jbc.M114.620047

Wu, X., Bishopric, N.H., Discher, D.J., Murphy, B.J., Webster, K.A., 1996. Physical and functional sensitivity of zinc finger transcription factors to redox change. Mol. Cell. Biol. 16, 1035–1046. https://doi.org/10.1128/mcb.16.3.1035

Yuan, T.-F., Gu, S., Shan, C., Marchado, S., Arias-Carrión, O., 2015. Oxidative Stress and Adult Neurogenesis. Stem Cell Rev. Rep. 11, 706–709. https://doi.org/10.1007/s12015-015-9603-y

Zeitvogel, A., Baumann, R., Starzinski-Powitz, A., 2001. Identification of an invasive, N-cadherin-expressing epithelial cell type in endometriosis using a new cell culture model. Am. J. Pathol. 159, 1839–1852. https://doi.org/10.1016/S0002-9440(10)63030-1

Zhang, L., Wang, N.-L., Zhang, W., Chang, Z.-J., 2008. [Suppression of cell proliferation by inhibitors to redox signaling in human lens epithelial cells]. Zhonghua Yan Ke Za Zhi Chin. J. Ophthalmol. 44, 622–628.

Zhang, S.C., 2001. Defining glial cells during CNS development. Nat. Rev. Neurosci. 2, 840–843. https://doi.org/10.1038/35097593

9   Appendix

9.1   List of Figures:

9.2   List of Tables:

9.3   List of Abbreviations:

B	BCA	Bicinchoninic acid
	BrdU	Bromodeoxyuridine
	BSA	Bovine serum albumin
C	CNPase	2',3'-cyclic nucleotide 3'-phosphodiesterase
	CNS	Central nervous system
	CRMP2	Collapsin response mediator protein 2
	CSPG4	Chondroitin sulphate proteoglycan 4
	Ctrl	Control
D	dpf	days post fertilization
	DNA	Deoxyribonucleic acid
	DTT	Dithiothreitol
E	EGF	Epidermal growth factor
	EGFR	Epidermal growth factor receptor
	EMSA	Electrophoretic mobility shift assay

F	FCS	Fetal calf serum
	FeS	Iron sulfur
	FGF	Fibroblast growth factor
G	GAPDH	Glyceraldehyde-3-phosphate-dehydrogenase
	GBM	Glioblastoma
	GFP	Green fluorescent protein
	GPxS	Glutathione peroxidases
	Grx	Glutaredoxin
	GSH	Glutathion
	GSSG	Glutathione disulfide
H	H_2O_2	Hydrogen peroxide
	H3	Histon 3
	hpf	hours post fertilization
I	ICC	Immunocytochemistry
	IHC	Immunohistochemistry
	IRL	Inner retinal layer
M	MACS	Magnetic associated cell sorting
	MAPK	Mitogen activated protein kinase
	MBP	Myelin basic protein
	MitA	Mithramycin A
	MO	Morpholino
	MS	Multiple sclerosis
N	NADPH	Nicotinamide adenine dinucleotide phosphate
	NDPK	Nucleoside diphosphate kinase
	NG2	Neuron-glial protein 2
	NGS	Normal goat serum
	NO	Nitric oxide
	NO·	Nitric oxide radical
	NPC	Neural precursor cell
	Nrf2	nuclear factor erythroid 2–related factor
O	O_2·	Superoxide
	OCT	Optical coherence tomography
	OH·	Hydroxyl radical
	Olig2	Oligodendrocyte transcription factor 2

	OMR	Optomotor response
	ONOO-	Peroxnitrite
	OPC	Oligodendrocyte progenitor cell
P	PBS	Phosphate buffered saline
	PCR	Polymerase chain reaction
	PDGF	Platelet-derived growth factor
	PDGFRα	Platelet-derived growth factor receptor-α
	PDIs	Protein disulfide isomerases
	Pen	Penicillin
	PFA	Paraformaldehyd
	PLL	Poly (L)-Lysin
	PLP	Proteolipid protein
	PNS	Peripheral nervous system
	Prxs	Peroxoredoxins
	PVP	Polyvinylpyrrolidone
Q	qRT-PCR	Quantitative real time PCR
R	RNA	Ribonucleic acid
	RNS	Reactive nitrogen species
	ROS	Reactive oxygen species
	RT	Room temperature
	RU	Relative units
S	SDS-PAGE	Sodium dodecyl sulfate polyacrylamide gel electrophoresis
	SEM	Standard error of the mean
	-SH	Thiol group
	SOD2	Superoxide dismutase 2
	Sp1	Specificity protein 1
	Strep	Streptomycin
T	TBP-2	thioredoxin binding protein 2
	TMZ	Temozolomide
	TRT	Total retinal thickness
	Trx	Thioredoxin
	TrxR	Thioredoxin reductase
V	VEGF-C	Vascular endothelial growth factor C

10   Acknowledgements

11   Declaration

Ich versichere an Eides statt, dass die Dissertation von mir selbstständig und ohne unzulässige fremde Hilfe unter Beachtung der „Grundsätze zur Sicherung guter wissenschaftlicher Praxis an der Heinrich-Heine-Universität Düsseldorf" erstellt worden ist.

Die Dissertation wurde weder in dieser noch in einer abgewandelten Form bereits einer anderen Fakultät vorgelegt.

Ich habe bisher keine erfolglosen Promotionsversuche unternommen.

Düsseldorf, den 04.05.2021

....

Christina Wilms